Stony Brook University

Role of NF-κB Recognition Sites in RTA Transactivation of Lytic Gene Expression during Murine Gammaherpesvirus 68 Infection.

A Dissertation Presented

by

Alexis Leah Santana

to

The Graduate School

in Partial Fulfillment of the

Requirements

for the Degree of

Doctor of Philosophy

in

Molecular Genetics and Microbiology

Stony Brook University

August 2015

Stony Brook University

The Graduate School

Alexis Leah Santana

We, the dissertation committee for the above candidate for the Doctor of Philosophy degree, hereby recommend acceptance of this dissertation.

Laurie T. Krug, Ph.D.
Dissertation Advisor
Assistant Professor, Department of Molecular Genetics and Microbiology

Patrick Hearing, Ph.D.
Chairperson of Defense
Professor, Department of Molecular Genetics and Microbiology

Sumita Bhaduri-McIntosh, M.D. Ph.D.
Associate Professor, Department of Pediatrics, Molecular Genetics and Microbiology

Ed Luk, Ph.D.
Assistant Professor, Department of Biochemistry and Cell Biology

Kenneth B. Marcu, Ph.D.
Professor, Department of Biochemistry and Cell Biology

This dissertation is accepted by the Graduate School

Charles Taber
Dean of the Graduate School

Abstract of the Dissertation

Role of NF-κB Recognition Sites in RTA Transactivation of Lytic Gene Expression during Murine Gammaherpesvirus 68 Infection.

by

Alexis Leah Santana

Doctor of Philosophy

in

Molecular Genetics and Microbiology

Stony Brook University

2015

Herpesviruses establish life-long infections in the host, characterized by phases of productive lytic replication, latency, and reactivation from latency. Gammaherpesvirus infections are associated with the development of lymphomas and tumors; the incidence of cancer is increased upon loss of host immune control. Murine gammaherpesvirus 68 (MHV68) naturally infects small rodents and has genetic and biologic parallels with the human gammaherpesviruses, Epstein-Barr virus and Kaposi's sarcoma-associated herpesvirus. This model pathogen system provides a platform to examine the interplay of viral and host determinants that shape the latent or lytic fate of an infected cell. The replication and transcription activator (RTA) drives the lytic cascade of viral gene expression during *de novo* infection and reactivation from latency. The NF-κB signaling pathway promotes inflammation and many aspects of B cell biology. NF-κB subunits were previously found to promote MHV68 latency in primary B cells. There are multiple NF-κB recognition sites in the viral genome, but the roles of these sites the regulation of viral gene expression is not known. A latent B cell line inducible for RTA expression was generated to examine the impact of NF-κB binding sites in the lytic ORF6 gene promoter upon RTA induction and stimulation of NF-κB signaling by lipopolysaccharide (LPS). The NF-κB binding sites in the viral genome were neither directly responsive to NF-κB activation nor did they influence RTA transactivation of the ORF6 promoter. Taken together, we conclude that the NF-κB recognition sites in the ORF6 promoter do not influence RTA transactivation. Next, a novel RTA recognition element in the right origin of lytic replication was identified by chromatin immunoprecipitation. To validate RTA occupancy of the viral genome in primary B

cells, a recombinant virus was generated to enable the biotinylation of RTA in transgenic mice expressing the BirA ligase. Biotinylated RTA was detected in complex with the viral genome upon LPS stimulation of B cells from infected mice. The inducible reactivation system coupled with the *in vivo* RTA biotinylation system are important tools for further mechanistic investigations of the interplay of host signaling with RTA transactivation function.

Table of Contents

List of figures

List of tables

List of Abbreviations

DNA – deoxyribonucleic acid

IE – Immediate Early

E - Early

L – Late

MZ – Marginal Zone

MOI - Multiplicity of infection

BAC - Bacterial artificial chromosome

aa - Amino acid

PFU - Plaque forming unit

IN - Intranasal

IP - Intraperitoneal

PEC - Peritoneal exudate cell

FBS - Fetal bovine serum

MEF - Mouse embryonic fibroblast

HSV-1 - Herpes simplex virus strain 1

HSV-2 - Herpes simplex virus strain 2

VZV - Varicella zoster virus

MHV68 - Murine gammaherpesvirus 68

EBV - Epstein-Barr virus

KSHV - Kaposi's sarcoma associated herpesvirus

RRV – Rhesus monkey rhadinovirus

HVS - Herpesvirus saimiri

HHV-6A - Human herpesvirus 6A

HHV-6B - Human herpesvirus 6B

HHV-7 - Human herpesvirus 7

γHV - gammaherpesvirus

NF-κB - Nuclear factor kappa B

IKKβ/IKK2 - Inhibitor of nuclear factor kappa-B subunit 2

TPA - 12-O-tetradecanoylphorbol-13-acetate

TSA – Trichostatin A

AP1- activator protein 1

SP1- specificity protein 1

CBP/p300 - CREB-binding protein

XBP-1 - X-box binding protein 1

STAT6 - signal transducer and transactivator of transcription 6

HMGB-1 - high mobility group box 1

CPE - Cytopathic effect

Hpi – hours post infection

RIG-I - Retinoic acid induced gene I

MAVS - Mitochondrial antiviral signaling protein

IFN - Interferon

PEL - Primary effusion lymphoma

KS - Kaposi's sarcoma

MCD - Multicentric Castleman's disease

PTM – Post-translational modification

Chapter 1: Introduction

1.1 *Herpesviridae*

The *Herpesviridae* represent a family of large double-stranded DNA viruses with genomes ranging from ~125 - 240 kb in size encoding over 70 genes (1, 2). Surrounding the exterior of the virion is the envelope composed of viral glycoproteins necessary for attachment and entry (**Fig.1.1**). The tegument layer, located beneath the outer envelope, is made up of viral proteins symmetrically positioned around the capsid. The core is comprised of the viral double-stranded DNA genome packaged in the center of an icosahedron shaped capsid. Upon attachment and entry, the viral capsid traffics along host microtubule networks, and docks at the nucleus into which the viral genome enters. Once in the nucleus, viral gene expression follows an ordered cascade beginning with immediate early (IE) followed by early (E) and late (L) gene expression. IE genes are expressed independent of viral protein synthesis and IE gene activation is proposed to be mediated by viral tegument proteins delivered into the cell following infection **(3-7)**. IE gene expression follows the same pattern for E and L genes whereby transcripts are spliced before being transported to the cytoplasm for protein translation. After translation, IE proteins are transported back into the nucleus to regulate subsequent E gene expression. E gene expression occurs before viral DNA replication. E genes encode enzymes involved in initiating DNA replication and host shutoff. L gene expression depends on viral DNA replication initiated by E genes. L genes encode the structural components of the virion and envelope and proteins necessary for viral egress from the infected cell.

Herpesviruses support two distinct phases of infection: lytic infection and latency (8-12). Lytic infection is characterized by tightly regulated viral gene expression, linear DNA replication, and the production of infectious virus particles. During latency a small number of viral genes are expressed and the viral genome is maintained as a non-integrated episome in the nucleus of the infected cell with no infectious virus particles released. Latency permits herpesviruses to establish life-long persistent infection that upon lytic reactivation contributes to seeding of other latent reservoirs via transmission of infectious particles throughout the host and to other hosts.

The herpesvirus family is divided into alpha (α), beta (β), and gamma (γ) subfamilies based on genetic and biological differences. The cell type in which latency is established differs dramatically between herpesvirus family members. The α-herpesviruses, varicella zoster virus (VZV) and herpes-simplex virus (HSV) -1 and -2, replicate in epithelial cells which is essential for establishing long-term latency in neurons. The β-herpesviruses are murine and human cytomegalovirus (MCMV and HCMV), human herpesvirus -6A and -6B (HHV-6A/B) and human herpesvirus -7 (HHV-7). For β-herpesviruses, latency is established in different types of hematopoietic cells. MCMV and HCMV establish latent infection in CD34+ hematopoietic stem cells and monocytes (13, 14). HHV-6A and -6B establish latent infection in bone marrow progenitor cells and both HHV-6 and HHV-7 establish latency in T cells (15). The γ-herpesviruses establish latency in lymphocytes and consist of the human Epstein-Barr virus (EBV) and Kaposi's sarcoma associated herpesvirus (KSHV), the primate herpesvirus saimiri (HVS) and rhesus monkey rhadinovirus (RRV), the murine gammaherpesvirus 68 (MHV68) and

other non-primate viruses. The γ-herpesviruses are further divided into two genera the (lymphocryptovirus) γ1- and (Rhadinovirus) γ2- herpesviruses based on viral sequence homology. EBV is considered a γ1-herpesvirus with the γ2-herpesvirus subfamily comprised of KSHV, HVS, RRV, and MHV68.

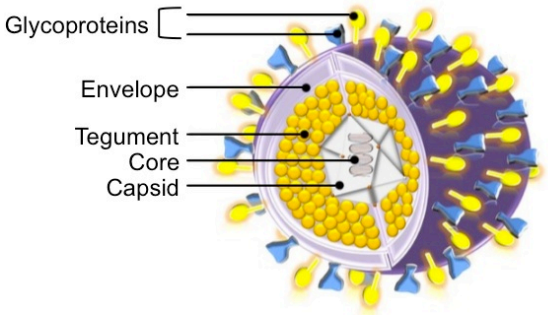

Figure 1.1 Herpesvirus virion composition.
The lipid envelope is comprised of glycoproteins necessary for cell entry. The tegument is positioned around the nucleocapsid (core and capsid). The viral genome is packaged within the capsid.

1.2 Gammaherpesvirus infection and associated malignancies

The human gammaherpesviruses are important pathogens associated with the development of lymphomas and neoplasms. In 1964, Epstein-Barr virus (EBV) was identified in Burkitt's lymphoma, a childhood tumor commonly found in sub-Saharan Africa (16). This was the first human tumor virus to be discovered and established a role for human viruses in cancer. EBV infection is ubiquitous in humans. Primary EBV infection may present clinically as infectious mononucleosis that is spontaneously resolved, resulting in life-long latency in B lymphocytes. Although mostly benign in the human population, EBV infection poses an increased cancer risk in immunocompromised patients. For instance, EBV is associated with Burkitt's lymphoma, nasopharyngeal carcinoma, and detected in a number of Hodgkin's and non-Hodgkin's lymphomas in immunocompromised hosts. Equally important, EBV infections are associated with the development of post-transplant lymphoproliferative disorders (PTLD) (17). PTLD is a complication upon transplantation of EBV-infected allogenic stem cells into an immunocompromised naïve recipient or in the case of solid organ transplants, upon EBV reactivation from the donor organ or transplant recipient that is immunosuppressed to prevent organ rejection. The disease is more common in children than adults and can require aggressive treatment for solid organ transplants, with a potential for fatal outcomes in the case of bone marrow transplants.

Kaposi's sarcoma-associated herpesvirus (KSHV) was first described as the causative agent of Kaposi's sarcoma (18). In addition, KSHV infection is associated with the development of multicentric Castleman's disease and primary effusion lymphoma (19, 20). KSHV infects

lymphoid and epithelial cells similar to EBV, but also infects a broader range of cells such as endothelial cells, macrophages, monocytes and dendritic cells (21).

The mechanisms by which EBV and KSHV ensure survival in the host cell can lead to uncontrolled proliferation and the development of lymphomas. The two most common malignancies associated with gammaherpesvirus infection, non-Hodgkin lymphomas and Kaposi's sarcoma, are predominately found in individuals co-infected with HIV (22). Despite the effectiveness of HAART therapy, both gammaherpesvirus-induced lymphomas remain the most common cancer-related cause of death in HIV-infected patients. Due to the ineffectiveness of antivirals in combating latent infections and the lack of vaccines, studies on virus-host interactions could provide valuable knowledge for the design of targeted therapeutics that disrupt latency. However, studies on the role of virus-host factors and how they influence pathogenesis in EBV and KSHV have been hampered due to the inability to perform synchronous *de novo* infection in cell culture, strict host tropism, and the lack of suitable small animal models (23, 24). Murine gammaherpesvirus (MHV68), a natural pathogen of murid rodents, provides a relevant and powerful model system for assaying factors that affect gammaherpesvirus pathogenesis (25-28)

1.3 MHV68 infection of mice as a model of gammaherpesvirus pathogenesis

Murine gammaherpesvirus 68 (MHV68) represents one of five gammaherpesvirus strains isolated from bank voles in Slovakia in 1980 (29). Additional strains have been isolated throughout northern Europe in wood mice and other rodents that display homology to those previously identified (30-33). Since MHV68 represents a natural pathogen of mice, it is capable of infecting a diverse number of inbred and outbred mouse strains (34-37). The natural route of MHV68 transmission is unknown, but low dose intranasal infection has been proposed as one method by which infection occurs (38).

Intranasal infection of mice results in high titer viral lytic replication in lung alveolar epithelial cells, peaking at approximately 7 days post-infection (**Fig. 1.2**) (37-39). Shortly afterwards, rapidly expanding populations of immune cells clear the acute phase of infection, with CD8+ T cells playing a central role in this process (40, 41). Viral clearance in the lung by two weeks post-infection coincides with dissemination to the spleen, marked by an increase in the size of spleen (splenomegaly) (**Fig. 1.2**) (37, 42). Direct infection of CD11c+ dendritic cells residing in the lung transport virus to adjacent supraclavicular lymph nodes where B cell infection occurs (43). B cell infection is necessary for viral persistence in the spleen, as infection of B cell knockout mice displayed clearance of viral replication and establishment of latency at the sites of infection, but no colonization of the spleen (44, 45). Although the process of trafficking of MHV68-infected B cells in the supraclavicular lymph node to the spleen is not known, viral splenic colonization begins with the transfer of virions from marginal zone (MZ) macrophages to MZ B cells, which then relocate to follicular dendritic cells (46, 47). Next,

follicular dendritic cells transfer virions to germinal center B cells. Memory B cells immunoglobulin isotype class-switched are the predominant reservoir of MHV68 latency (46, 48-50). Latency can also be established in dendritic cells, macrophages, epithelial, and endothelial cells (51-53). The peak of viral latency occurs at 16 days post-infection with viral genomes detectable up to nine months later (**Fig.1.2**). Intraperitoneal infection bypasses the lung to directly seed the spleen; latency is established in peritoneal exudate and splenic cells (45). For EBV and KSHV, previous work has shown that plasma cell differentiation is involved in B cell reactivation from latency (54-56). MHV68 infection of plasma cells has been confirmed at the peak of splenic latency and is associated with MHV68 reactivation (57). Moreover, ectopic expression of the virally encoded M2 protein drives plasma cell differentiation in the absence of infection (58). This data supports the hypothesis that latent B cells undergo reactivation via M2 protein expression which drives plasma cell differentiation.

Systems for genetic manipulation of both the host Mus musculus and MHV68 are well-established, permitting researchers to investigate the importance of host and viral genes during the course of a natural infection (59). Multiple techniques have been developed to assay different stages of the virus life cycle including lytic replication, latency, and reactivation from latency in the context of the host. In addition, the accessibility of lytic and latent tissue culture models and the ability of MHV68 to replicate to high titer in tissue culture facilitate mechanistic *in vitro* studies. Thus, MHV68 poses a model system to better understand the molecular basis of latency regulation in the context of its host (60).

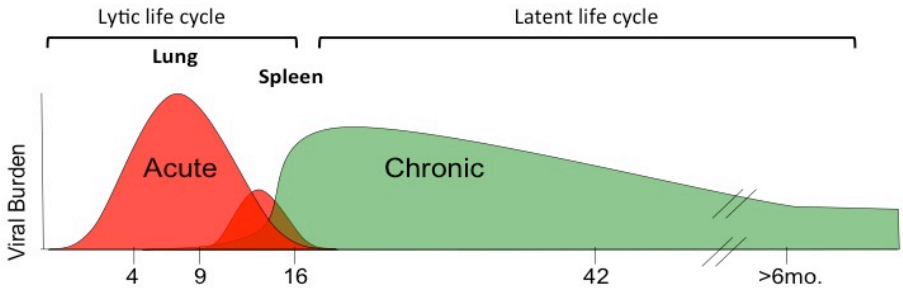

Figure 1.2 Course of an MHV68 infection in mice.
Acute lytic replication occurs in the lung (intranasal infection) or in the spleen (intraperitoneal infection). Ongoing replication is cleared typically by 12 days. The peak of latency is measured 16-18 days post-infection in secondary lymphoid tissues such as the spleen. Maintenance of latency is scored at 42 days post-infection or later. B cells are the predominant latency reservoir, followed by macrophages, dendritic cells, and endothelial cells.

1.4 Similarities and differences of MHV68 with human gammaherpesviruses

The MHV68 genome is approximately 120 kb long and contains approximately 80 open reading frames, a majority display homology as well as genetic co-linearity with the genomes of HVS and KSHV, and EBV (61-63). MHV68 is more closely related to the γ2-herpesviruses in terms of genome structure and organization. Transposon mutagenesis screening of MHV68 genes established a number of genes essential for virus growth that are conserved within the gammaherpesvirus family (64, 65). The MHV68 genome encodes 14 unique M genes that are located throughout the viral genome. On left end of MHV68, M1-M4 genes are found interspersed with eight vtRNA-miRNA non-coding RNAs expressed during latency (25, 66, 67). Deletion of the left end of the MHV68 genome, in which M1-M4 and the eight vtRNA-miRNAs are located, does not affect lytic replication in cell culture but does promote viral latency in the host. The MHV68 genome is flanked by 1.2 kb repeated regions (terminal repeats), a conserved feature of the gammaherpesvirus family, that upon the process of rolling circle DNA replication provides a substrate for cleavage and packaging of unit length viral genomes (63, 68-73). Similar to HVS, EBV and KSHV, the MHV68 encoded M11 gene is a viral homolog of the cellular anti-apoptotic bcl-2 protein that has both anti-apoptotic and anti-autophagic functions (74-78). In addition, MHV68, HSV, and KSHV encode functional homologs of host genes including the IL-8 receptor (MHV68-ORF74 or vGPCR), cyclin D (MHV68-ORF72 or v-cyclin), and the complement regulatory protein (MHV68-ORF4).

Intranasal infection of mice with MHV68 results in acute productive infection in the lung and induces an EBV-like infectious mononucleosis syndrome that contributes to enlarged lymph nodes and splenomegaly (48, 79, 80). Similar to EBV, initial infection is cleared by CD8+ T cells in the lung of MHV68 infected mice and latency is established in memory B cells generated from germinal center reactions (41, 46, 49, 50, 81-84). EBV and KSHV are associated with the development of lymphomas and tumors in immunocompromised hosts. Likewise, MHV68 infected mice treated with the immunsouppresive drug cyclosporin A (85) or transgenic mice lacking CD8 T cells or IFNγ signaling (86, 87) are prone to develop lymphoproliferative disease.

The latently infected B lymphoma cell line (S11) was derived from long-term MHV68-infected mice that spontaneously developed lymphoproliferative disease (88). KSHV and HVS encode cyclin D homologs that have oncogenic properties and are expressed to high levels in transformed cells (89, 90). Although EBV does not encode a cyclin D homolog, LMP-1 overexpression upregulates cyclin D protein levels and has been shown to induce epithelial cell carcinomas (91-94). The cyclin D homolog of MHV68 is encoded by ORF72 (v-cyclin) and overexpression of the protein has been demonstrated to drive lymphomas in primary lymphocytes (95). In addition, MHV68 can drive fetal liver B cell immortalization and latency programs are associated with the development of B cell lymphomas in mice (96).Therefore, MHV68 has the propensity to drive cancer progression and has been shown to induce lymphomas in the context of an immunocompromised mouse.

1.5 The RTA protein

During the herpesvirus lytic life cycle, viral gene expression follows an ordered cascade beginning with immediate early (IE), to early (E) and then late (L) genes. The immediate early protein, replication and transcription activator (RTA) is encoded by open reading frame 50 (ORF50) and is a conserved gammaherpesvirus transcription factor (97-101). RTA initiates lytic replication or the switch from latency to lytic replication by regulating transcription of E and L lytic genes. For the γ2-herpesviruses, KSHV, RRV, HVS, and MHV68, RTA has been shown to be necessary and sufficient to initiate viral lytic replication during *de novo* infection (98, 100, 102, 103). Moreover, ectopic expression of RTA in quiescently infected cells disrupts latency and induces lytic reactivation (97, 98, 101, 104, 105). The γ1-herpesvirus, EBV requires the viral transactivator protein ZTA (BZLF1) for lytic replication, and RTA (BRLF1) serves as a critical co-factor (106-112).

RTA plays a key role in driving viral gene expression; thus its expression must be stringently regulated for latency establishment and maintenance. RTA has been shown to auto-regulate its expression, yet there are no known RTA DNA binding sites in the ORF50 promoter. Host transcription factors are proposed to drive RTA transcription upon viral 'sensing' of specific cell contexts and environmental stimuli (104, 113-115). The ORF50 promoter has H3K27me3 repressive chromatin marks and is linked to the latency locus of the viral genome by cohesins and CTCF (116). Treatment of cells with histone deacetyltransferase inhibitors sodium butyrate, trichostatin A (TSA), valproic acid or 12-O-tetradecanoylphorbol-13-acetate (TPA) trigger ORF50 expression and reactivation (116). TPA treatment induces Activator protein-1 (AP-1) expression and AP-1 binding sites in the ORF50 promoter drive protein expression and

KSHV reactivation (117-130). Conversely, sodium butyrate induction of KSHV reactivation is mediated by Sp1 and Sp3 transcription factors at the ORF50 promoter (131, 132). Similar to KSHV, the MHV68 ORF50 promoter contains an AP-1 responsive element and mutagenesis of the site impairs virus lytic replication (133).

Terminal cell differentiation has been associated with the initiation of reactivation for KSHV (134-136). The host X-box binding protein 1 (XBP-1) protein is associated with terminal B cell differentiation, a process that induces KSHV reactivation from latency (54, 137). XBP-1 upregulates ORF50 expression and had been shown to bind to the ORF50 promoter and is presumed as the mechanism by which reactivation occurs (138, 139). Moreover, XBP-1 has been shown to promote Hypoxia-inducible factor 1 α (HIF-1α) gene expression and HIF-1α as well as -2α enhances MHV68 RTA promoter activity (140, 141). The KSHV ORF50 promoter contains Oct-1 binding sites that were required for RTA auto-regulation of transcription, an interaction that was increased by high mobility group box 1 (HMGB-1) expression yet requires Oct-1 binding sites (142, 143). In addition, CAAT/Enhancer-binding protein α (C/EBPα) binds to the KSHV ORF50 promoter and shown to activate its gene expression upon reactivation (144).

For MHV68, signal transducer and transactivator of transcription 6 (STAT6) has been shown to bind to a STAT6 DNA binding site located in an alternative ORF50 promoter region upstream of Exon 0 called (N4/N5) in infected IL-4-stimulated macrophages (145). In addition, interferon γ (IFN-γ) treatment and STAT1 expression were linked to ORF50 promoter inhibition in macrophages that was not dependent on STAT1 DNA binding sites (122).

The major KSV, HVS, and MHV68 ORF50 transcripts are composed of two exons separated by an intron that is spliced to generate the ORF50 transcript; although other alternatively spliced transcripts have been identified and some have been shown to affect RTA coding sequence (97-99, 121, 146-151). Upon translation, the RTA protein contains an N-terminal DNA binding domain and C-terminal transactivation domain. In addition, KSHV and MHV68 RTA contain cysteine rich domains that exhibit an E3 ubiquitin ligase function (152, 153). Alignment of the γ2-herpesviruses, RRV, MHV68, and KSHV, RTA protein amino acid sequence reveals a high degree of similarity (154). Interestingly, the highest degree of amino acid similarity occurs within the region encoding the RTA DNA binding domain. This may explain why the RRV and MHV68 RTA proteins have the capacity to trans-activate a similar subset of KSHV encoded genes, albeit at a lower level than KSHV RTA (154).

The KSHV RTA C-terminal transactivation domain was mapped by generating truncation mutants of the RTA protein that were fused to the yeast GAL4 DNA binding domain and tested for their capacity to activate a reporter gene containing the GAL4 DNA binding site (99, 155, 156). The amino acids 486-691 within the C-terminal domain of RTA were shown to be necessary for transactivation function (99). Deletion of amino acids within the C-terminal transactivation domain generates an RTA protein with the ability to bind DNA but is unable to activate gene expression and reactivate virus from latency and even has been shown to interfere with WT RTA function (99). Similarly, C-terminal MHV68 RTA truncation mutants were confirmed for loss of transactivation ability for the ORF57 promoter (157). Moreover, stable cell lines harboring a RTA C-terminal transactivation mutants were unable to undergo lytic

replication and generate infectious particles. Since immediate early gene expression was not compromised in the cell lines, RTA transactivation function was proposed to be necessary and sufficient for inducing viral gene expression.

KSHV and MHV68 RTA migrate at higher molecular weight than predicted based on their amino acid content, from 64 to 90 kDa for MHV68 and 76 to 110 kDa for KSHV (99, 157). Phosphatase treatment decreases KSHV RTA mobility to ~90 kDa suggesting that phosphorylation contributes in large to the change in RTA protein mobility (99). Mass spectrometric analysis of KSHV RTA identified serine/threonine residues that were phosphorylated and replacement of residues 634 and 636 from serine to alanine impairs RTA transactivation and reduces reactivation (158). Similarly, the MHV68 RTA is phosphorylated in vitro by the IKKβ kinase at groups of serine/threonine residues $S_{550}T_{552}S_{556}$ (STS) or $T_{561}T_{562}S_{564}$ (TTS) and replacement of the residues to alanine impairs RTA transactivation and MHV68 viral growth for the TTS mutant virus (159). Taken together, RTA phosphorylation plays a role in regulating RTA-mediated viral gene expression which impacts lytic replication and reactivation.

Numerous investigations have attempted to uncover the molecular mechanism by which RTA activates lytic gene expression in infected cells and suggest regulation occurs via both direct binding or indirectly in complex with other transcription factors. KSHV RTA activates its own promoter and that of the following genes: vIL6, polyadenylated nuclear RNA (PAN), ORF6, ORF21, ORF57, ORF59, ORF74, K1, K5, K8, K9, K12, K15 (129, 160-170). Of the KSHV RTA responsive genes listed above, DNA binding motifs was confirmed for PAN, K8, ORF57, v-IL6, and K12 and binding motifs were predicted based on them. However, only PAN

and K12 promoter RTA binding motifs contain significant homology (160). In a separate study, latent BCBL-1 cells harboring an inducible Flag-tagged RTA DNA binding domain were used for ChIP-seq analysis (162). Multiple novel and previously identified RTA binding sites in the KSHV genome were found and used to generate the consensus binding motif (TTCCAGGAT(N)0–16 TTCCTGGGA) (162). Interestingly, RTA binding does not require the entire consensus motif and some RTA binding sites identified contained half or partial sites (162).

To date, MHV68 RTA responsive elements (RREs) have been identified in the promoters of ORF57, ORF72, MK3, ORF18, M1, ORF48 and ORF50 itself (115, 151, 171-175). The MHV68 ORF72 gene encodes the v-cyclin protein that is essential for reactivation from latency (95). The ORF72 promoter has a 30 bp RRE, yet mutagenesis of this region only partially impairs expression (171). ORF57 contains two RREs, RRE-A and RRE-B that span a 83 and 57 bp region in its promoter and are homologous to RREs identified in the KSHV PAN and ORF57 promoters, respectively (115). For the MK3 gene, a minimal RRE was identified that spans ~400 bp upstream of the gene (172). The M1 and ORF50 RREs share a homologous 5'-CAGAAG-3' site which upon mutagenesis results a loss of RTA transactivation (173). For the RREs mentioned, it is unclear whether RTA directly interacts with the viral genome or interacts with other transcription factors to drive gene expression. Two RTA RREs were identified upstream of ORF18 in the left oriLyt and were shown to be directly bind RTA *in vitro* and *in vivo* (174). Three other RREs were predicted in the left oriLyt based on their homology to a 15 bp sequence (5'-CTTTTTGATGTGTTT-3') present in the RREs confirmed for RTA occupancy upstream of

ORF18 but were not investigated further. Recently, an RRE was identified upstream of the MHV68 ORF48 gene and shown to mediate RTA transactivation as mutation of the site disrupts gene expression (175). In addition, RTA DNA binding was confirmed via EMSA and chromatin immunoprecipitation to the identified RRE upstream of ORF48.

A number of cellular proteins have been identified as co-factors that synergize with RTA to regulate RTA-responsive promoters. For example, RBP-Jκ, CCAAT/enhancer binding proteins alpha and beta (C/EBP α/β), octamer binding protein 1 (OCT-1), c-Jun, CREB-binding protein (CREB), and high-mobility group B1 (HMGB1) have been demonstrated to interact with and upregulate KSHV RTA's transcriptional activity promoting lytic replication (124, 144, 176-179). The KSHV RTA was shown to activate the k-bZIP promoter via direct interactions with OCT-1 and RBPJ/κ (180). In a separate study, RTA and RBPJ/κ tetrameric protein complexes were identified and shown to bind a core "CANT" DNA sequence present in the MTA promoter (181).

Interestingly, some cellular factors have been reported to inhibit gammaherpesvirus lytic replication by inhibiting RTA expression or activity thereby promoting latency. For instance, PARP-1, KSHV RTA-binding protein (K-RBP), and nuclear factor kappa B (NF-κB) are examples of cellular proteins that inhibit lytic replication (182-184). The molecular interplay between MHV68 RTA and cellular proteins in affecting viral gene expression has not been as extensively studied as with KSHV. The cellular interferon regulatory factor 4 (IRF4) plays an important role in plasma cell differentiation and immunoglobulin class switching and has been shown to synergize with and enhance RTA transactivation of the M1 promoter (173). The

cellular HMGB-1 protein has been implicated as important for promoting MHV68 lytic replication (177). HMGB-1 co-expression with RTA enhanced its transactivation capacity of ORF57 and M3 reporters. Infection of HMGB-1 deficient cells impairs MHV68 lytic replication and linked to lessened RTA transactivation capacity. In addition, cellular proteins such as NF-κB have been demonstrated as important factor in inhibiting lytic gene expression, and will be discussed below (182, 185, 186).

1.6 The NF-κB signaling pathway

The Nuclear Factor Kappa B (NF-κB) pathway is a signaling process that involves upstream phosphorylation events that culminate in the proteosomal processing of regulatory proteins that enable the nuclear translocation of transcription factors into the nucleus. Often initiated upon engagement of cell surface receptors, the NF-κB signaling pathway regulates expression of genes involved in diverse processes including immunity, stress responses, cell death, differentiation and development.

Toll-like receptors (TLR) are a family of conserved pathogen recognition receptors that orchestrate innate immunity against invading pathogens in response to pathogen associated molecular patterns (PAMPs) (187, 188). TLR engagement activates the MyD88-IRAK-TRAF6 signaling pathway leading to activation of several transcription factors, activator protein 1 (AP-1), NF-κB, and interferon regulatory factors 3/7 (IRFs). These transcription factors play key roles in activating innate immune signal transduction and cytokine production. In resting cells, NF-κB complexes are retained in the cytoplasm by inhibitors of NF-κB (IκBs). IκBs are phosphorylated by IκB kinase (IKK) complexes resulting in activation of canonical or alternative NF-κB pathways. The NF-κB family consists of five subunits, p65 (RelA) RelB, cRel, p50/p105 (NF-κB1), and p52/p100 (NF-κB2) that can form homo- or hetero-dimers. Depending on the composition of the dimers and other variables such as post-translational modification and interactions with other factors, NF-κB dimers can both induce or repress gene expression through direct binding to DNA sequences in the regulatory region of target genes (189). The

canonical pathway is activated by the IKKα/β/γ complex and results in IKKβ-mediated phosphorylation and ubiquitin-mediated proteosomal processing of IκBα proteins, which sequester NF-κB subunits p50/p65 in the cytoplasm. Degradation of IκBα unmasks the nuclear localization signals of the subunits, permitting their nuclear translocation. The non-canonical pathway is activated by IKKα homodimers and phosphorylation of p100 results in proteosomal processing to p52 (190, 191). Processing of p100 to p52 reveals its nuclear localization signal and nuclear translocation of p52/RelB heterodimers.

Canonical and non-canonical NF-κB signaling pathways are utilized by B lymphoid cells, the primary latency reservoir for gammaherpesviruses, to drive transcription of genes important for B cell maturation, responses to infection, proliferation, protection from apoptosis, and immunoglobulin isotype class switching (192). Mechanistic understanding of how the NF-κB signaling pathway regulates gene expression requires identification of subunits that directly interact with DNA or other regulatory factors in promoter regions.

1.7 Gammaherpesviruses modulation of the NF-κB pathway

The human gammaherpesviruses encode lytic and latent proteins that activate the NF-κB signaling pathway during infection. During latency, EBV encodes two proteins, latent membrane protein 1 and 2 (LMP1/2), that mimic B cell signals that are involved in germinal center reactions and the process of memory B-cell differentiation. The EBV encoded LMP1 protein functions is a constitutively active CD40 receptor homolog and activates the canonical and noncanonical NF-κB pathways to promote the survival and proliferation of infected B cells (193-197). LMP2 has dual roles in promoting NF-κB signaling via Syk and Lyn kinases and enhances LMP1 signaling by controlling LMP1-interacting cellular TRAF2 transcription (198, 199). During lytic replication, the viral dUTPase encoded by BLLF3 signals through TLR2 in a MyD88-dependant fashion (200). In addition, the EBV protein BGLF4 encoded by ORF36 is a viral kinase that has been shown to phosphorylate cellular UTX to inhibit NF-κB signaling and promote RTA transactivation of lytic reporters (201).

KSHV encodes NF-κB activating proteins, viral-flice inhibitor protein (vFLIP), viral G protein-coupled receptor (vGPCR), K1, K15, and ORF75 (202-208). KSHV vFLIP is considered the major NF-κB activator expressed during latency and activates the signaling pathway by direct binding to NEMO (IKKγ) (202, 207, 208). The KSHV ORF75 tegument protein was the second highest NF-κB activator identified in an *in vitro* screen for NF-κB activators and is delivered by the virion during initial infection (202). In addition, the KSHV vGPCR and K15 activate NF-κB during lytic replication and K15 expression has also been reported at low levels

during latency (202, 204-206). The role of K1 as an NF-κB activator is cell-specific; its expression promotes NF-κB signaling in B cells yet is inhibits it in HEK293 cells (202, 209). Similar to KSHV, the MHV68 ORF75 homolog (ORF75C) has been shown to activate RIG-I to promote NF-κB signaling during initial infection (210). In addition, the MHV68 encodes a vGPCR that activates NF-κB signaling in response to chemokines (211).

Interestingly, the gammahepesvirus major lytic transactivator proteins inhibit NF-κB signaling during viral replication. For EBV, the major lytic transactivator Zta (BZLF1) inhibits p65 transactivation function; overexpression of which stunts RTA transactivation (212, 213). In addition, p65 overexpression impairs KSHV and MHV68 RTA transactivation of lytic promoters, both RTA proteins have been demonstrated to target p65 for degradation (153, 182, 214). Moreover, MHV68 LANA was demonstrated to target p65 for degradation in 293T co-transfection studies, suggesting that MHV68 may modulate p65 expression during latent infection (215).

Taken together, gammaherpesviruses encode proteins that function to exploit and/or modulate different components of the NF-κB signaling pathway in an attempt to regulate different stages of the virus life cycle, lytic replication or latency. This further highlights importance of the NF-κB pathway as a conserved host factor during viral infections.

1.8. Disruption of NF-κB signaling pathways impairs MHV68 pathogenesis

In vivo investigations have demonstrated that disruption of NF-κB signaling impairs MHV68 latency establishment in B cells of infected mice. In one approach, a recombinant MHV68 expressing a constitutively active form of the IκBα protein (MHV68-IκBαM) was used to infect mice (186). Infection with MHV68-IκBαM did not impair viral growth in the lungs, demonstrating that NF-κB activation is dispensable for lytic replication. However, inhibition of NF-κB activation led to a significant reduction of latency establishment in lung and spleen B cells *in vivo* (186). The NF-κB p50 subunit is activated during both lytic and latent infection *in vitro* (185). In a second study, our laboratory generated bone marrow chimeras with a 80/20% mix of wild-type to p50-/- hematopoietic cells (185). Upon infection of these mice, MHV68 failed to establish latency efficiently in the p50-/- B cells as compared the WT B cell counterparts. The p50-/- B cells also had defects in germinal center formation and isotype class switching. To summarize, these results demonstrated that p50 is required to support MHV68 latency and that defect correlates with the inability of the B cells to transit the germinal center. Unlike the latency establishment defect of the p50-/- B cells in the p50+/- mixed bone marrow chimeric mice, infection of CD40+/- mixed bone marrow chimeras revealed a defect in the long-term maintenance of latency, as the number of CD40-/- B cells harboring latent virus decreased at late times after infection (216). The Toll-like receptor responsive MyD88 is an upstream activator of the canonical arm of the NF-κB pathway. Infection of MyD88+/- mixed bone marrow chimeric mice revealed a defect in B cell latency establishment and decreased B cell

activation, germinal center formation, and class switching at early times post-infection in the MyD88-/- B cells (217). In addition, infection of MyD88 knockout mice with the MHV68-IκBαM virus increased the latency defect in B cells.

Taken together, the results suggest the following: inhibition of NF-κB signaling impacts latency at different stages of chronic infection that coincide with B cell activation, germinal center differentiation, and the formation of long term memory B cells. What remains unclear is the mechanism for this latency defect: are these phenotypes due to a defect in B cell biology and/or a dysregulation of the viral latency program? We propose that gammaherpesviruses have usurped NF-κB signaling during B cell activation, germinal center reactions, and during homeostatic maintenance to promote the viral latency program. Thus, it becomes important to determine if specific viral genes are directly under the control of activated, canonical NF-κB subunits. and if specific NF-κB binding site in the promoters of viral genes mediate this regulation. This knowledge will enable us to target those regions for mutagenesis and genetically separate the role of NF-κB in B cell biology from its function as a regulator of gammaherpesvirus gene regulation *in vivo*.

Chapter 2: Role of NF-κB Recognition Sites in RTA Transactivation of Lytic Gene Expression during Murine Gammaherpesvirus 68 Infection

Introduction

Herpesviruses establish a dynamic infection in the host, characterized by productive lytic replication, a quiescent form of infection known as latency, and reactivation from latency. The human gammaherpesviruses Epstein Bar virus (EBV) and Kaposi's sarcoma-associated herpesvirus (KSHV) establish latency in B lymphocytes and stromal cells; their latent programs are associated with the development of lymphomas, neoplasms, and tumors (218-220). Cancer incidence increases with the loss of immune function and reactivation from latency is believed to play a critical role in disease progression (218-221). Murine gammaherpesvirus 68 (MHV68) naturally infects small rodents and shares many genetic and biological properties with the human gammaherpesviruses (60). The MHV68 pathogen system provides a platform to examine the interplay of virus and host determinants that regulate viral gene expression to determine the latent or lytic fate of an infected cell.

The immediate early protein replication and transcription activator (RTA) is a conserved gammaherpesvirus transcription factor that, for the Rhadinoviruses, is necessary and sufficient to initiate viral lytic replication during *de novo* infection and reactivation (98, 99, 103, 222, 223). While the RTA homolog of EBV (BRLF1) is sufficient to induce reactivation and lytic replication in some cell systems, BRLF1 typically functions in conjunction with the immediate

early protein Zebra (ZTA) to activate viral lytic gene expression (109, 224-226). RTA of KSHV and MHV68 transactivate lytic genes by direct binding to RTA-responsive elements (RREs) in the viral genome or indirectly via interaction with cellular transcription factors (113, 118, 141, 162, 164, 168, 170, 178, 227-233).

NF-kB signaling can determine the outcome of gammaherpesvirus infection in cell culture and in the infected host. Overexpression of the p65/RelA NF-κB subunit inhibits lytic gene promoter activation by MHV68 and KSHV RTA, while pharmacological inhibition of NF-κB promotes EBV and KSHV reactivation from latency (182). However, inhibition of canonical NF-κB activation by infection with a recombinant MHV68 expressing IκBαM, a dominant negative mutant form of the NF-κB inhibitor IκBα, had no impact on lytic replication, but led to a severe defect in the establishment of latency B cells of infected mice (186). Along similar lines, loss of upstream activators including the CD40 (216, 234) and the BAFF receptors (235) or the downstream NF-κB subunit p50 in NF-κB1 knock-out mice in mixed bone marrow chimera studies impaired MHV68 latency in B cells *in vivo* (185, 186). Toll-like receptors (TLR) orchestrate innate and adaptive immune defenses against invading pathogens (187, 236). TLR engagement of the MyD88-IRAK-TRAF6 axis leads to several downstream signaling events including stimulation of the IKK signalosome leading to the nuclear translocation of activated canonical NF-κB subunits. Inhibition of NF-κB signaling by loss of the TLR signaling component MyD88 in knock-out mice impaired the establishment of viral latency (216, 217, 234). Thus, NF-κB signaling is a critical host determinant of gammaherpesviruses latency *in vivo*; but its mechanism of action remains unclear and requires further characterization.

In contrast to the role of NF-κB signaling in promoting gammaherpesvirus latency, engagement of NF-κB signaling via toll-like receptors has differential effects on MHV68 reactivation from latent B cell reservoirs and lytic replication in culture. Lipopolysaccharide (TLR4) or CpG DNA (TLR9) triggers reactivation of MHV68 from latency in cell culture (237); and lipopolysaccharide (LPS) administration drives reactivation from latent splenocytes in mice (237). In contrast, TLR -7 or -9 engagement has been demonstrated to suppress MHV68 reactivation from the S11 latent B cell line, but promotes reactivation *in vivo* (238). A series of recent reports support a role for RTA of MHV68 in usurping IKKβ activation in response to tegument protein-mediated activation of RIG-I and MAVS to enhance the transcriptional activity of RTA that, in turn, targets the p65/RelA NF-κB subunit for ubiquitin-mediated degradation during *de novo* infection of permissive cell types (153, 159). These data are consistent with a role for NF-κB transcription factors in regulating viral gene expression to promote latency, a function that is counteracted by RTA upon *de novo* infection. However, the role of the lytic cycle-associated NF-κB complexes p65/p50 and the latency-associated subunits c-Rel/p50 as direct regulators of MHV68 gene expression is not known.

Because the interplay of RTA and NF-κB signaling is clearly complex, herein we sought to delineate the role of NF-κB subunits in regulating MHV68 genes during lytic replication and reactivation from latency. We identified multiple NF-κB recognition sites located in upstream regulatory regions of latent and lytic MHV68 genes. Next, we examined the response of two NF-κB recognition elements upstream of the ORF6 gene in response to NF-κB subunits alone or in

combination with the lytic transactivator RTA. To assess the role of these NF-κB binding sites in the context of reactivation, we generated latent MHV68+ B cell lines inducible for RTA expression. We found that TLR4 activation by LPS treatment in combination with doxycycline-induced RTA expression significantly enhanced virus reactivation, but did not reveal any role for the NF-κB binding sites in the ORF6 promoter. In primary splenocytes, RTA occupancy of a novel RTA recognition element in the right oriLyt was validated with an *in vivo* biotinylation system. Taken together, while LPS enhances reactivation and RTA transactivation functions, the NF-κB recognition sites in the viral genome do not seem to influence lytic transactivation by RTA.

Materials and Methods

Cells and mice. NIH3T12 murine fibroblasts and HEK293T cells were maintained in Dulbecco's Modified Eagle Medium (DMEM) supplemented with 100 U/mL of penicillin and 100 mg/mL of streptomycin at 37°C in 5% CO_2. NIH3T12 and HEK293T cells were maintained in 8% and 10% fetal bovine serum (FBS), respectively. S11 lymphoma (88), A20-derived HE2.1 cells (239), and A20-HE2-RIT (described below) are MHV68+ latent B cell lines, and were maintained in RPMI 1640 supplemented with 10% FBS, 100 U of penicillin/mL, 100 mg of streptomycin/mL, and 50 mM 2-mercaptoethanol at 37°C in 5% CO_2. HE2 cells were selected and cultured in RPMI containing 300 μg/mL hygromycin B sulfate (Invivogen, San Diego, CA). Primary murine embryonic fibroblasts were maintained in DMEM supplemented with 10% FBS supplemented with 100 U/mL penicillin and 100 mg/mL of streptomycin at 37°C in 5% CO_2.

C57BL/6 mice were purchased from Jackson laboratories (Bar Harbor, Maine) or bred in the animal facilities at Stony Brook University. ROSA26HABirA mice ubiquitously express *birA*, an HA-tagged bacterial biotin ligase (http://jaxmice.jax.org/strain/010920.html). The ROSA26HABirA mice (herein referred to as ROSA BirA mice) were a gift from Dr. Ming Li (Memorial Sloan Kettering Cancer Center, New York) and were bred in the animal facilities at Stony Brook University. All protocols were approved by the Institutional Animal Care and Use Committee of Stony Brook University**.**

Plasmids. The ORF6p luciferase reporter contains the putative regulatory region of the ORF6 gene (genomic coordinates 9,894-11,218 bp, GenBank accession no. U97553) cloned into the HSP70-luc firefly luciferase reporter vector (240). Mutation of NF-kB binding sites in the

promoter of ORF6 (ORF6p) was performed using a Stratagene QuikChange II site-directed mutagenesis kit (Agilent Technologies, Santa Clara, CA) according to the manufacturer's protocol, and primers described in **Table 1**. For the -765 bp, -525 bp, and -331 bp, truncation mutants, PCR products were amplified from the ORF6p vector using the ORF6p reverse primer and forward primers described in Table 1. PCR products were digested and cloned into the SacI and XhoI sites of the HSP70-luc firefly reporter vector, courtesy of Dr. David Lukac (Rutgers Medical School, New Jersey) (164). NdeI and SacI digestion of the full length ORF6p in HSP70-Luc followed by Klenow blunting and ligation of the vector was performed to generate the -909 bp truncation mutant. To generate the -136 bp truncation mutant, the ORF6p vector was digested with HindIII, blunted by Klenow blunting, and digested with XhoI prior to ligation into the SmaI and XhoI sites of HSP70-luc. The -58 bp truncation mutant was generated by annealing the synthetic oligonucleotides described in Table 1.

p65, cRel, and p50 cFlag pcDNA3 expression vectors were gifts from Dr. Stephen Smale (Addgene plasmid# 20012, 20013, 20018) (241). pCMV-IκBαM expression vector encodes the mutant super-repressor form of IκBα with serine-to-alanine mutations at amino acids 32 and 36 (Stratagene). The pCMV empty vector was generated by BamHI and HindIII digestion of pCMV-IκBαM to excise the IκBαM insert, Klenow blunting and religation. The RTA expression vector (pSG50) and empty vector (pCMV-Tag2B) were gifts from Dr. Samuel H. Speck (Emory University) (103).

Cloning of PGK-puro-pTRE3G-RTA-FLAG-IRES-tdTomato began with PCR amplification of tdTomato from tdTomato vector (Invitrogen, Carlsbad, CA) and cloning into

EcoRV and BamHI sites of pTRE3G-IRES (Clontech, Mountain View, CA). Next, FLAG-tagged RTA was amplified from pcDNA5-Topo-TA-RTA-FLAG vector (a gift from Dr. Pinghui Feng, Keck School of Medicine of University of Southern California) (159). After PCR amplification of RTA-Flag, the product was digested with EagI, Klenow blunted, and digested with SalI. The product was ligated into pTRE3G-IRES-tdTomato that had been digested with BglII followed by Klenow blunting and SalI digestion. Last, PGK-puro was excised via EcoRV and EcoRI digestion from the pSico-PGK-puro vector, a gift from Tyler Jacks (Addgene plasmid# 11586) (242). The excised PGK-puro construct was ligated into ZraI/EcoRI digested pTRE3G-RTA-FLAG-IRES-tdTomato vector, in the opposite orientation of transcription of the Tet3G transactivator initiated by EF1α. The biotinylation tag (Precission-FLAG-V5-TEV-TEV-Biotin acceptor) was a gift from Dr. Meinrad Busslinger (The Research Institute of Molecular Pathology, Vienna, Austria). The Precission-FLAG-V5-TEV-TEV-Biotin acceptor tag contains FLAG and V5 epitope tags that are flanked by precission and two sequential TEV sites, respectively. The biotin acceptor sequence follows the second TEV site. The biotinylation tag was amplified by PCR (primers described in Table 1) followed by digestion with XhoI and ApaI and ligation to XhoI and ApaI sites of pcDNA5-Topo-TA-RTA-FLAG to generate the RTA-Bio construct.

Generation of doxycycline inducible B cell lines. A20-HE2.1 B cells are latently infected with a recombinant MHV68 that encodes a hygromycin resistance and enhanced green fluorescent fusion protein (239). HE2.1 B cells were nucleofected with the pTRE3G-EF1α vector encoding the Tet-On 3G transactivator protein (Clontech). 24 h post-nucleofection cells

were treated with 300 μg/mL G418 and hygromycin B sulfate (Invivogen, San Diego, CA). Serial dilution of the cells into 96-well plates was performed six days later in the presence of G418 and hygromycin B sulfate to isolate individual cells. Clones from individual cells were screened for inducible expression of luciferase 24 h after nucleofection with the pTRE3G-luc vector and doxycycline treatment (50 mg/mL); the cell line clone (C10) had the highest doxycycline inducible activity. Next, the HE2-C10 cells were nucleofected with PGK-puro-pTRE3G-RTA-FLAG-IRES-tdTomato construct and treated with 2 μg/mL puromycin (Invivogen), 300 μg/mL G418 and hygromycin B sulfate for eight days prior to serial dilution to isolate individual cells. After approximately three weeks colonies derived from single cells were validated for RTA induction by immunoblot. Two clones, designated RIT-G3 and RIT-F1, demonstrated robust RTA-Flag and tdTomato-Red expression in response to doxycycline treatment.

Recombinant viruses. The MHV68-H2BYFP genome was cloned into a bacterial artificial chromosome (BAC), kindly provided by Dr. Samuel Speck (243). MHV68-H2BYFP-RTA-Bio virus was generated using *en passant* mutagenesis (244). For generation of MHV68-H2BYFP-RTA-Bio, an intermediate was synthesized which contains RTA-Bio targeting construct with a kanamycin selection cassette and I-SceI site flanked by WT MHV68 sequence on either side (Genewiz, South Plainfield, NJ). The product was excised from the pUC57 vector by EcoRV digestion and transformed into electrocompetent *Escherichia coli* GS1783.5 harboring the MHV68-H2BYFP BAC. After recovery, the cells were plated on chloramphenicol (30 μg/mL) and kanamycin (25 μg/mL) plates, at 30°C for 48 h. The kanamycin selection marker

was PCR amplified to verify insertion into the MHV68-H2BYFP BAC. Using the protocol outlined previously (244), the kanamycin selection marker was removed via induction of the I-SceI homing enzyme, leaving behind the desired insertion. PCR amplification was performed to verify insertion of the Bio tag using 100 ng Qiagen purified BAC DNA and primers described in Table 1. Two independent clones were isolated.

Analysis of Recombinant viral BAC DNA. BAC DNA was prepared by column purification (Qiagen, Hilden, Germany). Restriction analysis was performed using 10 μg of BAC DNA digested overnight with MfeI and then resolved in a 0.8% agarose gel in 0.5X Tris-acetate-EDTA. For complete genome sequencing, 1 μg BAC DNA was prepared for multiplex, 200-cycle, paired-end read sequencing using Nextera XT DNA Library Preparation Kit (Illumina, San Diego, CA) with Miseq reagent kit v2 (Illumina) on an Illumina MiSeq by the Stony Brook Microarray Facility. Whole genome sequence data was aligned to the reference genome sequences using bowtie2 (245) and local alignment mode. Samtools mpileup with default options and vcfutils (246) were used to identify variants at depth coverage over 1000.

Electrophoretic mobility shift assays. Transcription Element Search Software ((http://www.cbil.upenn.edu/tess/) was used to search for candidate NF-κB binding sites in the MHV68 genome based on the consensus binding site (GGGAMTTYCC) allowing for a one nucleotide mismatch in the consensus sequence. Unlabeled double-stranded oligonucleotides with putative NF-κB binding sites are provided in **Table 2**. For nuclear extracts, MHV68+ latent S11 B lymphoma cells or lytic infected MEF cells (MOI 5) were harvested and washed once in

cold PBS. The cell pellet was resuspended in ice cold hypotonic lysis buffer (10.0 mM HEPES pH 7.9, 10.0 mM KCl, 1.5 mM $MgCl_2$, 0.1 mM EDTA, 1.0 mM DTT, 0.5 mM PMSF, one mini EDTA-free proteinase inhibitor cocktail tablet (Roche, Basel, Switzerland), and left on ice 15 min. Next, 10% NP40 was added and cells were vortexed briefly before spinning at 10,000 x g for 5 min at 4°C. The nuclei pellet was washed with hypotonic buffer and resuspended in high salt buffer (25% glycerol, 20mM HEPES pH 7.9, 420 mM NaCL, 1.5 mM $MgCl_2$, 0.2 mM EDTA, 0.5 mM DTT, 0.5 mM PMSF, EDTA-free proteinase inhibitor cocktail tablet) with vigorous shaking for 2-3 h at 4°C before centrifugation at 10,000 x g for 10 min at 4°C.

For analysis of direct binding, either a ^{32}P-labeled or infrared (LiCor) oligonucleotide containing the underlined NF-κB consensus site, 5'-AGTTGAGGGGACTTTCCCAGGC-3', was incubated at room temperature for 30 min with 2.5 μg of nuclear extracts in binding buffer (2.0 mM HEPES pH 7.9, 1.0 mM EDTA, 5.0 mM DTT, 0.05% Triton X-100, 5% glycerol, and 2.0 μg poly dI-dC). For cold competition analysis, unlabeled oligonucleotides containing putative WT or mutant NF-κB binding sites were added at 10- and 100- fold molar excess of labeled probe. Nucleoprotein complexes were run in 5% native polyacrylamide gels at 190V, dried under vacuum, and exposed to phosphor storage plate before and scanned using the Storm 840 PhosphoImager(GE Healthcare,Piscataway,NJ). Competition with 100-fold excess unlabeled oligonucleotides was calculated as a percentage of the signal lost compared to that detected for the ^{32}P-labeled WT oligonucleotide in the absence of competitor. For EMSA supershifts, overnight incubation of nuclear extracts with 0.2 to 2.0 μg of antibodies against NF-κB subunits (all purchased from Santa Cruz, Dallas,Texas): p65 (sc-109x), (sc-114x), cRel (sc-71x), RelB

(C-19x), p52 (K-27x), IgG rabbit (sc-2027) was performed at 4°C prior to incubation with nuclear extracts.

Luciferase reporter assays. To examine the minimal regulatory region of the ORF6 promoter, HEK 293T cells were seeded at 3.0 x 10^5 cells per well into 24-well plates one day prior to calcium phosphate transfection with 1.0 μg of the full length ORF6p luciferase reporter or promoter mutants along with either 0.5 μg RTA (pSG50) or empty vector (EV, pCMVTag2B) and 355 ng pRL-TK (103, 240). At 48 h post-transfection the cells were lysed in 1X passive lysis buffer (Promega, Madison, WI) and luciferase assay performed using pRL-TK to normalize. For NF-κB subunit co-transfection experiments in HEK 293T cells, plasmids expressing NF-κB subunits p50, cRel or p65 or pcDNA3 empty vectors were transfected at 1:1 ratios with pSG50. Protein content was used for normalization.

For ORF6p analysis in HE2 B cells, 2.0 x 10^6 cells were nucleofected, using electroporation solution (Mirus Bio LLC, Madison, WI), with 1.0 μg of either the full length ORF6p luciferase reporter or ORF6p truncation mutants and 0.5 μg RTA-Flag (RTA-FLAG-pcDNA5-Topo-TA) or EV (pcDNA5-Topo-TA) for 24 h. For NF-κB superrepressor experiments, HE2 B cells were nucleofected with 0.5 μg full length ORF6p reporter vector or the double NF-κB site mutant (ORF6p DM), 0.25 μg RTA-Flag (RTA-FLAG-pcDNA5-Topo-TA) or EV (pCDNA5-Topo-TA) and 0.25 μg IκBaM (pCMV-IκBαM) or pCMV empty vectors. To verify impact of NF-κB signaling components, nucleofection was performed using pGL-4.32, 0.25 μg p65 or 0.25 μg IκBαM (pCMV-IκBαM), and luciferase values were normalized to protein content.

To examine ORF6p transactivation in the context of infection, NIH3T12 cells were seeded at 8.0 x 10^5 cells per 10 cm dish one day prior to transfection with 15 μg pGL4.32 or ORF6p-luc by Superfect (Qiagen). The next day 1.0 x 10^5 cells per well were seeded into 12-well plates and then infected the following day with MHV68- IκBαM or MHV68-IκBαM.MR (186) at a multiplicity of infection (MOI) of 5. Luciferase assays were performed 24 hpi.

Antibodies and immunoblot analysis. For immunoblot analysis, A20-HE2-RIT cells were subcultured 1:3 one day prior without drug selection. The following day the cells were seeded at 1.0 x 10^6 cells/mL and treated with 100 μg/mL doxycycline and/or 20 ng/mL 12-O-tetradecanoylphorbol-13-acetate (TPA) (Sigma-Aldrich, St Louis, MO). Cells were lysed in RIPA and whole cell lysates were resolved by SDS-PAGE and transferred to PVDF membrane. For RTA-Bio immunoblot analysis, HEK 293T cells were transfected with empty vector (pcDNA5-TOPO-TA) or RTA-Bio with or without the mCherry-BirA Ligase expression vector using LT1 transfection reagent (Mirus Bio LLC, Madison, WI) 72 h post-transfection cells were lysed in RIPA and immunoblot was performed. Immunoblot was performed using ROSA26HABirA MEFs infected at MOI 5. Blots were probed with primary antibodies against FLAG (Sigma-Aldrich), V5 (AbD Serotec, Raleigh, NC), GAPDH (Sigma-Aldrich) and ORF59 (Gallus Immunotech, Fergus, Canada) (247). Antibody against ORF65 (M9) was a gift from Dr. Ren Sun (University of California, Los Angeles) (248). Secondary antibodies were goat anti-mouse (GE Healthcare), goat anti-rabbit (GE Healthcare), and goat anti-chicken (Gallus Immunotech) and anti-streptavidin (Rockland antibodies, Limerick, PA), all conjugated to

horseradish peroxidase. Chemiluminescent signals (ThermoScientific, Boston, MA) were detected by audioradiography film or a LAS 500 Chemiluminesence Imager (GE Healthcare).

Quantitative PCR. Quantitative PCR was performed on A20-HE2-RIT cells after single or combination treatment with 100 mg/mL of doxycycline and/or 20 μg/mL of LPS. Total DNA from A20-HE2-RIT cells lines was column-purified (Qiagen, Hilden, Germany). 150 ng of DNA was input into a quantitative PCR reaction (SYBR green low ROX mix; Thermo Scientific) and primers for the viral ORF50 (forward, 5'-GGCCGCAGACATTTAATGAC-3'); (reverse, 5'-GCCTCAACTTCTCTGGATATGCC-3') and host GAPDH (forward, 5'-CCTGCACCACCAACTGCTTAG-3'); (reverse, 5'-GTGGATGCAGGGATGATGTTC-3') genes. Copy number of viral genomes is calculated as fold increase in viral DNA copy number normalized to cellular GAPDH genomes over untreated cultures.

Chromatin Immunoprecipitation. Chromatin immunoprecipitation was performed using EZ-Magna ChIP^{TM} G kit (EMD Millipore, Billerica, MA). Briefly, 1.0 x 10^7 A20-HE2-RIT cells were induced with doxycycline as described above or in combination with LPS. Primary splenocytes were resuspended at 6.0 x 10^6 cells/mL in 10 mL DMEM and treated with 100 ng/mL LPS for 18 hrs. After treatment, cross-linking was performed with formaldehyde, terminated with glycine, and the cells were washed twice with 1X PBS containing protease inhibitors. Cell lysis was performed and nuclear extracts were resuspended in 0.5 mL of nuclear lysis buffer. Nuclear lysates were sonicated to ~100 bp to 500 bp fragments using a Branson Sonifier 450 (Danbury, CT). Sonicates were centrifuged at 10,000 X g at 4°C for 10 minutes to remove insoluble material. Lysates were pre-cleared with protein A/G agarose (Life

Technologies, Grand Island, NY) slurry for 30 min at 4°C. Immunoprecipitation was performed overnight with anti-FLAG M2 magnetic beads (Sigma-Aldrich) or streptavidin conjugated beads. Immunocomplexes were washed sequentially using EZ-Magna ChIP^{TM} low salt immune complex buffer, high salt immune complex buffer, LiCl immune complex buffer, and TE buffer. Elution was performed using the provided EZ-Magna ChIP^{TM} elution buffer, followed by proteinase K digestion overnight at 62°C. DNA was recovered by phenol-chloroform extraction and ethanol precipitation.

DNA samples were analyzed for viral genomic regions of interest using primers described in Table 1 in a 384-well qPCR Roche LightCycler ® 480 machine (Roche, Basel, Switzerland). Technical replicates of three biological replicates were analyzed for each condition and normalized by 1% input DNA. Immunoprecipitates recovered by anti-Flag conjugated beads were analyzed by qPCR which was designed to amplify ORF6p, ORF65 RREC and RRED-E (sequences described in **Table 2**)

Viruses and plaque assays. The recombinant MHV68-IκBαM and MHV68-IκBαM.MR viruses (186) were propagated as previously described (45). For plaque assays performed on A20-HE2-RIT cell lines, inductions were performed with indicated drugs for 48 h and cell homogenates were generated by 3 freeze-thaw cycles. For growth curves, 1.0 x 10^5 ROSA BirA MEFs were seeded in 12-well tissue culture plates prior to infection with recombinant MHV68 at a multiplicity of infection (MOI) of 5. Triplicate wells were harvested per time point, and cells with conditioned medium stored at -80°C. NIH3T12 cells were seeded at 2 x 10^5 cells per well in 6-well, and the next day were incubated with cell homogenate for 1 hour prior to overlaying with

1.5% methylcellulose in DMEM containing 5%FBS. Nine days later, methylcellulose was removed and cells were washed twice with 1X PBS prior to methanol fixation and staining with 0.1% crystal violet solution in 10% methanol.

Infections and organ harvests. Eight- to ten-week-old ROSA26HABirA mice were infected by intranasal inoculation or intraperitoneal injection with 1000 PFU of either MHV68-H2B-YFP or MHV68-H2B-YFP-RTA-Bio viruses under isoflurane anesthesia. Inoculum titers were determined to confirm infectious dose. Mice were sacrificed by the application of terminal isoflurane anesthesia. For acute titers, mouse lungs were harvested in 1 mL of DMEM supplemented with 10 % FBS and stored at -80°C prior to disruption in a Mini-Bead Beater using 1.0 mm size beads (Bio-spec, Bartlesville, OK). Viral titers of the homogenates were determined by plaque assay. For latency, reactivation, and ChIP experiments, mouse spleens were homogenized and treated with Tris-buffered ammonium chloride to remove red blood cells, and then filtered through 100 um pore sized nylon. For peritoneal cells, 10 mL of media was injected into the peritoneal cavity, agitated, and withdrawn using an 18-gauge needle. Peritoneal exudate cells were pelleted by centrifugation and resuspended in 1 mL of DMEM supplemented with 10% FBS.

Limiting dilution PCR detection of MHV68 genome positive cells. For determining the frequency of cells harboring the viral genome, single cell suspensions were prepared and used in single-copy sensitive nested PCR. Six 3-fold serial dilutions of cells were plated into 96-well PCR plates in a background of 3T12 cells and lysed overnight with proteinase K at 56°C. The plate was subject to an 80-cycle nested PCR with primers specific for MHV68 ORF50 (45).

At each serial dilution, twelve replicates were analyzed and plasmid DNA at 0.1, 1, and 10 copies included to verify single-copy sensitivity of the assay.

Limiting dilution *ex vivo* reactivation assay. In order to determine the frequency of cells that harbor latent virus capable of reactivation, single-cell suspensions were prepared from mice 16 or 18 days post-infection, resuspended in DMEM supplemented with 10% FBS and plated in 12 serial 2-fold dilutions onto a monolayer of C57BL/6 MEFs in 96-well tissue culture plates (41, 45). Twenty-four replicates were plated per serial dilution and wells were scored for cytopathic effect 2-3 weeks after plating. Parallel samples were mechanically disrupted using a mini-bead beater with 0.5 mm beads prior to plating on a monolayer of MEFs to release preformed virus to differentiate between preformed infectious virus and virus spontaneously reactivating upon explant.

Motif analysis. A fixed-size 22-bp Position Weight Matrix (PWM) was generated from known RRE-A and RRE-B RTA binding (174) using Glam2 (249). RTA consensus recognition elements in the MHV68 genomes were located with Find Individual Motif Occurrences (FIMO) utility with the p-value cutoff set at 1×10^{-6} (250). The background DNA zeroth-order Markov probabilities were generated automatically by FIMO from a non-redundant database (251).

Statistical analyses. Data were analyzed using Prism 5 software (GraphPad, La Jolla, CA). Statistical significance was determined using one-way ANOVA, followed by Tukey's post-test or Student's t-test. Under Poisson distribution analysis, the frequency of latency establishment and reactivation from latency was the intersection of nonlinear regression curves with the line at 63.2, the significance was determined by paired t-test.

Table 1.1. Oligonucleotides used for cloning

Gene target[a]	Genomic strand[b]	Primer Sequence[c]
ORF6p distal site mutant	F	5′-TGGAGTGGCCAATCTCCATATGT-3′
ORF6p distal site mutant	R	5′-CATATGGGAGATTGGCCACTCCA-3′
ORF6p proximal site mutant	F	5′-TTTTGCCTCGAAATTCCCTGTGG-3′
ORF6p proximal site mutant	R	5′-CCACAGGGAATTTCGAGGCAAAA-3′
ORF6p -765bp truncation mutant	F	5′-GATCGAGCTCGTGAGGGACCCGGGTGGACA-3′
ORF6p -526bp truncation mutant	F	5′-GATCGAGCTCGATGGGCACTCCTATGTGAC-3′
ORF6p -331bp truncation mutant	F	5′-GATCGAGCTCACGGCGTCCCCAGTCACTCA-3′
ORF6p reverse truncation mutant	R	5′-GATCCTCGAGCATGATGAGTGTCCAAAAGCAGAGAGG -3′
ORF6p -58bp	F	5′-CAAAATCCCAATTCTCCTCA-3′

A		
ORF6p -58bp B	F	5′-TGCTAGTCGCGTCCTCTCTG-3′
ORF6p -58bp C	F	5′-CTTTTGGACACTCATCATGC-3′
ORF6p -58bp D-	R	5′-ATTGGGATTTTGAGCT-3′
ORF6p -58bp E-	R	5′-CGACTAGCATGAGGAGA-3′
ORF6p -58bp F-	R	5′-CCAAAAGCAGAGAGGACG-3′
ORF6p -58bp G-	R	5′-TCGAGCATGATGAGTGT-3′
tdTomato	F	5′-GATCGATATCATGGTGAGCAAGGGCGAGGAG-3′
tdTomato	R	5′- GATCGGATCCGGCACAGTCGAGGCTG-3′
Flag-tagged RTA	F	5′-GATCGTCGACATGGCCTCTGACTCGGATTCC-′3
Flag-tagged RTA	R	5′-GATCCGGCCGCAGTAGCAGCAGGA-3′
Bio-tag[d]	F	5′- GAATTCGGCCGGCCATGCATTTACAATTGGGCGGTGGAGGTCTG GAAGTTCTGTTCC AGGGACCTGACTACAAGGACGATGACGATAAAGGGAAGCCAATC CCTAATCCCCTTCTGG GACTCGACTCTACCGAAAACTTGTACTTCCAGGGACCACGGGAA AATCTGTACTTTCAGG GAATGGCATCGAGTCTACGGCAAATCCTCGACTCGCAGAAGATG GAGTGGCGCTCAAACG CCGGAGGCTCGTGACCATGGCGCGCCGAATTC-3′.
RTA-Bio	F	5′-GATCCTCGAGGTTAACGGAATTCGGCC-3′

RTA-Bio	R	5′-GATCGGGCCCGCCATGGTCACGAGCCT-3′
RTA-Bio BAC PCR	F	5′-CCATTTTCACCCATTAGCCCT—3′
RTA-Bio BAC PCR	R	5′-ACTTAAGGATTTAGAAATGTCTTGT-3′
ChIP-ORF6 (0-150)	F	5′-AGACTCTGAAGTGCTGACTCGGC-3′
ChIP-ORF6 (0-150)	R	5′-GATGAGTGTCCAAAAGCAGAGAGGA-3′
ChIP-ORF65	F	5′-CGTCAGACATAGACCCTGGAT-3′
ChIP-ORF65	R	5′-TGGCCCTCTACCTTCTGTTGA-3′
ChIP-RREC	F	5′-GCCTGGGGAGCCAAAGCGAG-3′
ChIP-RREC	R	5′-GCAATAGGCCAGGTGGGCCG-3′
ChIP-RRED-E	F	5′-CGGACCAATCACCAACTTGACG-3′
ChIP-RRED-E	R	5′-TCGGTTTGCGGTTAGACCAGGC-3′

[a] Genomic target of PCR primer for cloning or qPCR

[b] F=Forward primer, R=Reverse primer

[c] Primer sequence used for PCR amplification

[d] Sequence of Bio tag inserted at the C-terminus of RTA, Flag (underlined), V5 (bold), Biotin acceptor sequence (bold and underlined)

Results

Identification of NF-κB binding sites in MHV68 genome. To identify potential binding sites for NF-κB subunits in the MHV68 genome, we performed an *in silico* analysis. Fifty-seven candidate binding sites with strong scores to a weighted consensus matrix for NF-κB were identified (**Fig. 2.1**). Nuclear extracts from S11 MHV68+ latent B cell lines were incubated with ^{32}P-labeled oligonucleotides containing the consensus NF-κB recognition site. Competitive electrophoretic mobility shift assay (EMSA) was performed with 10- and 100-fold molar excess of unlabeled 22 to 30 mer oligonucleotides from the MHV68 genome that contained the candidate NF-κB binding sites (**Table 2**). At 100-fold molar excess, 14 out of 57 candidate sites competed for binding such that the shifted complex with the labeled WT NF-κB consensus oligonucleotide was reduced by at least 50% (red lollipops in **Fig. 2.1**). Seven of the eight sites tested also competed for NF-κB binding against the labeled NF-κB consensus site oligonucleotide using nuclear extracts from murine embryonic fibroblasts (MEFs) undergoing lytic infection (**Fig. 2.1B**). Based on previous boundaries of MHV68 ORFs defined by 5' RACE and tiled microarray analysis (173, 240, 252), eight of the fourteen sites were located within an approximately ~1.2 kb region upstream of the transcription start sites of six MHV68 genes: M1 (latency), M2 (latency), ORF6 (lytic single-stranded DNA binding protein), ORF21 (lytic

thymidine kinase), ORF75B (lytic vFGAM tegument) and ORF75C (lytic vFGAM tegument) (**Fig. 2.2A**). A weighted consensus matrix was derived from the degree of binding for the oligonucleotides that competed for binding to the WT oligonucleotide and found to closely match the canonical NF-κB recognition site (**Fig. 2.2B**).

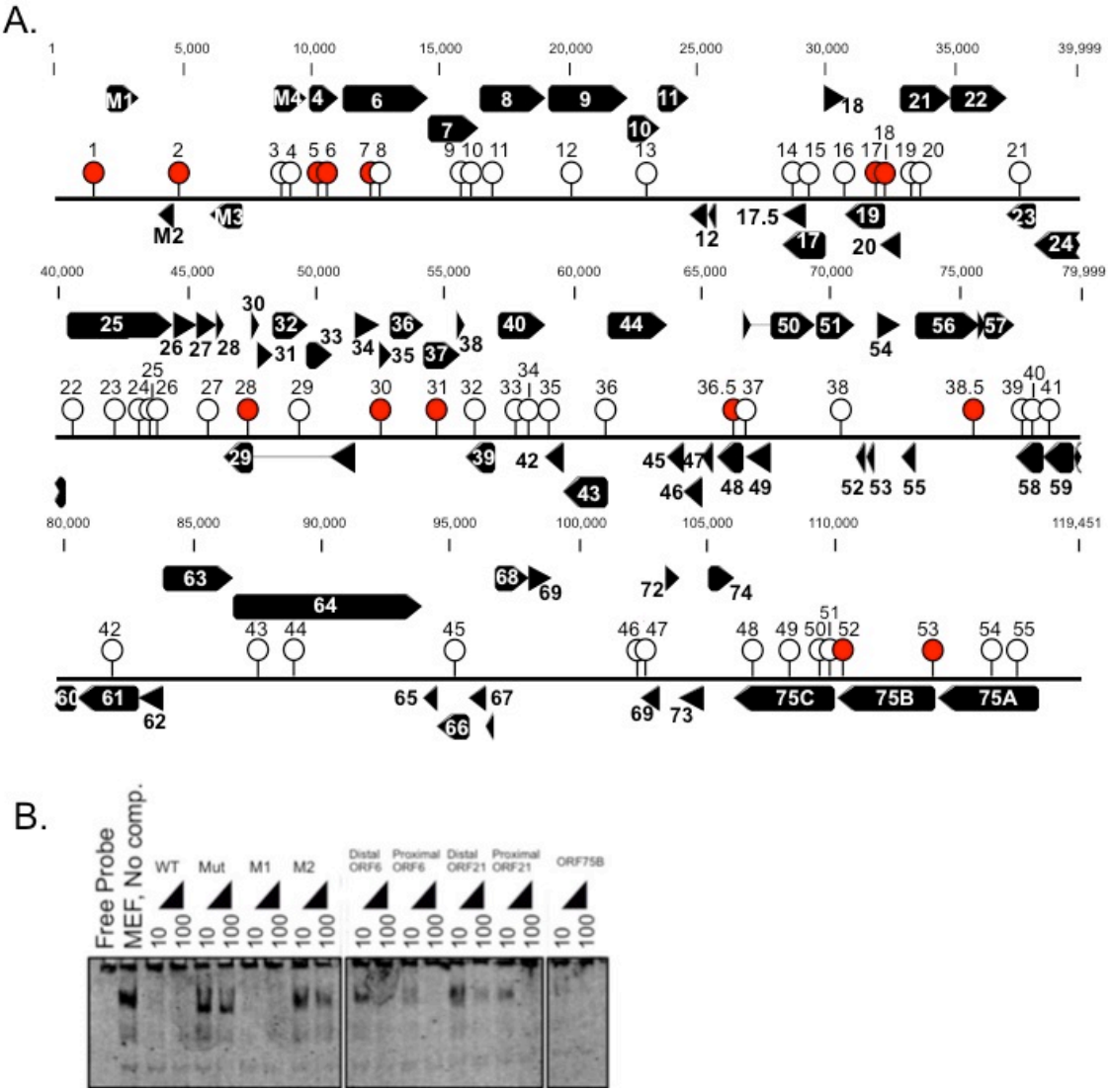

Figure 2.1. Identification of NF-κB recognition sites in MHV68.
(A) Diagram of murine gammaherpesvirus 68 genome illustrating location of 57 putative NF-κB sites (lollipops) identified by *In silico* analysis using Transcription Element Search Software (TESS). Oligonucleotides from the genomic sequences that encompass the putative binding sites were used at 100-fold molar excess as competition against ^{32}P-labeled NF-κB consensus oligonucleotide upon incubation with latent MHV68+ S11 nuclear extracts. Red lollipops indicate putative NF-κB binding sites which competed at greater than 50% of WT ^{32}P-labeled NF-κB consensus oligonucleotide. (B) Lytic infected MEF nuclear extracts were incubated with the infrared-labeled NF-κB consensus WT oligonucleotide for competitive EMSA with 10- and 100-fold molar excess of unlabeled oligonucleotide as indicated.

Table 2.2. Oligonucleotides used in electrophoretic mobility shift assays

Oligonucleotide number	MHV68 Sequence	Percent competition
Wild type oligo	AGTTGAGGGGACTTTCCCAGGC	100.0
Mutant oligo	AGTTGAGGCGACTTTCCCAGGC	35.0
1	ATGTCTGGGAATTCCCCAATGAC	100.0
2	AGCACAGGACTTTCCCTGCTCAC	77.1
3	GTGTCCATGAAATTTAGATCCAG	16.7
4	CTACCATAAATCTCATCAACCAG	17.7
5	TGGAGTGGGGAATCTCCCATATGT	92.7
6	TTTTGCCTGGAAATTCCCTGTGGC	91.6
7	GTGGAGGGGACCTCCCAGCCGTG	66.3
8	GAGGGACAGATTTCCTCAGGTGC	18.9
9	GCAAGGGAAAAGTCCCAATTTAT	24.2
10	ATCTGGGAAAAATCCCTGTCCAT	41.4
11	CTAACAGGGAATATCCAAAGATA	33.3
12	ATTATTCAAATTTCCTGTGTCAC	0.0
13	GCCCCACAAATTTCATATTTCCA	0.0
14	CTGGAAATGAGACTTGGTCCTCC	0.0
15	GATTGCAGAAATTTCCCCTGGTT	0.0
16	CTTTCCAGGAGATTCCCACTGCC	0.0
17	GGAAGGGGGAAGGCCCTTTTCTT	70.2

18	GCAGGGGGGAGTCCCCTAGTTAA	66.0
19	GGATGTCAGGTCTCCCAGGCCAC	0.0
20	TGAGCACAGATTTCCCGGCAGGC	0.0
21	TTTTGGGGGAAATGTACTGTTGG	0.0
22	CCTTGTTATGAAATCTGCCCACA	4.9
23	TACCCAGGGAAATCTATCTGATC	0.0
24	GTGGCACAAGTCTCCCATGCTCA	0.0
25	AGACATGGGAATCCACTGTCAGG	4.4
26	GTTGCTGGAATTACTACAGACAT	0.0
27	GATGGAGGGAAGTACCATGTGTG	0.0
28	TCACGAGGGACTTTCTCCCACAT	62.9
29	CTTCTTTATGAAATTTGCTTCAT	19.6
30	AGATTTGGAAAATCCCACAGTCT	54.6
31	ATGGAATTTTTGGAGTTTCCCTGG	76.3
32	GCCAGTAGGGACATTTGAATGTT	34.0
33	TGTTATCAGGTCTCCTCTAGCAG	6.4
34	ACGTAGGGGATATTACAGTCTCA	18.1
35	TTGACTGTGAAATTTGGGTGATA	14.9
36	TTACAACAAATATCCCTGATATG	21.9
36.5	ATAACAAAATTCCCTGGAATCAT	42.7
37	CTACGAGGGAATTTCTGCAGCGA	0.0
38	CTCCACCAAATATCCCAGCTGAC	47.9
38.5	ACGTGACGTCATAACTGCAACACTTATGAG	0.0

39	TCATCAGGGAAATTTCAGGGCTG	63.5
40	CAATGTACATCTCATATGGGCAG	0.0
41	ACAGGCGTGAAACTTGACTCTTG	0.0
42	GTATGCCAAATCTCCATATAGGC	0.0
43	AGGTCTGGGACGTCCCTCCCAAG	18.7
44	CCATGCCAGATCTCACAACCATC	1.6
45	AATTATGGGAAACTTGCATGAGA	1.5
46	CCATACGCAAATCTCGCACAGAA	0.0
47	TAACAGATGAGATCTGTACTCAG	11.5
48	GATCCACACATTTCACAGGCCTC	0.0
49	CTTGACTGGAAATCCCCCATCAA	12.3
50	CAGATTCAGGTCTCATAATGCTC	0.0
51	TCCACGGGGGCTCTCCCAGCCTC	71.0
52	ATCTAGGGGTAGTCCCAGGTTGC	87.3
53	GATTTTGGAAAGTCCCACCTAA	94.9
54	TTGCCAAGGAAATCTGACATGGT	0.0
55	GAAACAGGGGATATCCGGTGCCA	58.8

A.

Oligo		Sequence			Putative promoter
1	5′-	ATGTCT	GGGAATTCCC	CAATGAC -3′	M1
2	5′-	AGCACA	GGACTTTCCC	TGCTCAC -3′	M2
5	5′-	TGGAGTG	GGGAATCTCC	ATATGT -3′	ORF6 distal
6	5′-	TTTTGCCT	GGAAATTCCC	TGTGGC -3′	ORF6 proxmial
17	5′-	GGAAGG	GGGAAGGCCC	TTTTCTT -3′	ORF21 distal
18	5′-	GCAGGG	GGGAGTCCCC	TAGTTAA -3′	ORF21 proximal
52	5′-	ATCTAG	GGGTAGTCCC	AGGTTGC -3′	ORF75C
53	5′-	GATTTT	GGAAAGTCCC	ACCTAA -3′	ORF75B

B.

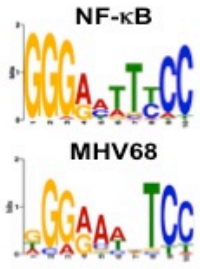

Figure 2.2. Alignment of NF-κB recognition sites in MHV68.
(A) Sequence alignment of putative NF-κB binding sites in the MHV68 genome identified by competitive EMSA (filled lollipops in A) Binding sites were located in the proximal promoter region of the indicated MHV68 encoded genes. (B) NF-κB binding site motif for NF-κB subunits p65 and p50, based on a weighted consensus matrix. NF-κB binding motif for MHV68 genome. Binding sites presented as a position weight matrix determined from MEME analysis (Multiple EM for Motif Elicitation v4.8.0[10]).

The ORF6 regulatory region contains two NF-κB binding sites. We previously mapped the 5' transcriptional start site of the ORF6 gene and demonstrated that a luciferase reporter under the control of a 1.3 kb region upstream of the start (ORF6p) is responsive to both MHV68 infection and co-transfection with the viral replication and transcription activator (RTA) (240). To examine whether the putative NF-κB recognition sites located in the distal and proximal ORF6 regulatory region were bound by NF-κB subunits, we mutated key nucleotides in the consensus site and tested for loss of binding (**Fig. 2.3A**). Competitive EMSA using nuclear extracts from latent S11 B cells demonstrated competition by the WT oligonucleotides but not by oligonucleotides with mutations in either the distal or proximal NF-κB sites in the ORF6 promoter (**Fig. 2.3B**). Next, to identify the NF-κB subunits that are recognized by the distal and proximal sites, WT oligonucleotides corresponding to each site were labeled and incubated with nuclear lysates and antibodies to each NF-κB subunit, alone or in combination. Lytic infected MEF nuclear extracts incubated with antibody against NF-κB p65 resulted in either a loss of shift or supershift for the distal and proximal site oligonucleotides (**Fig. 2.4A**). Addition of antibody against p50 resulted in a supershift of the distal site oligonucleotide. Using latent B cell nuclear extracts, we observed two major shifted complexes (**Fig. 2.4B**). Addition of antibody

against NF-κB p50 resulted in the loss of the upper complex and an additional shift in the mobility of the lower complex for both distal and proximal site oligonucleotides. Antibody against cRel ablated the upper complexes for both sites. Taken together, p65 and p50 subunits comprise the complex bound to the distal and proximal NF-κB binding sites in lytic infection while p50 and cRel recognize the distal and proximal sites of the ORF6 promoter in a latent infection.

A.

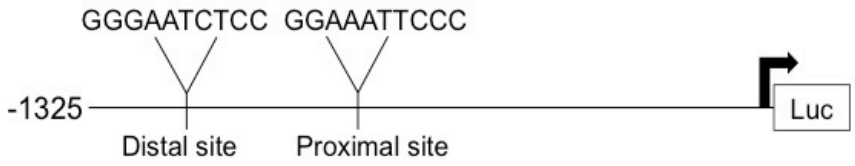

B.

NF-κB consensus WT	5′-AGTTGAG GGGACTTTCC CAGGC-3′
NF-κB consensus mut	5′-AGTTGAG GcGACTTTCC CAGGC-3′
ORF6p distal WT	5′-TGGAGTG GGGAATCTCC ATATGT-3′
ORF6p distal mut	5′-TGGAGTG GccAATCTCC ATATGT-3′
ORF6p proximal WT	5′-TTTTGCCT GGAAATTCCC TGTGGC-3′
ORF6p proximal mut	5′-TTTTGCCT cGAAATTCCC TGTGGC-3′

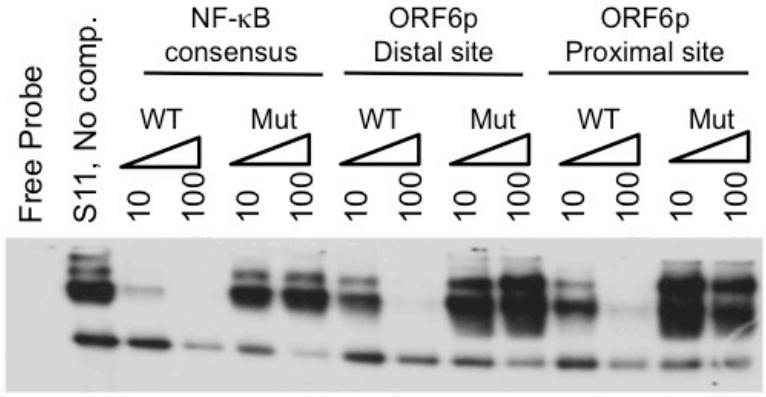

Figure 2.3. The ORF6 regulatory region contains two NF-κB recognition sites.
(A) Schematic of ORF6 regulatory region with position and sequence of distal and proximal NF-κB binding sites. Arrow denotes ORF6 transcriptional start site (240). (B) MHV68+ S11 nuclear extracts were incubated with the ^{32} P-labeled NF-κB consensus WT oligonucleotide for competitive EMSA with 10- and 100-fold molar excess of unlabeled oligonucleotide with a mutant NF-κB site or ORF6p distal and proximal site oligonucleotides as indicated.

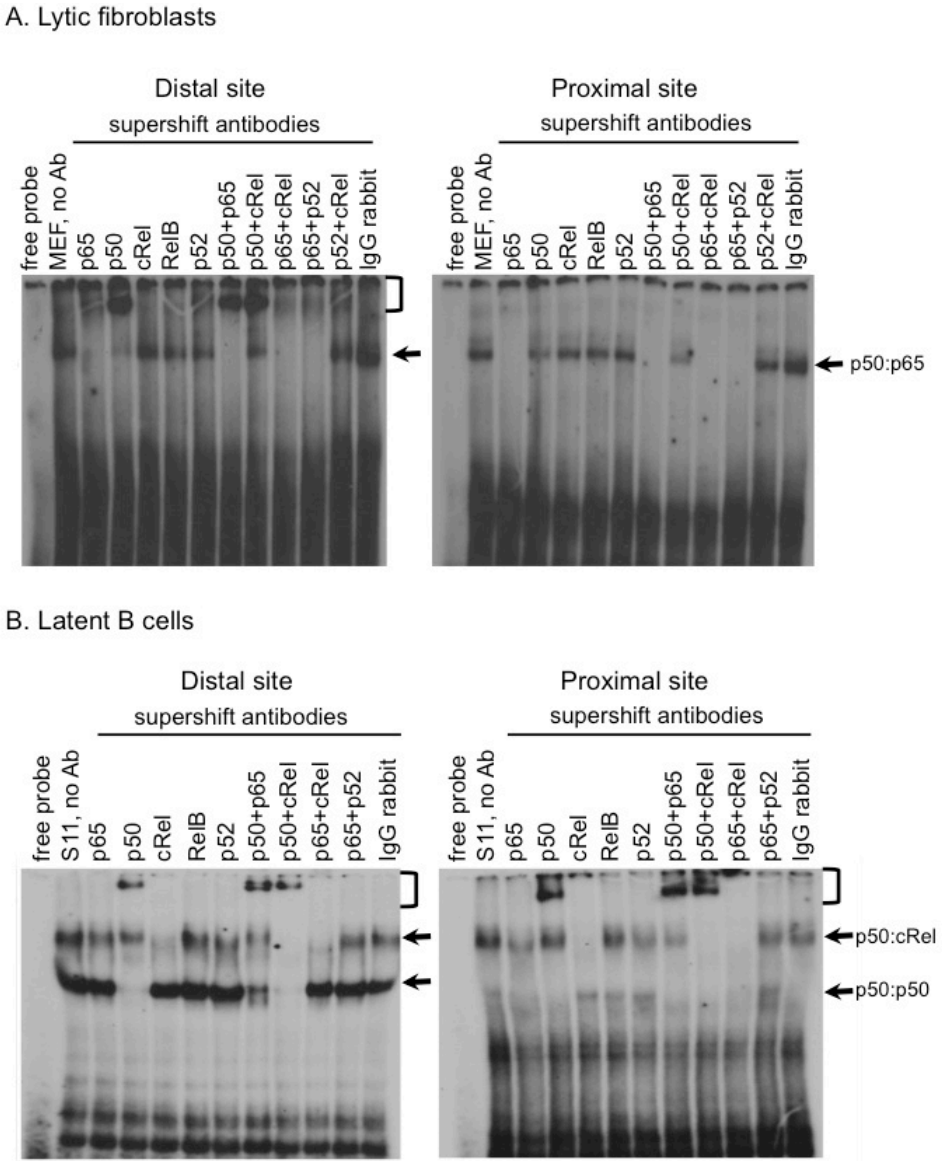

Figure 2.4. NF-κB subunits that bind to the ORF6 regulatory region vary with the type of infected cell.

(A) EMSA supershift analysis was performed using ^{32}P-labeled ORF6p distal and proximal NF-κB site oligonucleotides, nuclear extracts from MHV68+ infected mouse embryonic fibroblasts and the indicated antibodies. (B) EMSA supershift analysis was performed using ^{32}P-labeled ORF6p distal and proximal NF-κB site oligonucleotides, nuclear extracts from latent MHV68+ S11 B cells and the indicated antibodies. Arrows indicate shifts and brackets denote supershifts.

NF-κB subunits inhibit ORF6 transactivation by RTA independent of their DNA binding sites in the viral genome. NF-κB subunits have been found to antagonize MHV68 (182). To test if the NF-κB recognition sites regulate the RTA responsive region, we generated 5' truncation mutants of the ORF6p (**Fig. 2.5**). HEK293T cells were co-transfected with ORF6p truncation mutants in the absence or presence of the viral lytic transactivator RTA and luciferase levels were measured after 48 h. Truncation from -765 bp to -526 bp significantly enhanced RTA transactivation, suggesting the presence of an inhibitory element in this region. Truncation from -526 bp to -331 bp resulted in a significant loss in RTA transactivation suggesting the presence of an RTA responsive element. Lastly, truncation from -136 bp to -58 bp resulted in complete loss of RTA transactivation indicating that -136 bp constitutes the minimal RTA responsive region of the ORF6 promoter.

Next, we investigated if the proximal NF-κB binding site located in the -765 bp region that was lost with truncation to -526 bp, was inhibitory to RTA transactivation. Site-directed mutagenesis of the distal NF-κB site (distal mut), the proximal NF-κB site (proximal mut), or both NF-κB sites (double mut) in the ORF6p was performed based on mutations confirmed for loss of recognition of NF-κB subunits in competitive EMSA assays (**Fig. 2.3**). HEK293T cells

were transfected with proximal, distal, or double NF-κB site mutants and an RTA expression vector or empty vector (**Fig. 2.6A**). No significant loss of RTA transactivation was observed upon the individual or combined mutation of these NF-κB recognition sites.

We hypothesized that co-expression of NF-κB subunits might be necessary to reveal a role for the NF-κB recognition sites in response to RTA. To this end, we examined the activity of the WT ORF6p reporter or NF-κB site mutant reporters in the presence of RTA and the NF-κB subunits that were identified in nuclear extracts from MHV68+ latent B cells (**Fig. 2.4A**) and infected MEFs (**Fig. 2.4B**) were next examined. Expression of NF-κB subunits p50, cRel, or p65 alone did not affect basal activity of the ORF6 wild type or NF-κB site mutant reporter constructs in HEK293T cells, while the NF-κB responsive luciferase reporter pGL4.32 was activated in response to NF-κB subunit expression (data not shown). However, co-transfection of either NF-κB p50 and cRel or p50 and p65 subunits inhibited RTA transactivation of the ORF6 NF-κB site mutant reporters (**Fig. 2.6B**). This inhibitory effect occurred regardless of the integrity of the NF-κB binding sites, indicating that the NF-κB subunits were not impairing RTA transactivation by occupancy of their recognition sites in the ORF6 regulatory region.

We sought to determine if the ORF6 NF-κB sites influence ORF6p activation in the context of productive infection. MHV68-IκBαM is a recombinant virus that expresses a mutant form of IκBα which functions as a super-repressor of canonical NF-κB activation (186). NIH3T12 cells were first transfected with the NF-κB responsive luciferase reporter, pGL4.32, or the ORF6p reporter and then infected at a multiplicity of infection (MOI) 5 with the control MHV68 or MHV68-IκBαM (**Fig. 2.6C**). Infection with the control MHV68 vector activated the NF-κB reporter at 24 hpi, but MHV68-IκBαM infection did not activate the positive control NF-κB luciferase reporter, demonstrating that IκBαM can block canonical NF-κB activation occurring late during infection. In contrast, the ORF6p reporter did not show a change in promoter activity after infection with WT MHV68 or MHV68-IκBαM, which suggests that ORF6p reporter transactivation by RTA is not influenced by NF-κB subunit binding during lytic infection.

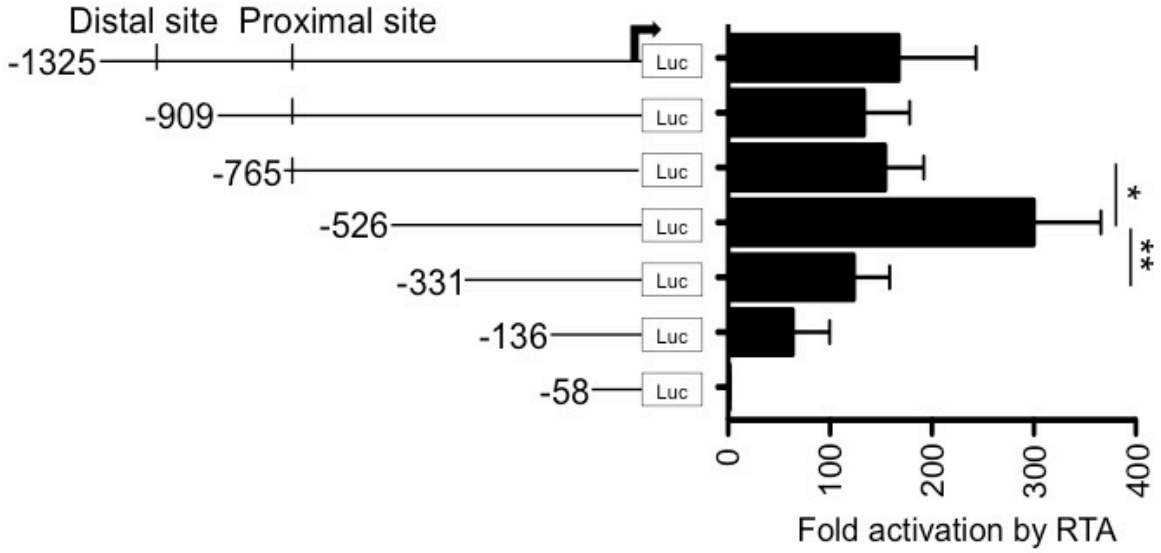

Figure 2.5. Response of ORF6 promoter 5' truncation mutants to RTA in HEK293T cells. Transcriptional activation by RTA was analyzed in HEK293T cells for the ORF6 promoter (ORF6p) at 48 h. ORF6p truncation mutants were transfected with the RTA expression vector or empty vector. Data is normalized by renilla luciferase and shown as fold activation by RTA over reporter alone. Bars represent fold activation relative to the untreated condition for triplicate samples +/- SD. Significance is determined by one-way ANOVA followed by Tukey post-test; *,$p<0.05$; **, $p<0.01$.

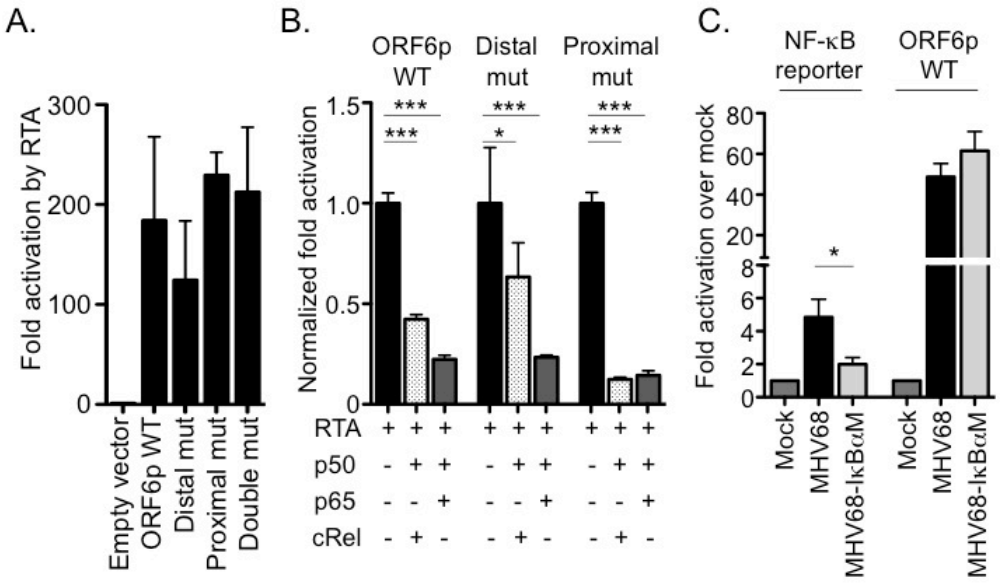

Figure 2.6. NF-κB subunits inhibit ORF6 promoter activity independent of NF-κB binding sites.

(A) Transcriptional activation by RTA of the full-length WT ORF6 promoter (ORF6p) or NF-κB site mutations in HEK293T cells. ORF6p NF-κB site mutants were transfected with the RTA expression vector or empty vector. Data is normalized by renilla luciferase and shown as fold activation by RTA over empty luciferase reporter. Bars represent fold activation relative to the untreated condition for triplicate samples +/- SD. (B) Co-transfection of HEK293T cells with either the ORF6p or NF-κB site mutant reporter constructs RTA and NF-κB subunits luciferase values were normalized to protein content and shown relative to RTA transactivation alone. Bars represent fold activation relative to the untreated condition for triplicate samples +/- SD. Significance is determined by one-way ANOVA followed by Tukey post-test; *,$p<0.05$; ***,$p<0.001$. (C) NIH3T12 cells were transfected with NF-κB or ORF6p reporters followed by infection with control MHV68 (MOI 5.0) WT or MHV68-IκBαM, that expresses the NF-κB superrepressor IκBαM. Luciferase assays were performed 24 h post-infection. Bars represent fold activation relative to the untreated condition for triplicate samples +/- SD. Data is shown as fold activation over uninfected cells and significance determined by Student's t-test, *p=0.013.

NF-κB inhibition does not alter ORF6 promoter activity in latent B cells or in the context of lytic replication. The HE2 B cell line is tightly latent with less that 1% of cells undergoing spontaneous reactivation (239). To map the minimal RTA responsive region of ORF6p upon *de novo* RTA expression, HE2 latent B cells were nucleofected with 5' truncation mutants of the ORF6p reporter in the presence or absence of the RTA expression vector (**Fig. 2.7**). Truncation from -909 bp to -765 bp led to enhanced transactivation by RTA. Truncation from -526 bp to -331 bp and -136 bp to -58 bp led to a loss in RTA transactivation. A minimal RTA responsive element positioned 136bp upstream of ORF6 in HE2 latent B cell (**Fig. 2.7**) is consistent with that demonstrated for HEK293T cells (**Fig. 2.5**). Next, nucleofection was performed with the full-length ORF6p or double NF-κB site mutant reporter constructs in the presence or absence of RTA alone or in combination with canonical NF-κB subunit super repressor IκBαM. In comparison to the NF-κB double site mutants, the basal activity of the wild type ORF6p promoter was enhanced by expression of IκBαM alone compared to the double site mutant (**Fig. 2.8**). In addition, the ORF6p double mutant had a decreased response to RTA when compared to the wild type reporter construct. NF-κB inhibition by IκBαM was confirmed by a

significant decrease in p65-mediated activation of the NF-κB reporter pGL4.32 (data not shown). These data indicate that NF-κB inhibition has a no effect on its RTA transactivation.

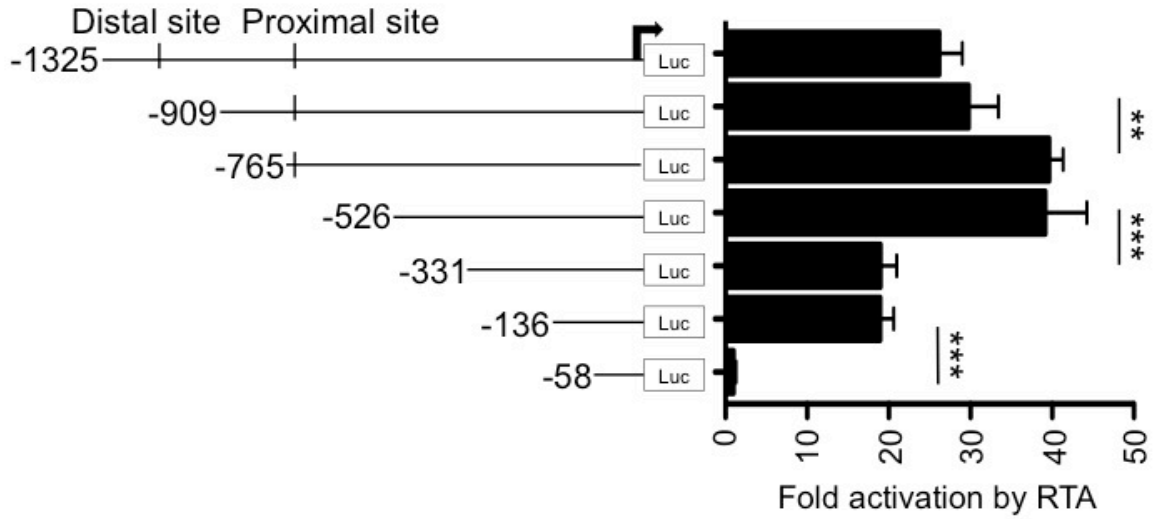

Figure 2.7. Response of ORF6 promoter 5' truncation mutants to RTA in latent B cells. (A) Schematic diagram of 5' deletions of the ORF6 promoter (ORF6p) firefly luciferase reporter. Transcriptional activation by RTA was analyzed in latent MHV68+ HE2 B cells. Data is normalized by protein content and shown as fold activation by RTA over reporter alone. Bars represent fold activation relative to the untreated condition for quadruplicate samples +/- SD. Significance is determined by one-way ANOVA followed by Tukey post-test; **, $p<0.01$; ***,$p<0.001$.

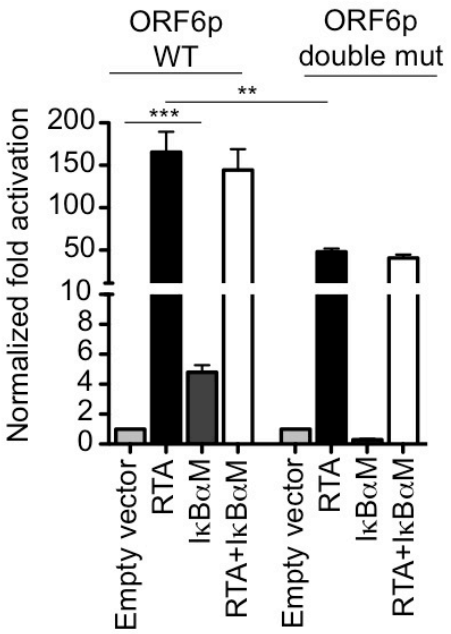

Figure 2.8. NF-κB inhibition does not affect ORF6 promoter activity in latent B cell lines. Latent MHV68+ HE2 B cell lines were nucelofected with RTA, NF-κB superrepressor IκBαM, or empty vectors and in the full-length WT or double mutant ORF6p reporter constructs and analyzed at 24h. Luciferase values normalized by protein content. Bars represent fold-activation relative to the untreated condition for quadruplicate samples +/- SD. Significance is determined by one-way ANOVA followed by Tukey post-test; **, $p<0.01$; ***,$p<0.001$.

Generation and characterization of RTA inducible A20-HE2 latent B cell lines.

Because previous studies suggested a role for TLR signaling and NF-κB kinase activity in enhancing viral reactivation (159, 217, 237), we next sought to characterize the contribution of upstream kinases affecting RTA transactivation of viral genes. In order to do this, we developed an assay in which we can induce RTA expression and stimulate TLR signaling. HE2 latent B cell lines were selected for the stable expression of an EF1α driven Tet-transactivator protein TET3G (**Fig. 2.9A**). In the presence of doxycycline, a conformational change in the Tet-transactivator permits binding to a consensus binding site in the P_{TRE3G} that activates transcription of downstream genes. HE2-TET3G cells (clone C10) were transfected with and selected for the integration of a Tet-responsive bicistronic construct encoding C-terminal Flag-tagged RTA followed by an IRES and the tomatoRed (tdTomato) reporter gene (termed HE-RITs) (**Fig. 2.9A**).

Addition of doxycycline to culture media induced expression of RTA-Flag as early as 12 h post-treatment in two individual clones, HE-RIT G3 and HE-RIT F1 (**Fig. 2.9B**). RTA-Flag levels remained relatively steady through two days post-treatment. tdTomato expression was confirmed by FACs analysis and was induced by doxycycline alone (**Fig. 2.9C**). Immunoblot for MHV68 lytic antigens confirmed the expression of the ORF65 capsid protein in HE-RIT clones

at 48 h post-doxycycline treatment, and ORF65 levels further increased when doxycycline treatment of the HE-RIT cells was coupled to treatment with the histone deacetylase inhibitor TPA (**Fig. 2.9D**). In addition, ORF59 expression was detected in lytic infected fibroblasts and in HE-RITs upon treatment with doxycycline and TPA, but not with doxycycline alone. Viral DNA replication was enhanced in both HE-RIT clones 48h post-treatment with doxycycline and TPA alone, and further increased with both doxycycline and TPA (**Fig. 2.9E**). A similar trend was observed for viral particle release measured by plaque assay (**Fig 2.9F**). Single treatment with doxycycline or TPA induced the production of infectious virus that was significantly enhanced when combined. In sum, HE-RIT cell lines are inducible for the expression of RTA-Flag that drives virus reactivation.

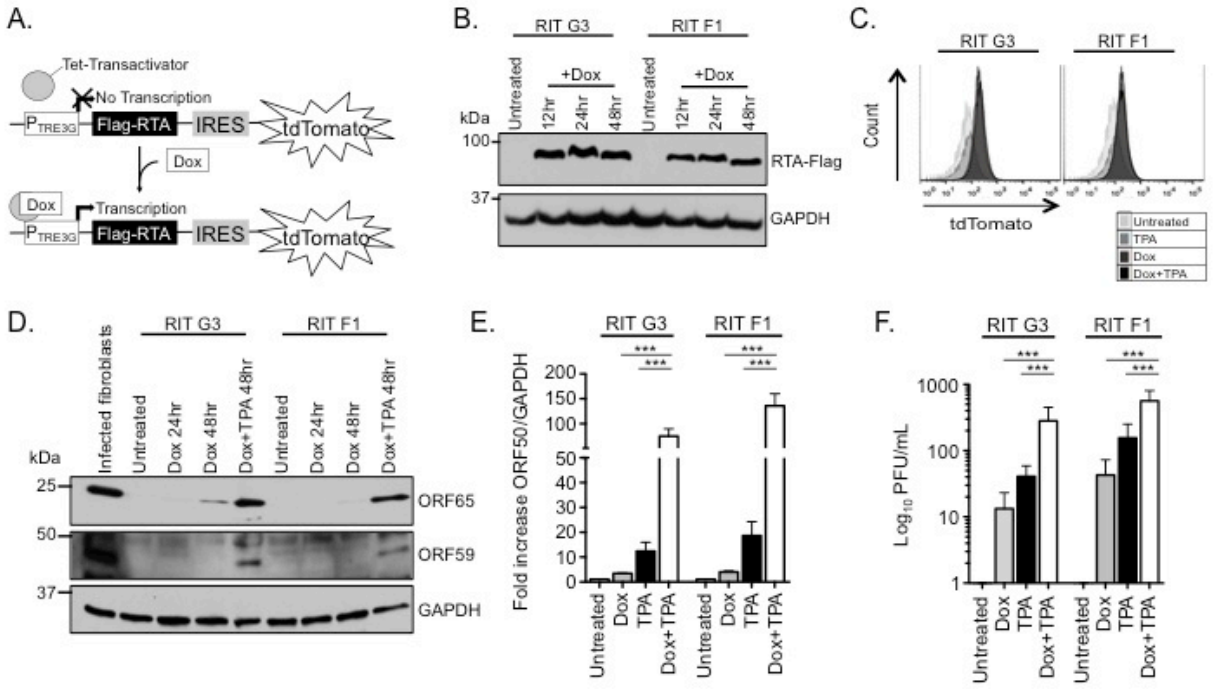

Figure 2.9. Characterization of a MHV68+ latent B cell line inducible for reactivation. (A) Schematic of reactivation inducible HE2 latent B cells lines (HE-RIT) whereby doxycycline (Dox) treatment induces expression of Flag-tagged RTA and tdTomato fluorescent protein. (B) Western blot of Flag-tagged RTA expression from two individual HE-RIT clones (G3 and F1) at indicated hours post-dox treatment. (C) Flow cytometry analysis of tdTomato fluorescence upon Dox or TPA treatment, alone or in combination for 24 h. (D) Immunoblot detection of lytic antigen expression after doxycycline induction of HE-RIT cell lines at the indicated times. (E) Quantitative PCR detection of viral DNA replication from HE-RIT cell lines 48 h after induction. The fold-increase in viral genome copy number was determined by viral ORF50 normalized to GAPDH over mock treated condition shown for triplicate samples. Bars represent fold-activation relative to the untreated condition for triplicate samples +/- SD. Significance determined by one way ANOVA, post-hoc Tukey test, ***$p<0.001$. (F) Plaque assay was performed 48 hours post-treatment with Dox and TPA alone or in combination. Bars represent fold-activation relative to the untreated condition for triplicate samples +/- SD. Significance determined by one way ANOVA, post-hoc Tukey's test, ***$p<0.001$.

Lipopolysaccharide treatment enhances viral gene transcription and RTA occupancy at the origin of lytic replication. We next investigated the role of upstream NF-κB activation in MHV68 reactivation from latency via TLR simulation. Lipopolysaccharide (LPS) is a bacterial pathogen associated molecular pattern recognized by TLR4. TLR4 activates the canonical NF-κB signaling cascade via the IKK-β/IKK2 kinase. RIT cells were nucleofected with the wild type ORF6p or the ORF6p double NF-κB site mutant reporter and treated with doxycycline and LPS, alone or in combination (**Fig. 2.10**). LPS treatment did not activate the wild type ORF6p reporter, indicating that exposure to LPS alone is not sufficient to regulate ORF6 expression. Doxycycline treatment enhanced the ORF6p and ORF6p double mutant activity to statistically significant levels. Interestingly, coupling doxycycline and LPS treatment significantly enhanced ORF6 and ORF6 double mutant reporter activity. These data indicate that LPS treatment enhances RTA gene transactivation, but the NF-κB recognition sites in the ORF6p do not play a role.

To examine whether LPS activation of ORF6p transactivation by RTA is accompanied by an increase in the occupancy of the viral genome by RTA, we performed chromatin immunoprecipitation of RTA-Flag in HE-RIT G3 cells treated with doxycycline alone or in combination with LPS at 24 h post-treatment. We observed that higher levels of RTA-Flag were

immunoprecipitated in HE-RIT cells treated with doxycycline and LPS (**Fig. 2.11A**). ChIP followed by qPCR did not detect RTA occupancy on the minimal ORF6 0-150 bp region (**Fig. 2.11B**). These data suggest that RTA transactivation of the ORF6p minimal promoter element may occur via an indirect mechanism that does not require direct RTA binding to ORF6p.

Hong et al. (174) previously reported an RTA recognition element (RRE) in the left origin of lytic replication (oriLyt) that controls ORF18 expression. Based on sequence conservation, three additional RRE elements were predicted in the right oriLyt. Indeed, we identified RTA-Flag occupancy on the right oriLyt by immunoprecipitation of a region that spans the predicted RRE-D and RRE-E sites (**Fig. 2.11B**). As expected, RTA-Flag did not pull down the previously characterized negative control ORF65 promoter region (**Fig. 2.11B**) (174). RTA-FLAG occupancy of the right oriLyt RRE-D and RRE-E sites was significantly increased by the addition of LPS to doxycycline treated RIT cells (**Fig. 2.11B**).

We examined if enhanced RTA occupancy of the right oriLyt upon LPS stimulation correlated with an increase in viral DNA replication (69, 253). Interestingly, doxycycline and LPS treatment at 48 h dramatically increased viral DNA replication when compared to either treatment alone, in both HE-RIT G3 and F1 cell lines (**Figs. 2.12A-B**). Immunoblot analysis detected enhanced RTA-Flag levels in HE-RIT cells treated with doxycycline and LPS compared

to doxycycline alone. To investigate whether LPS enhancement of reactivation was solely the result of enhanced RTA-Flag expression, we titrated the amount of doxycycline used to treat HE-RIT cells from 500 down to 5 ug/ml, which are 0.5 and 0.005-fold the previous concentrations used, either alone or in combination with LPS (**Fig. 2.13**). Decreasing doxycycline concentration resulted in less RTA-Flag and LPS-enhanced RTA-Flag at each concentration of doxycycline. However, when cells were treated with a high concentration of doxycycline to achieve comparable RTA-Flag levels to a very low level of doxycycline that was combined with LPS, the LPS treated condition led to a higher level of reactivation. Taken together, LPS treatment enhanced reactivation regardless of cellular levels of RTA-Flag.

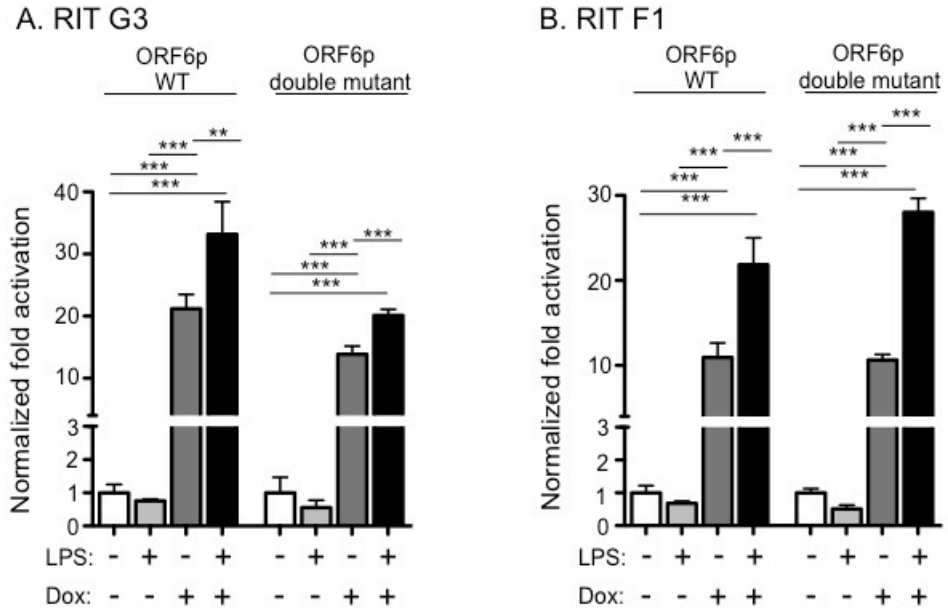

Figure 2.10. Lipopolysaccharide enhancement of reactivation is independent of NF-κB binding sites.

HE-RIT G3 (A) and HE-RIT F1 (B) cell lines were nucleofected with full-length ORF6p or ORF6p double NF-κB site mutant reporters and harvested at 24h for luciferase activity normalized by protein content. Bars represent fold-activation relative to the untreated condition for triplicate samples +/- SD. Significance was determined from one-way ANOVA followed by Tukey multiple comparison test; **,p<.01; ***p<0.001.

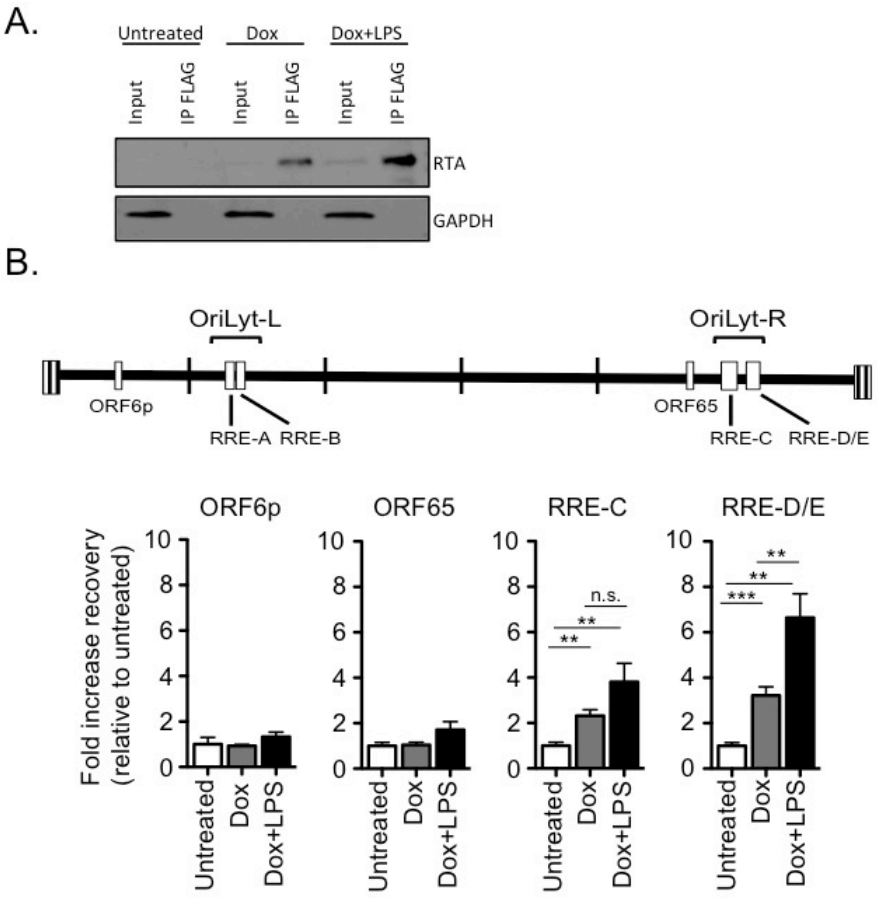

Figure 2.11. Chromatin immunoprecipitation of RTA on the right OriLyt is enhanced by LPS treatment.

(A) Western blot of immunoprecipitates recovered by anti-Flag conjugated beads in HE-RIT G3 cell lines. Input shown is 1% of total. (B) Quantitative PCR was used to measure the indicated genomic regions in complex with RTA-Flag. Data shown as fold-increase in % input recovery compared to untreated samples. Bars represent fold-activation relative to the untreated condition for triplicate samples +/- SD. Significance is determined by one-way ANOVA followed by Tukey post-test; **, $p<0.01$; ***,$p<0.001$.

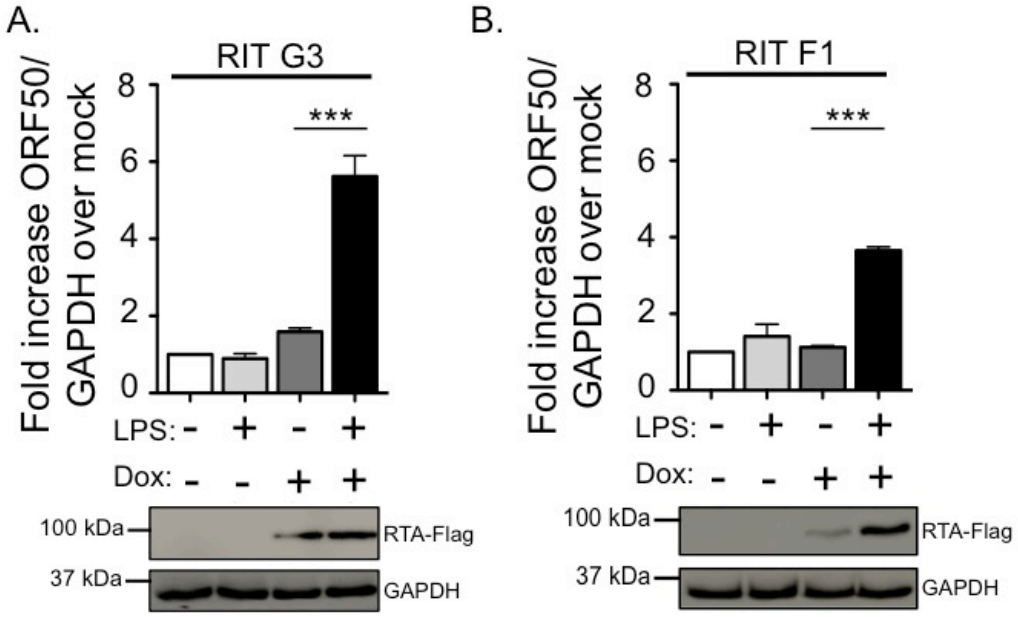

Figure 2.12. LPS treatment enhances viral DNA replication.
Quantitative PCR of viral genome load from the HE-RIT G3 (A) and F1 (B) cell lines 48 h after the indicated treatments. The fold-increase in viral ORF50 normalized to cellular GAPDH over mock treated condition is shown for triplicate samples. Immunoblot for RTA-Flag and GAPDH below. Bars represent fold-activation relative to the untreated condition for triplicate samples +/- SD. Significance is determined by one-way ANOVA followed by Tukey post-test; **, $p<0.01$; ***,$p<0.001$

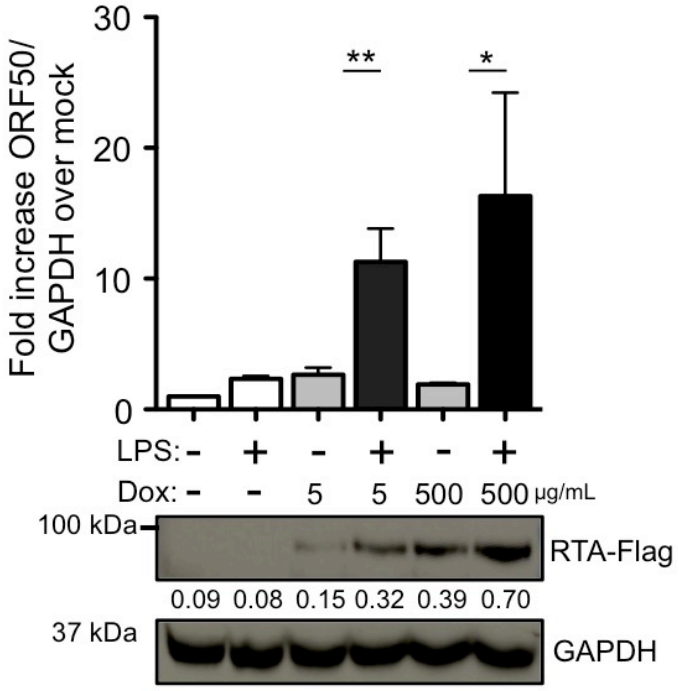

Figure 2.13. Lipopolysaccharide enhances reactivation independent of RTA protein amount.

Quantitative PCR of viral genome load from the HE-RIT G3 cell lines 48 h after treatment with LPS and the indicated concentration of doxycycline. The fold-increase in viral ORF50 normalized to host GAPDH over mock is shown from triplicate samples. Immunoblot for RTA-Flag and GAPDH below. Bars represent fold-activation relative to the untreated condition for triplicate samples +/- SD. Significance is determined by one-way ANOVA followed by Tukey post-test; **, $p<0.01$; ***,$p<0.001$.

Lipopolysaccharide treatment enhances RTA binding to viral genome in primary splenocytes upon explant reactivation. Previous studies indicated that LPS treatment of mice enhances virus reactivation from latency (237). We hypothesized that LPS treatment would increase RTA occupancy of the viral genome in primary splenocytes. To test the possibility that LPS treatment might increase RTA occupancy of the viral genome in primary splenocytes, we generated a recombinant MHV68 virus that encodes a tagged RTA to enhance the isolation of RTA-DNA complexes from the rare population of infected cells *in vivo*. The RTA-Bio construct encodes MHV68 RTA with a C-terminal fusion of FLAG, V5, and a biotin acceptor sequence. The biotin acceptor sequence is a 23 amino acid peptide tag that is biotinylated in the presence of the bacterial *Escherichia coli* BirA protein ligase (254). In mammalian cells, very few naturally occurring proteins are biotinylated, thus isolation of proteins covalently linked to biotin by strong streptavidin interactions is a powerful tool for enrichment from *in vivo* tissues (255, 256). *En passant* mutagenesis was performed to generate two independent recombinant viruses encoding RTA-Bio on the MHV68-H2BYFP reporter virus backbone (MHV68-H2BYFP-RTA-Bio.1 and .2) (**Fig. 2.14A**). MfeI or BamHI digestion of the BAC DNA and PCR amplimers confirmed genomic integrity and tag insertion, respectively (**Fig. 2.14B**). In addition, whole-genome sequencing of the parental MHV68 H2B-YFP and RTA-Bio.1 BAC DNA confirmed the

sequence of the C-terminal Bio tag and did not reveal any additional mutations in the entire unique sequence.

Mouse embryonic fibroblasts derived from transgenic mice that ubiquitously express the BirA gene (ROSA BirA MEFs) were infected with H2B-YFP or the RTA-Bio.1 virus at an MOI 5. Immunoblot analysis detected both RTA expression and biotinylation (**Fig. 2.15A**). In addition, ORF59 early gene expression increased throughout the 24h time-course for both WT and RTA-Bio1 viruses. Late gene products, the capsid protein ORF65 (M9) and tegument protein ORF75C, were detected at 12 and 24 h post-infection at comparable levels. Single-step growth curves were performed for WT and RTA-Bio.1 viruses (MOI 5) in WT C57/BL6 MEFs and ROSA BirA MEFs. RTA-Bio 1 virus replication was decreased when compared to H2BYFP (**Fig. 2.15B**). Given this slight attenuation in replication we infected ROSA BirA mice with 1000 PFU of MHV68-H2BYFP or RTA-Bio by the less restrictive intraperitoneal route of inoculation. The peak of MHV68 latency in the spleen (~16 dpi) coincides with germinal center formation as the host responds to infection. Regardless of the virus used to infect the ROSA BirA mice, the CD19+ B cells participated in germinal center reactions, as evidenced by similar percentages with upregulated of CD95+GL7+. The B cells from the ROSA BirA mice infected with WT H2BYFP and RTA-Bio underwent immunoglobulin class-switching to IgG2b at comparable

levels (**Fig. 2.16A**). We also characterized the splenic B cells harboring the parental MHV68-H2BYFP and RTA-Bio. The percentage of YFP+ CD19+ B cells were not altered by the tagged RTA (**Fig. 2.16B**). In addition, both viruses colonized CD95+GL7+ germinal center (**Fig. 2.16C**) and IgG2b+ IgD- class-switched (**Fig. 2.16D**) CD19+ B cells at equivalent frequencies (summarized in **Fig. 2.16E**).

The ability of the virus to colonize the germinal center and class-switched B cell population suggested that the normal B cell latency dynamics were not impacted by the C-terminal RTA bio tag. In agreement with the flow cytometry analysis, we did not observe a change in the establishment of latency (**Fig. 2.17A**) or defect in reactivation of the virus from latency upon explant (**Fig. 2.17B**). Infection of ROSA BirA mice with RTA-Bio clone 1 and 2 led to the same level of reactivation after splenic explant from primary splenocytes (data not shown). Latency establishment was also not impacted in cells of the peritoneal exudate compartment (PECs), which is another latency reservoir (**Fig. 2.17C**). However, in contrast to the splenocyte reservoir, there was a significant defect in reactivation from PECs after intraperitoneal infection (**Fig. 2.17D**). This indicates that the C-terminal tag impairs RTA function in some cell-types such as the PECs, but RTA-bio does not impact MHV68 latency or reactivation from latency in the splenocytes upon a direct intraperitoneal infection

ChIP-qPCR was performed using primary splenocytes isolated from BL6 and ROSA BirA infected mice at 16 days post-intraperitoneal infection. Primary splenocytes were left untreated or treated with LPS for 18 hours after explant. ChIP using streptavidin-conjugated beads to capture biotinylated RTA was followed by quantitative PCR with primers targeting the region of the right oriLyt that comprises the RRE-C and RRE-D and -E sites, which were bound by RTA-Flag in the HE-RIT experiments (**Fig. 2.11B**). ROSA BirA mice infected with the RTA-Bio virus were enriched for RTA occupancy on the right oriLyt, but not the ORF65 gene or ORF6 promoter regions (**Fig. 2.18A**). LPS treatment led to a statistically significant increase in RTA occupancy of the right oriLyt region in the ROSA BirA mice in comparison to the C57Bl/6 mice (**Fig. 2.18B**). We generated a position weight matrix based on the RRE binding sites. Searching the MHV68 genome with this matrix identified 7 potential binding sites with statistically significant p-values and q-values ($p < 1e\text{-}6$, $q < 0.1$) based on an analysis of background DNA Markov probabilities. Five of these sequences were the RRE sites and two additional regions with a consensus motif sequence to RREs were identified in regions upstream of ORF9 and ORF21 (**Fig. 2.18C**).

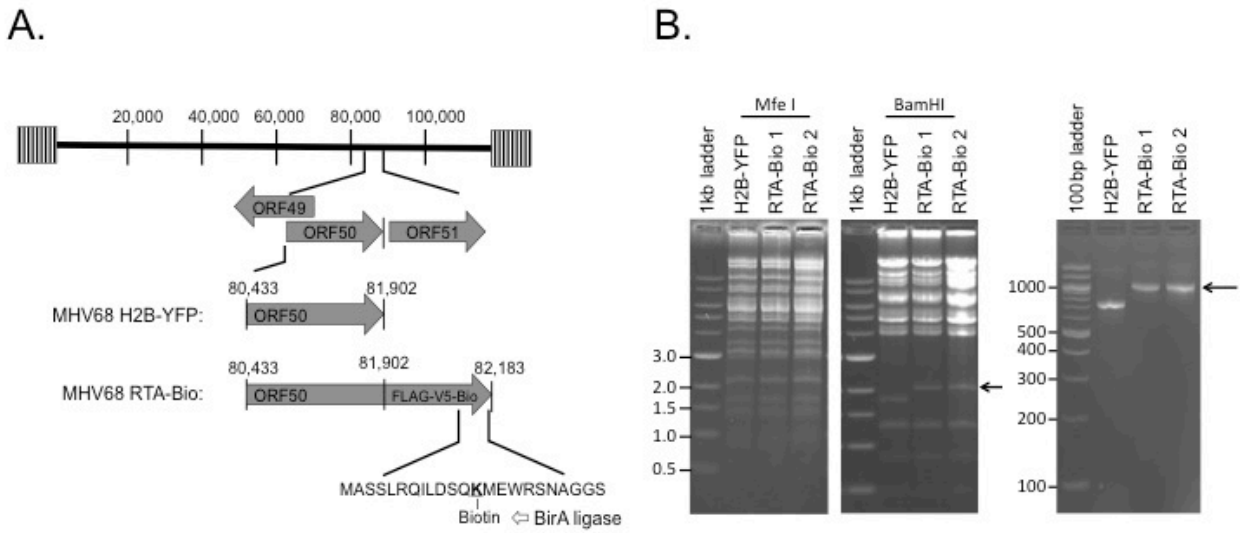

Figure 2.14. Construction of recombinant RTA-Bio virus.
(A) Schematic of the RTA-Bio virus indicated the he Bio tag insertion at the 3' end of RTA. Biotinylation occurs on lysine residue in presence of BirA ligase. (B) Confirmation of two independent clones of RTA-Bio virus by restriction fragment length polymorphism analysis. MfeI or BamHI digestion of BAC DNA. Arrows denote expected change in digested product size upon Bio-tag insertion. PCR confirms insertion of Bio-tag (indicated by arrow) in the RTA-Bio BAC DNA.

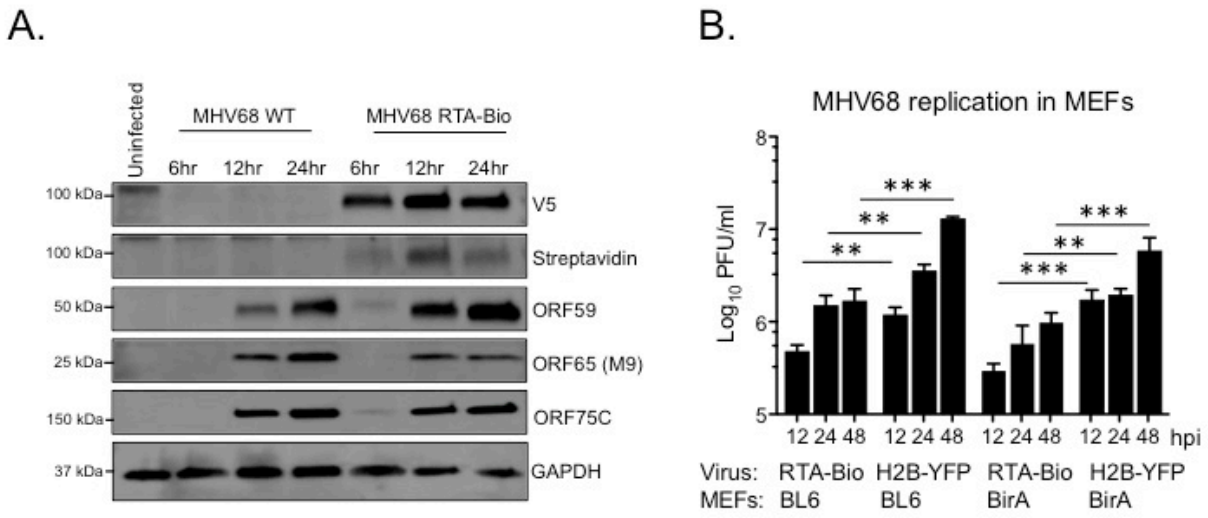

Figure 2.15. Characterization of recombinant RTA-Bio virus.
(A) Timecourse analysis of RTA-FLAG-V5-Bio and other viral gene products upon infection of BirA expressing MEFs with H2B-YFP or RTA-Bio viruses (MOI 5.0). (B) Virus growth in primary MEFs isolated from C57/BL6 (BL6) or Rosa BirA mice upon infection with H2B-YFP or RTA-Bio viruses (MOI 5.0). Bars represent fold activation relative to the untreated condition for triplicate samples +/- SD.

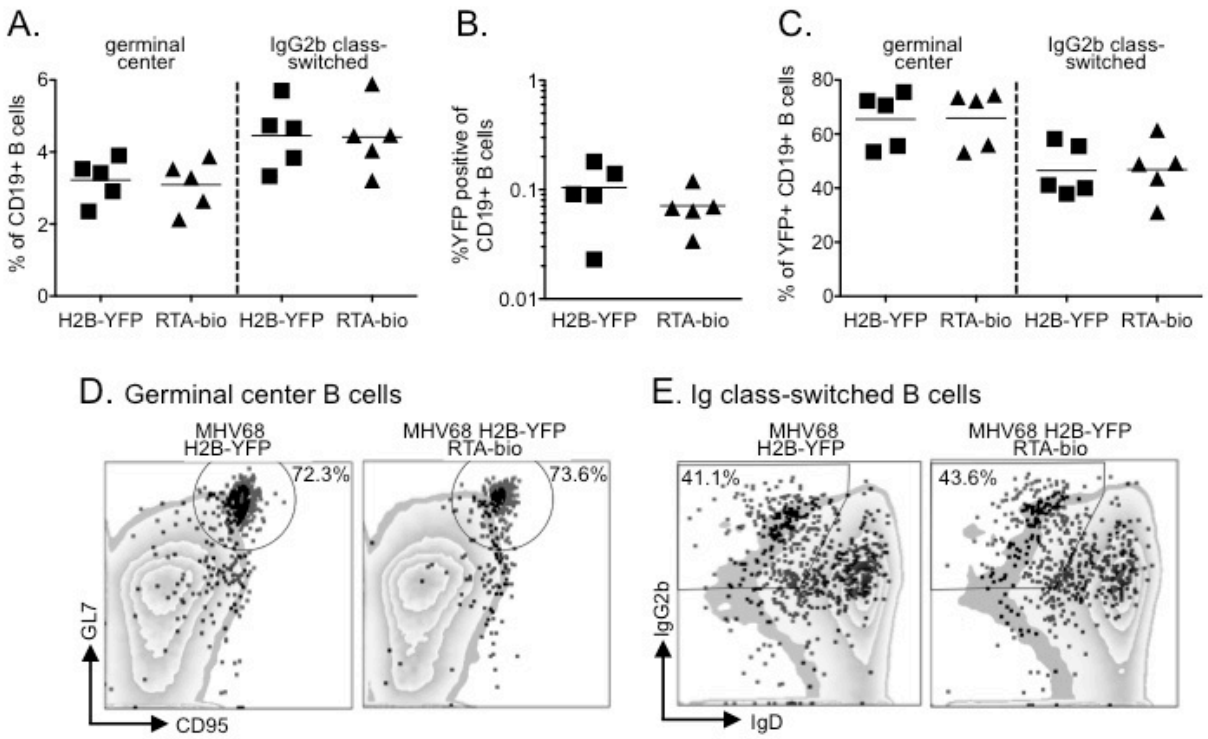

Figure 2.16. RTA-Bio virus detection in germinal center and class-switched B cells.
(A) Percentage of CD19+ B cells positive for germinal center or immunoglobulin class-switched to IgG2b. (B) Percentage of total CD19+ B cells positive for viral infection measured by YFP expression. (C) Percentage of germinal center or IgG2b+ class-switched CD19+ MHV68+ YFP expressing cells. (D) Percentage of GL7+ and CD95+ germinal center B cells. (E) Percentage of IgG2b+ IgD- class-switched B cells.

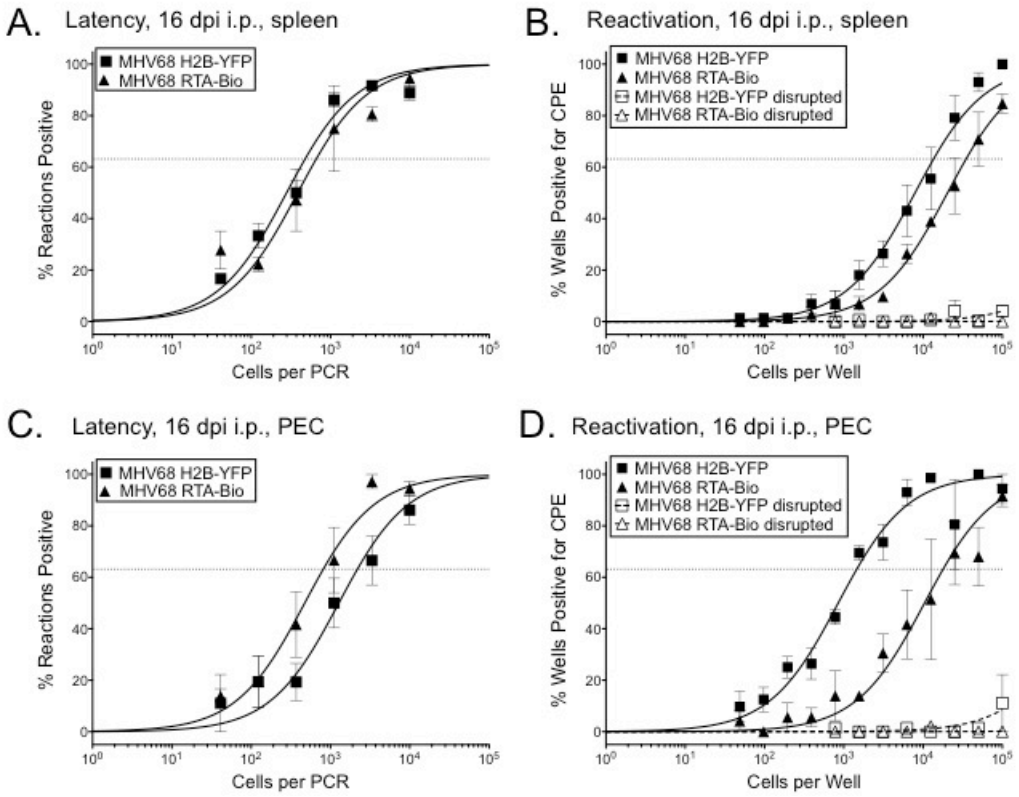

Figure 2.17. The RTA-Bio virus establishes latency in the spleen comparable to control virus.

(A) Latency was measured at 16 dpi in the spleen, as indicated by the frequency of intact splenocytes harboring the viral genome using a limiting-dilution nested-PCR assay. (B) Reactivation from latency was measured by using a limiting-dilution explant reactivation co-culture assay. (C) Latency of peritoneal exudate cells at 16 dpi. (D) Reactivation from latency from peritoneal exudate cells at 16 dpi. Dotted lines represent disrupted cells used to measure preformed infectious virus. The intersection of the nonlinear regression curves with dashed line at 63.2% is used to determine the frequency of cells that were positive for either the viral genome or reactivating virus. Graphs represent SEM of three independent experiments using three mice each.

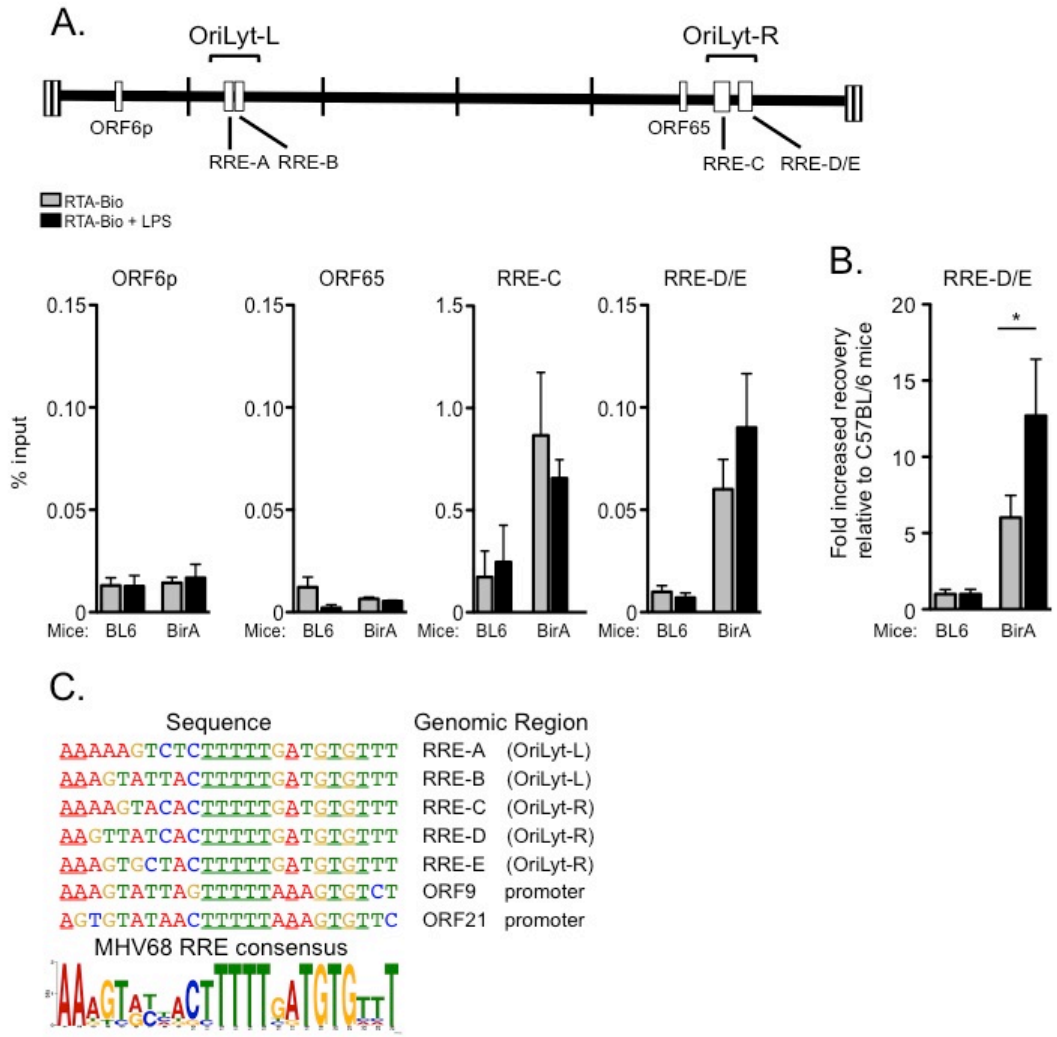

Figure 2.18. Chromatin immunoprecipitation of the right oriLyt with RTA-Bio from primary splenocytes isolated from infected C57BL/6 or Rosa BirA mice.
(A) C57/BL6 or BirA expressing transgenic mice were infected at 1000 pfu and primary splenocytes harvested 16 dpi. Cells were cultured in media for 18 h with or without LPS. Immunoprecipitates using streptavidin conjugated beads were analyzed by qPCR for the indicated genomic regions and calculated as a percentage of input DNA. Graphs represent SEM of three independent experiments using two mice each. (B) Enrichment of RTA occupancy on the oriLyt-R upon LPS stimulation. Data represents analysis of (A) as the fold-enrichment in recovery from the Rosa-BirA splenocytes compared to the recovery from the C57/BL6 splenocytes. Significance determined by one-way ANOVA followed by Tukey post-test, *$p<0.05$. (C) Find Individual Motif Occurrences (FIMO) was used to search the MHV68 genome for putative RTA binding elements based on known binding sites. An MHV68 consensus was generated based on the putative RTA responsive elements identified.

Conclusions

We and others have previously reported that NF-κB signaling impacts the lytic or latent outcomes of murine gammaherpesvirus 68 infection (185, 186, 216, 217), but the mechanism is not well-defined. To determine the potential role of NF-κB DNA binding sites in viral gene expression, we first identified putative NF-κB recognition sites in the regulatory regions of MHV68 genes. We observed that the specific subunit compositions of the NF-κB dimers recognizing the NF-κB consensus elements in the lytic ORF6 promoter varied with cell-type and status of infection. Importantly, mutation of NF-κB recognition sites in ORF6p did not impair RTA transactivation of the ORF6p, and over-expression of NF-κB subunits in combination with RTA inhibited gene expression regardless of whether these NF-κB binding sites were intact. Next, we developed tools to test the role of toll-like receptor activation of NF-κB signaling in promoting reactivation from latency in B cells. We generated a latent B cell line inducible for RTA-Flag expression. RTA expression alone drove a small degree of viral reactivation from latency that was significantly increased upon LPS treatment; but ORF6p activation was again independent of the integrity of the NF-κB binding sites. Likewise, generation of recombinant RTA Bio-tagged virus permitted further validation of RTA occupancy on the right oriLyt replication in the context of reactivation from B cells directly from the spleens of infected mice. RTA occupancy on the right oriLyt was enhanced by LPS, both in the reactivation-inducible cell lines as well as in primary splenocytes from infected mice.

Chapter 3: Discussion

Our current study indicates that the NF-κB recognition sites in the ORF6 promoter are not essential for RTA transactivation during productive infection. In addition to the analysis of this lytic gene, we also did not find any impact on pathogenesis upon the mutagenesis of the NF-κB binding site in the latency-associated M1 promoter of MHV68 (data not shown). However, LPS engagement did enhance reactivation and RTA occupancy of the right oriLyt. Given the previous report that IKKβ activates RTA, our data is consistent with a model whereby LPS drives canonical NF-κB signaling to enhance RTA transactivation and reactivation. In the process of investigating the interplay of NF-κB signaling and subunit function with RTA-mediated lytic gene expression we developed a B cell latency system inducible for reactivation by RTA and a recombinant virus that enables isolation of RTA from primary cells from the mouse. Significantly, these two novel tools will enable whole genome analysis of RTA occupancy and the identification of RTA binding partners in the context of latency and reactivation from latency in cell culture, and, importantly, in multiple aspects of gammaherpesvirus infection in primary latency reservoirs of the host.

NF-κB subunits promote latency

Disruption of NF-κB signaling upon Bay-11-7082 treatment of latent EBV+ or KSHV+ infected B cell lines induces reactivation (182). It has been proposed that NF-κB signaling promotes latency via interference of RTA transactivation of lytic genes. For example, the NF-κB p65 subunit inhibits transactivation of lytic luciferase reporters by MHV68, KSHV and EBV

RTA proteins; interestingly, the p65 DNA binding domain was not required (182). In addition, p65 antagonizes KSHV RTA activation of viral promoters that are co-regulated by RTA and RBP-Jκ by interfering with protein-DNA complex formation (257). We also found that co-transfection of NF-κB subunits p65, p50, or cRel with RTA has an inhibitory effect on RTA-mediated transactivation of the ORF6p reporter in 293T cells. However, NF-κB subunit inhibition of RTA transactivation occurs independently of the NF-κB recognition elements identified in the ORF6p reporter in 293T cells suggesting NF-κB inhibition of RTA transactivation may only occur via protein-protein interactions or by inducing the expression of other cellular repressors. Since RTA binds p65 and promotes its ubiquitination and degradation (174), the p65 subunit has the potential to directly interact and interfere with RTA transactivation of viral genes. Perhaps a certain threshold of NF-κB p65 that inhibits RTA function in some contexts must be overcome to enable RTA to transactivate viral genes. As for the NF-κB subunits p50 and cRel that are found in the nucleus of MHV68-infected cells, further experiments are required to test for interactions with RTA and the consequences of those interactions for RTA function. A direct role for NF-κB subunits in regulating viral gene expression may be revealed only where NF-κB binding sites overlap with genomic regions occupied by RTA.

Truncation of a portion of the ORF6 promoter that included the proximal NF-κB recognition site revealed an enhanced response to RTA that was not evident in HE2 latent B cell lines. This result suggests that the inhibitory role of NF-κB signaling could be a context-

dependent phenomenon. Grossman et al. (258) reported that the impact of NF-κB signaling in KSHV latency depends on the cellular context. Inhibition of NF-κB signaling impaired viral latency in PEL cells and promoted higher levels of lytic replication upon *de novo* infection of primary endothelial cells, yet was dispensable for the viral life cycle in human foreskin fibroblasts. KSHV lytic replication in endothelial, epithelial, and fibroblast cells was associated with higher levels of NF-κB activation (258, 259) as we observed for MHV68 at late times after fibroblast infection. Taken together, the impact of NF-κB subunits is likely cell type-specific due to the variation in active subunits and status of other transcription factors that is shaped by the microenvironment of the infected cell.

TLR signaling enhances reactivation from latency.

Previous studies demonstrated that toll-like receptor (TLR) stimulation increases MHV68 reactivation from latency in B cells *in vitro* (237, 260). TLR4 and TLR9 engagement, by LPS or CpG DNA, respectively, triggers increased reactivation of MHV68 42 days post-infection *in vivo*. In contrast, TLR7 and TLR9 ligand treatment of the latent S11B lymphoma cell line inhibits viral DNA replication and infectious virus production (238). In line with this observation, TLR7 ligand treatment of infected mice resulted in higher latency establishment in the spleen. Taken together, these studies suggest that TLR stimulation has the potential to enhance or inhibit lytic replication, and the outcome may be different in primary or transformed cells, or at different stages of the virus life cycle. Treatment of latent HE2 B cell lines with the TLR4 ligand lipopolysaccharide (LPS) enhances reactivation from latency (237). We observed a two-fold enhancement in viral DNA replication after LPS or doxycycline induction of RTA

expression in HE2-RIT cell lines and reactivation was dramatically enhanced with combinatorial treatment. In addition, RTA transactivation of the full-length WT ORF6 promoter and the double NF-κB site mutant reporter construct was significantly enhanced in HE2-RIT cell lines treated with doxycycline and LPS. This finding suggests that NF-κB signaling promotes RTA transactivation of viral genes independently of NF-κB recognition elements in the ORF6 promoter region.

Induction of RTA alone did not drive reactivation to the levels of TPA alone or the combinatorial induction of RTA with LPS treatment. IKKβ phosphorylation of RTA enhances its transcriptional activity and a mutant virus lacking RTA phosphorylation sites is impaired for lytic replication (153). Hence, the mechanism by which LPS activation of NF-κB signaling enhances RTA transactivation of the ORF6 promoter may likely be a result of IKKβ phosphorylation of RTA. To address this, we treated HE2-RIT cell lines with doxycycline and LPS alone, or in combination with SC514, a selective inhibitor of IKKβ kinase activity. We observed a loss in LPS-enhanced reactivation for cells treated with SC514 in addition to doxycycline and LPS (data not shown), consistent with a role for IKKβ phosphorylation of RTA, but our interpretation of this data was confounded by the significant loss of cell viability that accompanied the SC514 treatment (data not shown).

RTA occupancy of origins of lytic replication.

During the lytic phase of infection, replication of the viral genome occurs after recruitment of viral replication-associated proteins to the oriLyt. Similar to EBV and KSHV

(261-263), MHV68 contains two functional oriLyt sequences that each serve as sites for initiating viral DNA replication (69, 253). Binding of the EBV Zta protein to the oriLyt is essential for the initiation of DNA replication (264). For KSHV, the K8 protein is functionally analogous to the EBV Zta protein as it interacts in with the core replication machinery in the oriLyt to promote viral DNA replication (262, 265). KSHV RTA binds sites in the left oriLyt that are essential for viral DNA replication (266). RTA binding and transcription in the KSHV oriLyt generates a polyadenylated RNA (Ori-RNA). During KSHV reactivation from RTA-inducible latent BCBL1 cells, RTA was preferentially recruited to the Ori-RNA promoter during reactivation (267). Similarly, the MHV68 left origin of lytic replication contains two RTA responsive elements (RREs), RRE-A and RRE-B, that directly bind RTA (69, 174). The RRE-B site is necessary for transcription of the adjacent ORF18 gene (69, 174). Mutation of RRE-B disrupts expression of the essential ORF18 gene and impairs virus replication. Thus, transcription occurs in the left oriLyt region, but further studies are necessary to determine if RTA binding and transcription in this region are necessary for initiation of viral DNA replication. The RRE-A and RRE-B binding elements of the left oriLyt displayed homology to three other elements identified in the right oriLyt, RRE-C, RRE-D, and RRE-E; however, RTA occupancy was not evaluated at these sites (174). Here we confirm RTA occupancy of RRE-C and RRE-D and -E in the right oriLyt during reactivation from latent B cell lines in cell culture, thus expanding the known targets of MHV68 RTA. RTA occupancy at these newly validated RRE sites was enhanced by LPS treatment at 24 h. RTA was not found in complex with the minimal RTA responsive region of ORF6 or the previously identified ORF65 genomic region

negative for RTA binding (174). Since ORF6 is an early gene we attempted to perform chromatin immunoprecipitation for RTA at 6 h post-doxycycline treatment, but RTA protein was not consistently detectable (data not shown).

To confirm our finding of LPS-enhanced occupancy of RTA on the right oriLyt regions that was observed in the reactivation inducible B cell system, we generated a recombinant virus encoding a C-terminal modified RTA that has multiple epitope tags including a biotinylation site. Infection of ROSA BirA cells with the RTA-Bio tagged virus permits the detection of biotinylation by BirA ligase. While the RTA-Bio virus was slightly attenuated for replication in cell culture, our pathogenesis studies demonstrated that latency establishment and reactivation from latency were remarkably unperturbed as compared to WT virus upon intraperitoneal infection. Latency establishment in the PECs was also comparable for both the WT and RTA-Bio viruses16 dpi; but there was a significant defect in reactivation from latency for the RTA-Bio virus. Nevertheless, since the RTA-Bio virus established latency and reactivated similar to WT virus in splenic B cells, we used this experimental condition to examine RTA-bio interaction with the MHV68 genome. RTA occupancy of the right oriLyt region spanning RRE-D and RRE-E was confirmed using primary splenocytes isolated directly from the infected animal at 18 hours after explant. LPS treatment led to enhanced occupancy. We generated a consensus motif based on the RRE elements of the MHV68 oriLyt regions and identified two additional regions of the MHV68 genome that will be examined for recognition by RTA in future studies.

Model for the role of canonical NF-κB signaling in productive infection.

Taken together, the *in vivo* biotinylation of RTA enabled streptavidin-mediated isolation of RTA-viral genomic targets that validate the profile of RTA occupancy in the latent B cell lines upon reactivation stimulated by RTA induction or enhancement by TRL4 signaling. These data extend previous findings regarding the subversion of the canonical NF-κB signaling pathway by MHV68 RTA (153, 159, 210) and the enhancement of gammaherpesvirus reactivation from latent B cells by TLR engagement (237, 238, 268). As illustrated in the model (**Fig. 3.1**), RTA utilizes canonical NF-κB signaling to enhance productive infection, yet the process leading to IKK activation differs with the virus lifecycle: viral tegument may engage upstream signaling in the context of *de novo* infection while TLR ligands may provide co-stimulatory, enhancing signals in the context of a latent B cell primed for RTA-driven reactivation.

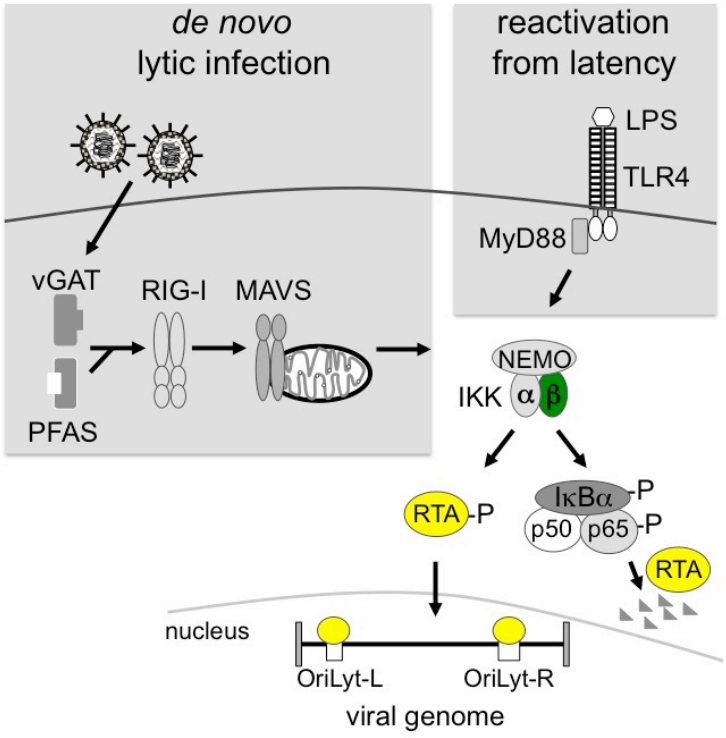

Figure 3.1. Model for the role of canonical NF-κB signaling in productive infection.
Model demonstrating RTA subversion of canonical NF-κB signaling to promote productive infection. Upon de novo infection, vFGARAT tegument-mediated activation of MAVS leads to IKKβ activation and phosphorylation of RTA, RTA targets p65 for degradation (153, 159, 210). In this report, TLR4 activation of LPS in a latent B cell line leads to enhanced RTA transactivation and occupancy of the right lytic origin of replication (oriLyt-R).

Future directions

An EMSA screen identified multiple viral elements that compete for NF-κB binding. We chose to investigate the role of two NF-κB binding sites identified in the ORF6 regulatory region and showed that they do not alter its regulation in transient assays. A thorough examination of NF-κB binding sites in the viral genome should be performed to address the role of additional sites identified in the EMSA screen. Primary experiments such as chromatin immunoprecipitation for NF-κB subunits in lytic and latent cell culture systems, in addition to primary MHV68+ splenocytes, would better define the repertoire of NF-κB subunits occupying the MHV68 genome during latency, lytic replication, and reactivation from latency. Initially, this study could focus on the identified NF-κB binding sites and then be expanded to cover the length of the MHV68 genome by an unbiased ChIP-seq analysis. Once confirmed for NF-κB occupancy during infection, mutagenesis of *bone-fide* NF-κB binding sites can be performed in the context of the viral genome and assayed for changes in viral gene regulation and pathogenesis *in vivo*. These experiments could highlight changes in NF-κB occupancy and possibly identify shifting subunit compositions that occur during the dynamic lifecycle of MHV68.

We describe a role for TLR4 signaling in enhancing transactivation and viral genome occupancy by RTA in the context of reactivation from latent B cells. Consistent with previous work (159), we propose that IKKβ kinase activity enhances RTA function in the context of reactivation, yet further studies are necessary to validate the IKKβ post-translational modification (PTM) of RTA that affects its functions. For instance, mass-spectrometry can be performed on RTA-Flag isolated from untreated (latent), doxycycline (reactivation), and LPS/doxycyline (enhanced reactivation) treated RIT cell lines to identify the PTM signature present during different stages of MHV68 infection. This method should confirm previously identified phosphorylation sites on RTA and reveal novel sites. It was shown that

IKKβ phorphorylates RTA, yet the role of individual phosphorylation sites in RTA and their impact on its function were not addressed (159). Moreover, mutations of individual RTA phosphorylation sites could be assayed for their impact on TLR4-enhanced reactivation from B cells. Once essential residues are identified, mutations in the viral genome can be performed in the RTA-bio virus to test for an impact on pathogenesis *in vivo*. In addition, the RTA-Bio virus provides a system in which RTA can be pulled-down using V5, Flag, or Bio epitope tags that are flanked by protease cleavage sites to purify and analyze RTA-protein or RTA-DNA complexes *in vivo*.

As found for KSHV RTA, a consensus DNA recognition element for MHV68 RTA has not been identified. Nuclear lysates from 293T cells expressing RTA-Flag bind two disparate sequences in the left oriLyt and the ORF48 promoter region (174). Binding sites identified in the left origin of lytic replication (oriLyt) influenced transcription of an adjacent gene. We have confirmed RTA occupancy in regions of the right oriLyt that were predicted as RREs based on homology to the RREs of the left oriLyt. It is not known if RTA activates transcription in this region. Interestingly, an expressed genomic region (EGR) had been identified adjacent to the right oriLyt and further experiments are necessary to address whether RTA initiates the transcription of this EGR (240, 269). An additional question in the field is whether or not transcription in the oriLyt is necessary for initiating DNA replication or if these processes occur separately. First, northern analysis, combined with 5' and 3' rapid amplification of cDNA ends (RACE) analysis can be performed to map the transcription in the genomic region within and adjacent to the right oriLyt based on predicted ORFs in the region. If transcription is identified in the region, mutagenesis of the RRE sites can be performed in the context of the virus to assay the effect on RTA-mediated gene expression in the region and levels of DNA replication. The right oriLyt was previously shown to be essential for DNA replication (253). Therefore, plasmid based DNA replication assays of single oriLyt can be performed to monitor changes in DNA replication upon mutagenesis.

Impact of these studies

RTA is a critical transcription factor for initiating the lytic cascade of gene expression during reactivation from latency and is conserved among MHV68, KSHV, and EBV. This study provides valuable insight as to how RTA functions to regulate gene expression during reactivation from latency, with respect to the functional interplay of RTA and NF-κB subunits at the level of NF-κB binding sites in the viral genome. Our findings are consistent with the idea that TLR4 signaling enhances IKKβ activity, which promotes RTA transactivation of viral genes and DNA replication during viral reactivation from latency. Since gammaherpesvirus reactivation is an inefficient process and not all cells will undergo reactivation simultaneously, this poses a challenge to the immune system in clearing infection. Adjuvants that promote IKKβ activity can be developed for use in lytic induction therapy as this would increase levels of reactivation by enhancing RTA function and can be administered in the presence of drugs that prevent further infection. Conversely, development of new molecular targets that interfere with either the conserved RTA DNA binding region or inhibit its phosphorylation could prevent viral growth.

REFERENCES

1. **Honess RW.** 1984. Herpes simplex and 'the herpes complex': diverse observations and a unifying hypothesis. The eighth Fleming lecture. The Journal of general virology **65 (Pt 12):**2077-2107.
2. **B R.** 1996. Herpesviridae., vol. 2. Lippincott-Raven, Philadelphia.
3. **Bresnahan WA, Shenk TE.** 2000. UL82 virion protein activates expression of immediate early viral genes in human cytomegalovirus-infected cells. Proceedings of the National Academy of Sciences of the United States of America **97:**14506-14511.
4. **Ling PD, Tan J, Sewatanon J, Peng R.** 2008. Murine gammaherpesvirus 68 open reading frame 75c tegument protein induces the degradation of PML and is essential for production of infectious virus. Journal of virology **82:**8000-8012.
5. **Moriuchi H, Moriuchi M, Straus SE, Cohen JI.** 1993. Varicella-zoster virus (VZV) open reading frame 61 protein transactivates VZV gene promoters and enhances the infectivity of VZV DNA. Journal of virology **67:**4290-4295.
6. **Nicholson IP, Sutherland JS, Chaudry TN, Blewett EL, Barry PA, Nicholl MJ, Preston CM.** 2009. Properties of virion transactivator proteins encoded by primate cytomegaloviruses. Virology journal **6:**65.
7. **Sewatanon J, Ling PD.** 2013. Murine gammaherpesvirus 68 ORF75c contains ubiquitin E3 ligase activity and requires PML SUMOylation but not other known cellular PML regulators, CK2 and E6AP, to mediate PML degradation. Virology **440:**140-149.
8. **Fakhari FD, Dittmer DP.** 2002. Charting latency transcripts in Kaposi's sarcoma-associated herpesvirus by whole-genome real-time quantitative PCR. Journal of virology **76:**6213-6223.
9. **Jenner RG, Alba MM, Boshoff C, Kellam P.** 2001. Kaposi's sarcoma-associated herpesvirus latent and lytic gene expression as revealed by DNA arrays. Journal of virology **75:**891-902.
10. **Paulose-Murphy M, Ha NK, Xiang C, Chen Y, Gillim L, Yarchoan R, Meltzer P, Bittner M, Trent J, Zeichner S.** 2001. Transcription program of human herpesvirus 8 (kaposi's sarcoma-associated herpesvirus). Journal of virology **75:**4843-4853.
11. **Sarid R, Flore O, Bohenzky RA, Chang Y, Moore PS.** 1998. Transcription mapping of the Kaposi's sarcoma-associated herpesvirus (human herpesvirus 8) genome in a body cavity-based lymphoma cell line (BC-1). Journal of virology **72:**1005-1012.
12. **Zhong W, Wang H, Herndier B, Ganem D.** 1996. Restricted expression of Kaposi sarcoma-associated herpesvirus (human herpesvirus 8) genes in Kaposi sarcoma.

Proceedings of the National Academy of Sciences of the United States of America **93:**6641-6646.
13. **Mendelson M, Monard S, Sissons P, Sinclair J.** 1996. Detection of endogenous human cytomegalovirus in CD34+ bone marrow progenitors. The Journal of general virology **77 (Pt 12):**3099-3102.
14. **Sinclair J.** 2008. Human cytomegalovirus: Latency and reactivation in the myeloid lineage. Journal of clinical virology : the official publication of the Pan American Society for Clinical Virology **41:**180-185.
15. **Miyake F, Yoshikawa T, Sun H, Kakimi A, Ohashi M, Akimoto S, Nishiyama Y, Asano Y.** 2006. Latent infection of human herpesvirus 7 in CD4(+) T lymphocytes. Journal of medical virology **78:**112-116.
16. **Epstein MA, Achong BG, Barr YM.** 1964. Virus Particles in Cultured Lymphoblasts from Burkitt's Lymphoma. Lancet **1:**702-703.
17. **Gupta S, Fricker FJ, Gonzalez-Peralta RP, Slayton WB, Schuler PM, Dharnidharka VR.** 2010. Post-transplant lymphoproliferative disorder in children: recent outcomes and response to dual rituximab/low-dose chemotherapy combination. Pediatric transplantation **14:**896-902.
18. **Cesarman E, Chang Y, Moore PS, Said JW, Knowles DM.** 1995. Kaposi's sarcoma-associated herpesvirus-like DNA sequences in AIDS-related body-cavity-based lymphomas. The New England journal of medicine **332:**1186-1191.
19. **Malnati MS, Dagna L, Ponzoni M, Lusso P.** 2003. Human herpesvirus 8 (HHV-8/KSHV) and hematologic malignancies. Reviews in clinical and experimental hematology **7:**375-405.
20. **Elgui de Oliveira D.** 2007. DNA viruses in human cancer: an integrated overview on fundamental mechanisms of viral carcinogenesis. Cancer letters **247:**182-196.
21. **Rappocciolo G, Jenkins FJ, Hensler HR, Piazza P, Jais M, Borowski L, Watkins SC, Rinaldo CR, Jr.** 2006. DC-SIGN is a receptor for human herpesvirus 8 on dendritic cells and macrophages. Journal of immunology **176:**1741-1749.
22. **Simard EP, Engels EA.** 2010. Cancer as a cause of death among people with AIDS in the United States. Clinical infectious diseases : an official publication of the Infectious Diseases Society of America **51:**957-962.
23. **Ganem D.** 1997. KSHV and Kaposi's sarcoma: the end of the beginning? Cell **91:**157-160.
24. **Crawford DH, Rickinson A, Johannessen Il.** 2014. Cancer virus : the story of Epstein-Barr Virus, 1st ed. Oxford University Press, Oxford, United Kingdom ; New York.
25. **Simas JP, Efstathiou S.** 1998. Murine gammaherpesvirus 68: a model for the study of gammaherpesvirus pathogenesis. Trends in microbiology **6:**276-282.
26. **Blackman MA, Flano E, Usherwood E, Woodland DL.** 2000. Murine gamma-herpesvirus-68: a mouse model for infectious mononucleosis? Molecular medicine today **6:**488-490.

27. **Speck SH, Ganem D.** 2010. Viral latency and its regulation: lessons from the gamma-herpesviruses. Cell host & microbe **8:**100-115.
28. **Barton E, Mandal P, Speck SH.** 2011. Pathogenesis and host control of gammaherpesviruses: lessons from the mouse. Annual review of immunology **29:**351-397.
29. **Blaskovic D, Stancekova M, Svobodova J, Mistrikova J.** 1980. Isolation of five strains of herpesviruses from two species of free living small rodents. Acta virologica **24:**468.
30. **Blasdell K, McCracken C, Morris A, Nash AA, Begon M, Bennett M, Stewart JP.** 2003. The wood mouse is a natural host for Murid herpesvirus 4. The Journal of general virology **84:**111-113.
31. **Chastel C, Beaucournu JP, Chastel O, Legrand MC, Le Goff F.** 1994. A herpesvirus from an European shrew (Crocidura russula). Acta virologica **38:**309.
32. **Kozuch O, Reichel M, Lesso J, Remenova A, Labuda M, Lysy J, Mistrikova J.** 1993. Further isolation of murine herpesviruses from small mammals in southwestern Slovakia. Acta virologica **37:**101-105.
33. **Svobodova J, Blaskovic D, Mistrikova J.** 1982. Growth characteristics of herpesviruses isolated from free living small rodents. Acta virologica **26:**256-263.
34. **Blaskovic D, Stanekova D, Rajcani J.** 1984. Experimental pathogenesis of murine herpesvirus in newborn mice. Acta virologica **28:**225-231.
35. **Mistrikova J, Blaskovic D.** 1985. Ecology of the murine alphaherpesvirus and its isolation from lungs of rodents in cell culture. Acta virologica **29:**312-317.
36. **Rajcani J, Blaskovic D, Svobodova J, Ciampor F, Huckova D, Stanekova D.** 1985. Pathogenesis of acute and persistent murine herpesvirus infection in mice. Acta virologica **29:**51-60.
37. **Sunil-Chandra NP, Efstathiou S, Arno J, Nash AA.** 1992. Virological and pathological features of mice infected with murine gamma-herpesvirus 68. The Journal of general virology **73 (Pt 9):**2347-2356.
38. **Milho R, Smith CM, Marques S, Alenquer M, May JS, Gillet L, Gaspar M, Efstathiou S, Simas JP, Stevenson PG.** 2009. In vivo imaging of murid herpesvirus-4 infection. The Journal of general virology **90:**21-32.
39. **Nash AA, Sunil-Chandra NP.** 1994. Interactions of the murine gammaherpesvirus with the immune system. Current opinion in immunology **6:**560-563.
40. **Doherty PC, Christensen JP, Belz GT, Stevenson PG, Sangster MY.** 2001. Dissecting the host response to a gamma-herpesvirus. Philosophical transactions of the Royal Society of London. Series B, Biological sciences **356:**581-593.
41. **Weck KE, Barkon ML, Yoo LI, Speck SH, Virgin HI.** 1996. Mature B cells are required for acute splenic infection, but not for establishment of latency, by murine gammaherpesvirus 68. Journal of virology **70:**6775-6780.
42. **Sunil-Chandra NP, Efstathiou S, Nash AA.** 1992. Murine gammaherpesvirus 68 establishes a latent infection in mouse B lymphocytes in vivo. The Journal of general virology **73 (Pt 12):**3275-3279.

43. **Gaspar M, May JS, Sukla S, Frederico B, Gill MB, Smith CM, Belz GT, Stevenson PG.** 2011. Murid herpesvirus-4 exploits dendritic cells to infect B cells. PLoS pathogens **7:**e1002346.
44. **Usherwood EJ, Stewart JP, Robertson K, Allen DJ, Nash AA.** 1996. Absence of splenic latency in murine gammaherpesvirus 68-infected B cell-deficient mice. The Journal of general virology **77 (Pt 11):**2819-2825.
45. **Weck KE, Kim SS, Virgin HI, Speck SH.** 1999. B cells regulate murine gammaherpesvirus 68 latency. Journal of virology **73:**4651-4661.
46. **Marques S, Efstathiou S, Smith KG, Haury M, Simas JP.** 2003. Selective Gene Expression of Latent Murine Gammaherpesvirus 68 in B Lymphocytes. Journal of Virology **77:**7308-7318.
47. **Frederico B, Chao B, May JS, Belz GT, Stevenson PG.** 2014. A murid gamma-herpesviruses exploits normal splenic immune communication routes for systemic spread. Cell host & microbe **15:**457-470.
48. **Flano E, Woodland DL, Blackman MA.** 2002. A mouse model for infectious mononucleosis. Immunologic research **25:**201-217.
49. **Moser JM, Upton JW, Allen RD, 3rd, Wilson CB, Speck SH.** 2005. Role of B-cell proliferation in the establishment of gammaherpesvirus latency. Journal of virology **79:**9480-9491.
50. **Willer DO, Speck SH.** 2003. Long-term latent murine Gammaherpesvirus 68 infection is preferentially found within the surface immunoglobulin D-negative subset of splenic B cells in vivo. Journal of virology **77:**8310-8321.
51. **Suarez AL, van Dyk LF.** 2008. Endothelial cells support persistent gammaherpesvirus 68 infection. PLoS pathogens **4:**e1000152.
52. **Weck KE, Kim SS, Virgin HI, Speck SH.** 1999. Macrophages are the major reservoir of latent murine gammaherpesvirus 68 in peritoneal cells. Journal of virology **73:**3273-3283.
53. **Flano E, Husain SM, Sample JT, Woodland DL, Blackman MA.** 2000. Latent murine gamma-herpesvirus infection is established in activated B cells, dendritic cells, and macrophages. Journal of immunology **165:**1074-1081.
54. **Yu F, Feng J, Harada JN, Chanda SK, Kenney SC, Sun R.** 2007. B cell terminal differentiation factor XBP-1 induces reactivation of Kaposi's sarcoma-associated herpesvirus. FEBS letters **581:**3485-3488.
55. **Crawford DH, Ando I.** 1986. EB virus induction is associated with B-cell maturation. Immunology **59:**405-409.
56. **Laichalk LL, Thorley-Lawson DA.** 2005. Terminal differentiation into plasma cells initiates the replicative cycle of Epstein-Barr virus in vivo. Journal of virology **79:**1296-1307.
57. **Collins CM, Boss JM, Speck SH.** 2009. Identification of infected B-cell populations by using a recombinant murine gammaherpesvirus 68 expressing a fluorescent protein. Journal of virology **83:**6484-6493.

58. **Liang X, Collins CM, Mendel JB, Iwakoshi NN, Speck SH.** 2009. Gammaherpesvirus-driven plasma cell differentiation regulates virus reactivation from latently infected B lymphocytes. PLoS pathogens **5:**e1000677.
59. **Adler H, Messerle M, Wagner M, Koszinowski UH.** 2000. Cloning and mutagenesis of the murine gammaherpesvirus 68 genome as an infectious bacterial artificial chromosome. Journal of virology **74:**6964-6974.
60. **Nash AA, Dutia BM, Stewart JP, Davison AJ.** 2001. Natural history of murine gamma-herpesvirus infection. Philosophical transactions of the Royal Society of London. Series B, Biological sciences **356:**569-579.
61. **Virgin HWt, Latreille P, Wamsley P, Hallsworth K, Weck KE, Dal Canto AJ, Speck SH.** 1997. Complete sequence and genomic analysis of murine gammaherpesvirus 68. Journal of virology **71:**5894-5904.
62. **Efstathiou S, Ho YM, Hall S, Styles CJ, Scott SD, Gompels UA.** 1990. Murine herpesvirus 68 is genetically related to the gammaherpesviruses Epstein-Barr virus and herpesvirus saimiri. The Journal of general virology **71 (Pt 6):**1365-1372.
63. **Efstathiou S, Ho YM, Minson AC.** 1990. Cloning and molecular characterization of the murine herpesvirus 68 genome. The Journal of general virology **71 (Pt 6):**1355-1364.
64. **Alba MM, Das R, Orengo CA, Kellam P.** 2001. Genomewide function conservation and phylogeny in the Herpesviridae. Genome research **11:**43-54.
65. **Song MJ, Hwang S, Wong WH, Wu TT, Lee S, Liao HI, Sun R.** 2005. Identification of viral genes essential for replication of murine gamma-herpesvirus 68 using signature-tagged mutagenesis. Proceedings of the National Academy of Sciences of the United States of America **102:**3805-3810.
66. **Bowden RJ, Simas JP, Davis AJ, Efstathiou S.** 1997. Murine gammaherpesvirus 68 encodes tRNA-like sequences which are expressed during latency. The Journal of general virology **78 (Pt 7):**1675-1687.
67. **Husain SM, Usherwood EJ, Dyson H, Coleclough C, Coppola MA, Woodland DL, Blackman MA, Stewart JP, Sample JT.** 1999. Murine gammaherpesvirus M2 gene is latency-associated and its protein a target for CD8(+) T lymphocytes. Proceedings of the National Academy of Sciences of the United States of America **96:**7508-7513.
68. **Deiss LP, Chou J, Frenkel N.** 1986. Functional domains within the a sequence involved in the cleavage-packaging of herpes simplex virus DNA. Journal of virology **59:**605-618.
69. **Deng H, Chu JT, Park NH, Sun R.** 2004. Identification of cis sequences required for lytic DNA replication and packaging of murine gammaherpesvirus 68. Journal of virology **78:**9123-9131.
70. **Deng H, Dewhurst S.** 1998. Functional identification and analysis of cis-acting sequences which mediate genome cleavage and packaging in human herpesvirus 6. Journal of virology **72:**320-329.
71. **Raab-Traub N, Flynn K.** 1986. The structure of the termini of the Epstein-Barr virus as a marker of clonal cellular proliferation. Cell **47:**883-889.

72. **Sun R, Spain TA, Lin SF, Miller G.** 1997. Sp1 binds to the precise locus of end processing within the terminal repeats of Epstein-Barr virus DNA. Journal of virology **71:**6136-6143.
73. **Varmuza SL, Smiley JR.** 1985. Signals for site-specific cleavage of HSV DNA: maturation involves two separate cleavage events at sites distal to the recognition sequences. Cell **41:**793-802.
74. **Bellows DS, Chau BN, Lee P, Lazebnik Y, Burns WH, Hardwick JM.** 2000. Antiapoptotic herpesvirus Bcl-2 homologs escape caspase-mediated conversion to proapoptotic proteins. Journal of virology **74:**5024-5031.
75. **Henderson S, Huen D, Rowe M, Dawson C, Johnson G, Rickinson A.** 1993. Epstein-Barr virus-coded BHRF1 protein, a viral homologue of Bcl-2, protects human B cells from programmed cell death. Proceedings of the National Academy of Sciences of the United States of America **90:**8479-8483.
76. **Nava VE, Cheng EH, Veliuona M, Zou S, Clem RJ, Mayer ML, Hardwick JM.** 1997. Herpesvirus saimiri encodes a functional homolog of the human bcl-2 oncogene. Journal of virology **71:**4118-4122.
77. **Sarid R, Sato T, Bohenzky RA, Russo JJ, Chang Y.** 1997. Kaposi's sarcoma-associated herpesvirus encodes a functional bcl-2 homologue. Nature medicine **3:**293-298.
78. **Wang GH, Garvey TL, Cohen JI.** 1999. The murine gammaherpesvirus-68 M11 protein inhibits Fas- and TNF-induced apoptosis. The Journal of general virology **80 (Pt 10):**2737-2740.
79. **Tripp RA, Hamilton-Easton AM, Cardin RD, Nguyen P, Behm FG, Woodland DL, Doherty PC, Blackman MA.** 1997. Pathogenesis of an infectious mononucleosis-like disease induced by a murine gamma-herpesvirus: role for a viral superantigen? The Journal of experimental medicine **185:**1641-1650.
80. **Usherwood EJ, Ross AJ, Allen DJ, Nash AA.** 1996. Murine gammaherpesvirus-induced splenomegaly: a critical role for CD4 T cells. The Journal of general virology **77 (Pt 4):**627-630.
81. **Babcock GJ, Decker LL, Volk M, Thorley-Lawson DA.** 1998. EBV persistence in memory B cells in vivo. Immunity **9:**395-404.
82. **Ehtisham S, Sunil-Chandra NP, Nash AA.** 1993. Pathogenesis of murine gammaherpesvirus infection in mice deficient in CD4 and CD8 T cells. Journal of virology **67:**5247-5252.
83. **Flano E, Kim IJ, Woodland DL, Blackman MA.** 2002. Gamma-herpesvirus latency is preferentially maintained in splenic germinal center and memory B cells. The Journal of experimental medicine **196:**1363-1372.
84. **Hochberg D, Middeldorp JM, Catalina M, Sullivan JL, Luzuriaga K, Thorley-Lawson DA.** 2004. Demonstration of the Burkitt's lymphoma Epstein-Barr virus phenotype in dividing latently infected memory cells in vivo. Proceedings of the National Academy of Sciences of the United States of America **101:**239-244.

85. **Sunil-Chandra NP, Arno J, Fazakerley J, Nash AA.** 1994. Lymphoproliferative disease in mice infected with murine gammaherpesvirus 68. The American journal of pathology **145:**818-826.
86. **Tarakanova VL, Suarez F, Tibbetts SA, Jacoby MA, Weck KE, Hess JL, Speck SH, Virgin HWt.** 2005. Murine gammaherpesvirus 68 infection is associated with lymphoproliferative disease and lymphoma in BALB beta2 microglobulin-deficient mice. Journal of virology **79:**14668-14679.
87. **Lee KS, Groshong SD, Cool CD, Kleinschmidt-DeMasters BK, van Dyk LF.** 2009. Murine gammaherpesvirus 68 infection of IFNgamma unresponsive mice: a small animal model for gammaherpesvirus-associated B-cell lymphoproliferative disease. Cancer research **69:**5481-5489.
88. **Usherwood EJ, Stewart JP, Nash AA.** 1996. Characterization of tumor cell lines derived from murine gammaherpesvirus-68-infected mice. Journal of virology **70:**6516-6518.
89. **Cesarman E, Nador RG, Bai F, Bohenzky RA, Russo JJ, Moore PS, Chang Y, Knowles DM.** 1996. Kaposi's sarcoma-associated herpesvirus contains G protein-coupled receptor and cyclin D homologs which are expressed in Kaposi's sarcoma and malignant lymphoma. Journal of virology **70:**8218-8223.
90. **Jung JU, Stager M, Desrosiers RC.** 1994. Virus-encoded cyclin. Molecular and cellular biology **14:**7235-7244.
91. **Arvanitakis L, Yaseen N, Sharma S.** 1995. Latent membrane protein-1 induces cyclin D2 expression, pRb hyperphosphorylation, and loss of TGF-beta 1-mediated growth inhibition in EBV-positive B cells. Journal of immunology **155:**1047-1056.
92. **Cannell EJ, Farrell PJ, Sinclair AJ.** 1996. Epstein-Barr virus exploits the normal cell pathway to regulate Rb activity during the immortalisation of primary B-cells. Oncogene **13:**1413-1421.
93. **Wilson JB, Weinberg W, Johnson R, Yuspa S, Levine AJ.** 1990. Expression of the BNLF-1 oncogene of Epstein-Barr virus in the skin of transgenic mice induces hyperplasia and aberrant expression of keratin 6. Cell **61:**1315-1327.
94. **Sinclair AJ, Palmero I, Holder A, Peters G, Farrell PJ.** 1995. Expression of cyclin D2 in Epstein-Barr virus-positive Burkitt's lymphoma cell lines is related to methylation status of the gene. Journal of virology **69:**1292-1295.
95. **van Dyk LF, Hess JL, Katz JD, Jacoby M, Speck SH, Virgin HI.** 1999. The murine gammaherpesvirus 68 v-cyclin gene is an oncogene that promotes cell cycle progression in primary lymphocytes. Journal of virology **73:**5110-5122.
96. **Liang X, Paden CR, Morales FM, Powers RP, Jacob J, Speck SH.** 2011. Murine gamma-herpesvirus immortalization of fetal liver-derived B cells requires both the viral cyclin D homolog and latency-associated nuclear antigen. PLoS pathogens **7:**e1002220.
97. **Wu TT, Usherwood EJ, Stewart JP, Nash AA, Sun R.** 2000. Rta of murine gammaherpesvirus 68 reactivates the complete lytic cycle from latency. Journal of virology **74:**3659-3667.

98. **Sun R, Lin SF, Gradoville L, Yuan Y, Zhu F, Miller G.** 1998. A viral gene that activates lytic cycle expression of Kaposi's sarcoma-associated herpesvirus. Proceedings of the National Academy of Sciences of the United States of America **95:**10866-10871.
99. **Lukac DM, Kirshner JR, Ganem D.** 1999. Transcriptional activation by the product of open reading frame 50 of Kaposi's sarcoma-associated herpesvirus is required for lytic viral reactivation in B cells. Journal of virology **73:**9348-9361.
100. **Feederle R, Kost M, Baumann M, Janz A, Drouet E, Hammerschmidt W, Delecluse HJ.** 2000. The Epstein-Barr virus lytic program is controlled by the co-operative functions of two transactivators. The EMBO journal **19:**3080-3089.
101. **Goodwin DJ, Walters MS, Smith PG, Thurau M, Fickenscher H, Whitehouse A.** 2001. Herpesvirus saimiri open reading frame 50 (Rta) protein reactivates the lytic replication cycle in a persistently infected A549 cell line. Journal of virology **75:**4008-4013.
102. **Xu Y, AuCoin DP, Huete AR, Cei SA, Hanson LJ, Pari GS.** 2005. A Kaposi's sarcoma-associated herpesvirus/human herpesvirus 8 ORF50 deletion mutant is defective for reactivation of latent virus and DNA replication. Journal of virology **79:**3479-3487.
103. **Pavlova IV, Virgin HW, Speck SH.** 2003. Disruption of Gammaherpesvirus 68 Gene 50 Demonstrates that Rta Is Essential for Virus Replication. Journal of Virology **77:**5731-5739.
104. **Gradoville L, Gerlach J, Grogan E, Shedd D, Nikiforow S, Metroka C, Miller G.** 2000. Kaposi's sarcoma-associated herpesvirus open reading frame 50/Rta protein activates the entire viral lytic cycle in the HH-B2 primary effusion lymphoma cell line. Journal of virology **74:**6207-6212.
105. **Lukac DM, Renne R, Kirshner JR, Ganem D.** 1998. Reactivation of Kaposi's sarcoma-associated herpesvirus infection from latency by expression of the ORF 50 transactivator, a homolog of the EBV R protein. Virology **252:**304-312.
106. **Chen H, Lee JM, Wang Y, Huang DP, Ambinder RF, Hayward SD.** 1999. The Epstein-Barr virus latency BamHI-Q promoter is positively regulated by STATs and Zta interference with JAK/STAT activation leads to loss of BamHI-Q promoter activity. Proceedings of the National Academy of Sciences of the United States of America **96:**9339-9344.
107. **Cox MA, Leahy J, Hardwick JM.** 1990. An enhancer within the divergent promoter of Epstein-Barr virus responds synergistically to the R and Z transactivators. Journal of virology **64:**313-321.
108. **Quinlivan EB, Holley-Guthrie EA, Norris M, Gutsch D, Bachenheimer SL, Kenney SC.** 1993. Direct BRLF1 binding is required for cooperative BZLF1/BRLF1 activation of the Epstein-Barr virus early promoter, BMRF1. Nucleic acids research **21:**1999-2007.
109. **Ragoczy T, Heston L, Miller G.** 1998. The Epstein-Barr virus Rta protein activates lytic cycle genes and can disrupt latency in B lymphocytes. Journal of virology **72:**7978-7984.

110. **Ragoczy T, Miller G.** 2001. Autostimulation of the Epstein-Barr virus BRLF1 promoter is mediated through consensus Sp1 and Sp3 binding sites. Journal of virology **75:**5240-5251.
111. **Russo JJ, Bohenzky RA, Chien MC, Chen J, Yan M, Maddalena D, Parry JP, Peruzzi D, Edelman IS, Chang Y, Moore PS.** 1996. Nucleotide sequence of the Kaposi sarcoma-associated herpesvirus (HHV8). Proceedings of the National Academy of Sciences of the United States of America **93:**14862-14867.
112. **Zalani S, Holley-Guthrie E, Kenney S.** 1996. Epstein-Barr viral latency is disrupted by the immediate-early BRLF1 protein through a cell-specific mechanism. Proceedings of the National Academy of Sciences of the United States of America **93:**9194-9199.
113. **Deng H, Young A, Sun R.** 2000. Auto-activation of the rta gene of human herpesvirus-8/Kaposi's sarcoma-associated herpesvirus. The Journal of general virology **81:**3043-3048.
114. **Liu P, Speck SH.** 2003. Synergistic autoactivation of the Epstein-Barr virus immediate-early BRLF1 promoter by Rta and Zta. Virology **310:**199-206.
115. **Pavlova I, Lin CY, Speck SH.** 2005. Murine gammaherpesvirus 68 Rta-dependent activation of the gene 57 promoter. Virology **333:**169-179.
116. **Shin HJ, DeCotiis J, Giron M, Palmeri D, Lukac DM.** 2014. Histone deacetylase classes I and II regulate Kaposi's sarcoma-associated herpesvirus reactivation. Journal of virology **88:**1281-1292.
117. **Bhende PM, Seaman WT, Delecluse HJ, Kenney SC.** 2005. BZLF1 activation of the methylated form of the BRLF1 immediate-early promoter is regulated by BZLF1 residue 186. Journal of virology **79:**7338-7348.
118. **Chang LK, Liu ST.** 2000. Activation of the BRLF1 promoter and lytic cycle of Epstein-Barr virus by histone acetylation. Nucleic acids research **28:**3918-3925.
119. **Chen J, Ueda K, Sakakibara S, Okuno T, Parravicini C, Corbellino M, Yamanishi K.** 2001. Activation of latent Kaposi's sarcoma-associated herpesvirus by demethylation of the promoter of the lytic transactivator. Proceedings of the National Academy of Sciences of the United States of America **98:**4119-4124.
120. **Countryman JK, Gradoville L, Miller G.** 2008. Histone hyperacetylation occurs on promoters of lytic cycle regulatory genes in Epstein-Barr virus-infected cell lines which are refractory to disruption of latency by histone deacetylase inhibitors. Journal of virology **82:**4706-4719.
121. **DeWire SM, McVoy MA, Damania B.** 2002. Kinetics of expression of rhesus monkey rhadinovirus (RRV) and identification and characterization of a polycistronic transcript encoding the RRV Orf50/Rta, RRV R8, and R8.1 genes. Journal of virology **76:**9819-9831.
122. **Goodwin MM, Molleston JM, Canny S, Abou El Hassan M, Willert EK, Bremner R, Virgin HW.** 2010. Histone deacetylases and the nuclear receptor corepressor regulate lytic-latent switch gene 50 in murine gammaherpesvirus 68-infected macrophages. Journal of virology **84:**12039-12047.

123. **Gray KS, Forrest JC, Speck SH.** 2010. The de novo methyltransferases DNMT3a and DNMT3b target the murine gammaherpesvirus immediate-early gene 50 promoter during establishment of latency. Journal of virology **84:**4946-4959.
124. **Gwack Y, Byun H, Hwang S, Lim C, Choe J.** 2001. CREB-binding protein and histone deacetylase regulate the transcriptional activity of Kaposi's sarcoma-associated herpesvirus open reading frame 50. Journal of virology **75:**1909-1917.
125. **Gwack Y, Hwang S, Lim C, Won YS, Lee CH, Choe J.** 2002. Kaposi's Sarcoma-associated herpesvirus open reading frame 50 stimulates the transcriptional activity of STAT3. The Journal of biological chemistry **277:**6438-6442.
126. **Klass CM, Krug LT, Pozharskaya VP, Offermann MK.** 2005. The targeting of primary effusion lymphoma cells for apoptosis by inducing lytic replication of human herpesvirus 8 while blocking virus production. Blood **105:**4028-4034.
127. **Luka J, Kallin B, Klein G.** 1979. Induction of the Epstein-Barr virus (EBV) cycle in latently infected cells by n-butyrate. Virology **94:**228-231.
128. **Shaw RN, Arbiser JL, Offermann MK.** 2000. Valproic acid induces human herpesvirus 8 lytic gene expression in BCBL-1 cells. Aids **14:**899-902.
129. **Wang SE, Wu FY, Chen H, Shamay M, Zheng Q, Hayward GS.** 2004. Early activation of the Kaposi's sarcoma-associated herpesvirus RTA, RAP, and MTA promoters by the tetradecanoyl phorbol acetate-induced AP1 pathway. Journal of virology **78:**4248-4267.
130. **Xie J, Pan H, Yoo S, Gao SJ.** 2005. Kaposi's sarcoma-associated herpesvirus induction of AP-1 and interleukin 6 during primary infection mediated by multiple mitogen-activated protein kinase pathways. Journal of virology **79:**15027-15037.
131. **Lu F, Zhou J, Wiedmer A, Madden K, Yuan Y, Lieberman PM.** 2003. Chromatin remodeling of the Kaposi's sarcoma-associated herpesvirus ORF50 promoter correlates with reactivation from latency. Journal of virology **77:**11425-11435.
132. **Ye J, Shedd D, Miller G.** 2005. An Sp1 response element in the Kaposi's sarcoma-associated herpesvirus open reading frame 50 promoter mediates lytic cycle induction by butyrate. Journal of virology **79:**1397-1408.
133. **Li X, Feng J, Chen S, Peng L, He WW, Qi J, Deng H, Sun R.** 2010. Tpl2/AP-1 enhances murine gammaherpesvirus 68 lytic replication. Journal of virology **84:**1881-1890.
134. **Staskus KA, Sun R, Miller G, Racz P, Jaslowski A, Metroka C, Brett-Smith H, Haase AT.** 1999. Cellular tropism and viral interleukin-6 expression distinguish human herpesvirus 8 involvement in Kaposi's sarcoma, primary effusion lymphoma, and multicentric Castleman's disease. Journal of virology **73:**4181-4187.
135. **Johnson AS, Maronian N, Vieira J.** 2005. Activation of Kaposi's sarcoma-associated herpesvirus lytic gene expression during epithelial differentiation. Journal of virology **79:**13769-13777.
136. **Du MQ, Liu H, Diss TC, Ye H, Hamoudi RA, Dupin N, Meignin V, Oksenhendler E, Boshoff C, Isaacson PG.** 2001. Kaposi sarcoma-associated herpesvirus infects

monotypic (IgM lambda) but polyclonal naive B cells in Castleman disease and associated lymphoproliferative disorders. Blood **97:**2130-2136.

137. **Reimold AM, Iwakoshi NN, Manis J, Vallabhajosyula P, Szomolanyi-Tsuda E, Gravallese EM, Friend D, Grusby MJ, Alt F, Glimcher LH.** 2001. Plasma cell differentiation requires the transcription factor XBP-1. Nature **412:**300-307.
138. **Dalton-Griffin L, Wilson SJ, Kellam P.** 2009. X-box binding protein 1 contributes to induction of the Kaposi's sarcoma-associated herpesvirus lytic cycle under hypoxic conditions. Journal of virology **83:**7202-7209.
139. **Wilson SJ, Tsao EH, Webb BL, Ye H, Dalton-Griffin L, Tsantoulas C, Gale CV, Du MQ, Whitehouse A, Kellam P.** 2007. X box binding protein XBP-1s transactivates the Kaposi's sarcoma-associated herpesvirus (KSHV) ORF50 promoter, linking plasma cell differentiation to KSHV reactivation from latency. Journal of virology **81:**13578-13586.
140. **Polcicova K, Hrabovska Z, Mistrikova J, Tomaskova J, Pastorek J, Pastorekova S, Kopacek J.** 2008. Up-regulation of Murid herpesvirus 4 ORF50 by hypoxia: possible implication for virus reactivation from latency. Virus research **132:**257-262.
141. **Chen X, Iliopoulos D, Zhang Q, Tang Q, Greenblatt MB, Hatziapostolou M, Lim E, Tam WL, Ni M, Chen Y, Mai J, Shen H, Hu DZ, Adoro S, Hu B, Song M, Tan C, Landis MD, Ferrari M, Shin SJ, Brown M, Chang JC, Liu XS, Glimcher LH.** 2014. XBP1 promotes triple-negative breast cancer by controlling the HIF1alpha pathway. Nature **508:**103-107.
142. **Sakakibara S, Ueda K, Chen J, Okuno T, Yamanishi K.** 2001. Octamer-binding sequence is a key element for the autoregulation of Kaposi's sarcoma-associated herpesvirus ORF50/Lyta gene expression. Journal of virology **75:**6894-6900.
143. **Harrison SM, Whitehouse A.** 2008. Kaposi's sarcoma-associated herpesvirus (KSHV) Rta and cellular HMGB1 proteins synergistically transactivate the KSHV ORF50 promoter. FEBS letters **582:**3080-3084.
144. **Wang SE, Wu FY, Yu Y, Hayward GS.** 2003. CCAAT/enhancer-binding protein-alpha is induced during the early stages of Kaposi's sarcoma-associated herpesvirus (KSHV) lytic cycle reactivation and together with the KSHV replication and transcription activator (RTA) cooperatively stimulates the viral RTA, MTA, and PAN promoters. Journal of virology **77:**9590-9612.
145. **Reese TA, Wakeman BS, Choi HS, Hufford MM, Huang SC, Zhang X, Buck MD, Jezewski A, Kambal A, Liu CY, Goel G, Murray PJ, Xavier RJ, Kaplan MH, Renne R, Speck SH, Artyomov MN, Pearce EJ, Virgin HW.** 2014. Coinfection. Helminth infection reactivates latent gamma-herpesvirus via cytokine competition at a viral promoter. Science **345:**573-577.
146. **Saveliev A, Zhu F, Yuan Y.** 2002. Transcription mapping and expression patterns of genes in the major immediate-early region of Kaposi's sarcoma-associated herpesvirus. Virology **299:**301-314.

147. **Tang S, Zheng ZM.** 2002. Kaposi's sarcoma-associated herpesvirus K8 exon 3 contains three 5'-splice sites and harbors a K8.1 transcription start site. The Journal of biological chemistry **277:**14547-14556.
148. **Wang Y, Chong OT, Yuan Y.** 2004. Differential regulation of K8 gene expression in immediate-early and delayed-early stages of Kaposi's sarcoma-associated herpesvirus. Virology **325:**149-163.
149. **Whitehouse A, Carr IM, Griffiths JC, Meredith DM.** 1997. The herpesvirus saimiri ORF50 gene, encoding a transcriptional activator homologous to the Epstein-Barr virus R protein, is transcribed from two distinct promoters of different temporal phases. Journal of virology **71:**2550-2554.
150. **Liu S, Pavlova IV, Virgin HWt, Speck SH.** 2000. Characterization of gammaherpesvirus 68 gene 50 transcription. Journal of virology **74:**2029-2037.
151. **Wakeman BS, Johnson LS, Paden CR, Gray KS, Virgin HW, Speck SH.** 2014. Identification of alternative transcripts encoding the essential murine gammaherpesvirus lytic transactivator RTA. Journal of virology **88:**5474-5490.
152. **Yu Y, Wang SE, Hayward GS.** 2005. The KSHV immediate-early transcription factor RTA encodes ubiquitin E3 ligase activity that targets IRF7 for proteosome-mediated degradation. Immunity **22:**59-70.
153. **Dong X, He Z, Durakoglugil D, Arneson L, Shen Y, Feng P.** 2012. Murine gammaherpesvirus 68 evades host cytokine production via replication transactivator-induced RelA degradation. Journal of virology **86:**1930-1941.
154. **Damania B, Jeong JH, Bowser BS, DeWire SM, Staudt MR, Dittmer DP.** 2004. Comparison of the Rta/Orf50 Transactivator Proteins of Gamma-2-Herpesviruses. Journal of Virology **78:**5491-5499.
155. **Wang S, Liu S, Wu M, Geng Y, Wood C.** 2001. Kaposi's sarcoma-associated herpesvirus/human herpesvirus-8 ORF50 gene product contains a potent C-terminal activation domain which activates gene expression via a specific target sequence. Archives of virology **146:**1415-1426.
156. **Seaman WT, Ye D, Wang RX, Hale EE, Weisse M, Quinlivan EB.** 1999. Gene expression from the ORF50/K8 region of Kaposi's sarcoma-associated herpesvirus. Virology **263:**436-449.
157. **Wu TT, Tong L, Rickabaugh T, Speck S, Sun R.** 2001. Function of Rta is essential for lytic replication of murine gammaherpesvirus 68. Journal of virology **75:**9262-9273.
158. **Tsai WH, Wang PW, Lin SY, Wu IL, Ko YC, Chen YL, Li M, Lin SF.** 2012. Ser-634 and Ser-636 of Kaposi's Sarcoma-Associated Herpesvirus RTA are Involved in Transactivation and are Potential Cdk9 Phosphorylation Sites. Frontiers in microbiology **3:**60.
159. **Dong X, Feng H, Sun Q, Li H, Wu TT, Sun R, Tibbetts SA, Chen ZJ, Feng P.** 2010. Murine gamma-herpesvirus 68 hijacks MAVS and IKKbeta to initiate lytic replication. PLoS pathogens **6:**e1001001.

160. **Chang PJ, Shedd D, Gradoville L, Cho MS, Chen LW, Chang J, Miller G.** 2002. Open Reading Frame 50 Protein of Kaposi's Sarcoma-Associated Herpesvirus Directly Activates the Viral PAN and K12 Genes by Binding to Related Response Elements. Journal of Virology **76:**3168-3178.
161. **Chang PJ, Shedd D, Miller G.** 2005. Two subclasses of Kaposi's sarcoma-associated herpesvirus lytic cycle promoters distinguished by open reading frame 50 mutant proteins that are deficient in binding to DNA. Journal of virology **79:**8750-8763.
162. **Chen J, Ye F, Xie J, Kuhne K, Gao SJ.** 2009. Genome-wide identification of binding sites for Kaposi's sarcoma-associated herpesvirus lytic switch protein, RTA. Virology **386:**290-302.
163. **Deng H, Song MJ, Chu JT, Sun R.** 2002. Transcriptional regulation of the interleukin-6 gene of human herpesvirus 8 (Kaposi's sarcoma-associated herpesvirus). Journal of virology **76:**8252-8264.
164. **Lukac DM, Garibyan L, Kirshner JR, Palmeri D, Ganem D.** 2001. DNA binding by Kaposi's sarcoma-associated herpesvirus lytic switch protein is necessary for transcriptional activation of two viral delayed early promoters. Journal of virology **75:**6786-6799.
165. **Song MJ, Deng H, Sun R.** 2003. Comparative study of regulation of RTA-responsive genes in Kaposi's sarcoma-associated herpesvirus/human herpesvirus 8. Journal of virology **77:**9451-9462.
166. **Song MJ, Li X, Brown HJ, Sun R.** 2002. Characterization of interactions between RTA and the promoter of polyadenylated nuclear RNA in Kaposi's sarcoma-associated herpesvirus/human herpesvirus 8. Journal of virology **76:**5000-5013.
167. **Ueda K, Ishikawa K, Nishimura K, Sakakibara S, Do E, Yamanishi K.** 2002. Kaposi's sarcoma-associated herpesvirus (human herpesvirus 8) replication and transcription factor activates the K9 (vIRF) gene through two distinct cis elements by a non-DNA-binding mechanism. Journal of virology **76:**12044-12054.
168. **Zhang L, Chiu J, Lin JC.** 1998. Activation of human herpesvirus 8 (HHV-8) thymidine kinase (TK) TATAA-less promoter by HHV-8 ORF50 gene product is SP1 dependent. DNA and cell biology **17:**735-742.
169. **Wen HJ, Minhas V, Wood C.** 2009. Identification and characterization of a new Kaposi's sarcoma-associated herpesvirus replication and transcription activator (RTA)-responsive element involved in RTA-mediated transactivation. The Journal of general virology **90:**944-953.
170. **Duan W, Wang S, Liu S, Wood C.** 2001. Characterization of Kaposi's sarcoma-associated herpesvirus/human herpesvirus-8 ORF57 promoter. Archives of virology **146:**403-413.
171. **Allen RD, 3rd, DeZalia MN, Speck SH.** 2007. Identification of an Rta responsive promoter involved in driving gammaHV68 v-cyclin expression during virus replication. Virology **365:**250-259.

172. **Coleman HM, Brierley I, Stevenson PG.** 2003. An internal ribosome entry site directs translation of the murine gammaherpesvirus 68 MK3 open reading frame. Journal of virology **77:**13093-13105.
173. **O'Flaherty BM, Soni T, Wakeman BS, Speck SH.** 2014. The murine gammaherpesvirus immediate-early Rta synergizes with IRF4, targeting expression of the viral M1 superantigen to plasma cells. PLoS pathogens **10:**e1004302.
174. **Hong Y, Qi J, Gong D, Han C, Deng H.** 2011. Replication and transcription activator (RTA) of murine gammaherpesvirus 68 binds to an RTA-responsive element and activates the expression of ORF18. Journal of virology **85:**11338-11350.
175. **Qi J, Han C, Gong D, Liu P, Zhou S, Deng H.** 2015. Murine Gammaherpesvirus 68 ORF48 Is an RTA-Responsive Gene Product and Functions in both Viral Lytic Replication and Latency during In Vivo Infection. Journal of virology **89:**5788-5800.
176. **Gwack Y, Baek HJ, Nakamura H, Lee SH, Meisterernst M, Roeder RG, Jung JU.** 2003. Principal role of TRAP/mediator and SWI/SNF complexes in Kaposi's sarcoma-associated herpesvirus RTA-mediated lytic reactivation. Molecular and cellular biology **23:**2055-2067.
177. **Song MJ, Hwang S, Wong W, Round J, Martinez-Guzman D, Turpaz Y, Liang J, Wong B, Johnson RC, Carey M, Sun R.** 2004. The DNA architectural protein HMGB1 facilitates RTA-mediated viral gene expression in gamma-2 herpesviruses. Journal of virology **78:**12940-12950.
178. **Liang Y, Chang J, Lynch SJ, Lukac DM, Ganem D.** 2002. The lytic switch protein of KSHV activates gene expression via functional interaction with RBP-Jkappa (CSL), the target of the Notch signaling pathway. Genes & development **16:**1977-1989.
179. **Liang Y, Ganem D.** 2003. Lytic but not latent infection by Kaposi's sarcoma-associated herpesvirus requires host CSL protein, the mediator of Notch signaling. Proceedings of the National Academy of Sciences of the United States of America **100:**8490-8495.
180. **Carroll KD, Khadim F, Spadavecchia S, Palmeri D, Lukac DM.** 2007. Direct interactions of Kaposi's sarcoma-associated herpesvirus/human herpesvirus 8 ORF50/Rta protein with the cellular protein octamer-1 and DNA are critical for specifying transactivation of a delayed-early promoter and stimulating viral reactivation. Journal of virology **81:**8451-8467.
181. **Palmeri D, Carroll KD, Gonzalez-Lopez O, Lukac DM.** 2011. Kaposi's sarcoma-associated herpesvirus Rta tetramers make high-affinity interactions with repetitive DNA elements in the Mta promoter to stimulate DNA binding of RBP-Jk/CSL. Journal of virology **85:**11901-11915.
182. **Brown HJ, Song MJ, Deng H, Wu TT, Cheng G, Sun R.** 2003. NF-kappaB inhibits gammaherpesvirus lytic replication. Journal of virology **77:**8532-8540.
183. **Gwack Y, Nakamura H, Lee SH, Souvlis J, Yustein JT, Gygi S, Kung HJ, Jung JU.** 2003. Poly(ADP-ribose) polymerase 1 and Ste20-like kinase hKFC act as transcriptional repressors for gamma-2 herpesvirus lytic replication. Molecular and cellular biology **23:**8282-8294.

184. **Yang Z, Wood C.** 2007. The transcriptional repressor K-RBP modulates RTA-mediated transactivation and lytic replication of Kaposi's sarcoma-associated herpesvirus. Journal of virology **81:**6294-6306.
185. **Krug LT, Collins CM, Gargano LM, Speck SH.** 2009. NF-kappaB p50 plays distinct roles in the establishment and control of murine gammaherpesvirus 68 latency. Journal of virology **83:**4732-4748.
186. **Krug LT, Moser JM, Dickerson SM, Speck SH.** 2007. Inhibition of NF-kappaB activation in vivo impairs establishment of gammaherpesvirus latency. PLoS pathogens **3:**e11.
187. **Kawai T, Akira S.** 2007. TLR signaling. Seminars in immunology **19:**24-32.
188. **Takeda K, Akira S.** 2007. Toll-like receptors. Current protocols in immunology / edited by John E. Coligan ... [et al.] **Chapter 14:**Unit 14 12.
189. **Oeckinghaus A, Ghosh S.** 2009. The NF-kappaB family of transcription factors and its regulation. Cold Spring Harbor perspectives in biology **1:**a000034.
190. **Connelly MA, Marcu KB.** 1995. CHUK, a new member of the helix-loop-helix and leucine zipper families of interacting proteins, contains a serine-threonine kinase catalytic domain. Cellular & molecular biology research **41:**537-549.
191. **Senftleben U, Karin M.** 2002. The IKK/NF-kappaB pathway. Critical care medicine **30:**S18-S26.
192. **Pasparakis M, Luedde T, Schmidt-Supprian M.** 2006. Dissection of the NF-kappaB signalling cascade in transgenic and knockout mice. Cell death and differentiation **13:**861-872.
193. **Le Clorennec C, Ouk TS, Youlyouz-Marfak I, Panteix S, Martin CC, Rastelli J, Adriaenssens E, Zimber-Strobl U, Coll J, Feuillard J, Jayat-Vignoles C.** 2008. Molecular basis of cytotoxicity of Epstein-Barr virus (EBV) latent membrane protein 1 (LMP1) in EBV latency III B cells: LMP1 induces type II ligand-independent autoactivation of CD95/Fas with caspase 8-mediated apoptosis. Journal of virology **82:**6721-6733.
194. **Grimm T, Schneider S, Naschberger E, Huber J, Guenzi E, Kieser A, Reitmeir P, Schulz TF, Morris CA, Sturzl M.** 2005. EBV latent membrane protein-1 protects B cells from apoptosis by inhibition of BAX. Blood **105:**3263-3269.
195. **Uchida J, Yasui T, Takaoka-Shichijo Y, Muraoka M, Kulwichit W, Raab-Traub N, Kikutani H.** 1999. Mimicry of CD40 signals by Epstein-Barr virus LMP1 in B lymphocyte responses. Science **286:**300-303.
196. **Zhao B, Barrera LA, Ersing I, Willox B, Schmidt SC, Greenfeld H, Zhou H, Mollo SB, Shi TT, Takasaki K, Jiang S, Cahir-McFarland E, Kellis M, Bulyk ML, Kieff E, Gewurz BE.** 2014. The NF-kappaB genomic landscape in lymphoblastoid B cells. Cell reports **8:**1595-1606.
197. **Ersing I, Bernhardt K, Gewurz BE.** 2013. NF-kappaB and IRF7 pathway activation by Epstein-Barr virus Latent Membrane Protein 1. Viruses **5:**1587-1606.

198. **Guasparri I, Bubman D, Cesarman E.** 2008. EBV LMP2A affects LMP1-mediated NF-kappaB signaling and survival of lymphoma cells by regulating TRAF2 expression. Blood **111:**3813-3820.
199. **Dawson CW, George JH, Blake SM, Longnecker R, Young LS.** 2001. The Epstein-Barr virus encoded latent membrane protein 2A augments signaling from latent membrane protein 1. Virology **289:**192-207.
200. **Ariza ME, Glaser R, Kaumaya PT, Jones C, Williams MV.** 2009. The EBV-encoded dUTPase activates NF-kappa B through the TLR2 and MyD88-dependent signaling pathway. Journal of immunology **182:**851-859.
201. **Chang LS, Wang JT, Doong SL, Lee CP, Chang CW, Tsai CH, Yeh SW, Hsieh CY, Chen MR.** 2012. Epstein-Barr virus BGLF4 kinase downregulates NF-kappaB transactivation through phosphorylation of coactivator UXT. Journal of virology **86:**12176-12186.
202. **Konrad A, Wies E, Thurau M, Marquardt G, Naschberger E, Hentschel S, Jochmann R, Schulz TF, Erfle H, Brors B, Lausen B, Neipel F, Sturzl M.** 2009. A systems biology approach to identify the combination effects of human herpesvirus 8 genes on NF-kappaB activation. Journal of virology **83:**2563-2574.
203. **Chaudhary PM, Jasmin A, Eby MT, Hood L.** 1999. Modulation of the NF-kappa B pathway by virally encoded death effector domains-containing proteins. Oncogene **18:**5738-5746.
204. **Brinkmann MM, Glenn M, Rainbow L, Kieser A, Henke-Gendo C, Schulz TF.** 2003. Activation of mitogen-activated protein kinase and NF-kappaB pathways by a Kaposi's sarcoma-associated herpesvirus K15 membrane protein. Journal of virology **77:**9346-9358.
205. **Prakash O, Tang ZY, Peng X, Coleman R, Gill J, Farr G, Samaniego F.** 2002. Tumorigenesis and aberrant signaling in transgenic mice expressing the human herpesvirus-8 K1 gene. Journal of the National Cancer Institute **94:**926-935.
206. **Samaniego F, Pati S, Karp JE, Prakash O, Bose D.** 2001. Human herpesvirus 8 K1-associated nuclear factor-kappa B-dependent promoter activity: role in Kaposi's sarcoma inflammation? Journal of the National Cancer Institute. Monographs**:**15-23.
207. **Guasparri I, Keller SA, Cesarman E.** 2004. KSHV vFLIP is essential for the survival of infected lymphoma cells. The Journal of experimental medicine **199:**993-1003.
208. **Guasparri I, Wu H, Cesarman E.** 2006. The KSHV oncoprotein vFLIP contains a TRAF-interacting motif and requires TRAF2 and TRAF3 for signalling. EMBO reports **7:**114-119.
209. **Seo T, Park J, Lim C, Choe J.** 2004. Inhibition of nuclear factor kappaB activity by viral interferon regulatory factor 3 of Kaposi's sarcoma-associated herpesvirus. Oncogene **23:**6146-6155.
210. **He S, Zhao J, Song S, He X, Minassian A, Zhou Y, Zhang J, Brulois K, Wang Y, Cabo J, Zandi E, Liang C, Jung JU, Zhang X, Feng P.** 2015. Viral pseudo-enzymes activate RIG-I via deamidation to evade cytokine production. Molecular cell **58:**134-146.

211. **Verzijl D, Fitzsimons CP, Van Dijk M, Stewart JP, Timmerman H, Smit MJ, Leurs R.** 2004. Differential activation of murine herpesvirus 68- and Kaposi's sarcoma-associated herpesvirus-encoded ORF74 G protein-coupled receptors by human and murine chemokines. Journal of virology **78:**3343-3351.
212. **Morrison TE, Kenney SC.** 2004. BZLF1, an Epstein-Barr virus immediate-early protein, induces p65 nuclear translocation while inhibiting p65 transcriptional function. Virology **328:**219-232.
213. **Gutsch DE, Holley-Guthrie EA, Zhang Q, Stein B, Blanar MA, Baldwin AS, Kenney SC.** 1994. The bZIP transactivator of Epstein-Barr virus, BZLF1, functionally and physically interacts with the p65 subunit of NF-kappa B. Molecular and cellular biology **14:**1939-1948.
214. **Yang Z, Yan Z, Wood C.** 2008. Kaposi's sarcoma-associated herpesvirus transactivator RTA promotes degradation of the repressors to regulate viral lytic replication. Journal of virology **82:**3590-3603.
215. **Rodrigues L, Filipe J, Seldon MP, Fonseca L, Anrather J, Soares MP, Simas JP.** 2009. Termination of NF-kappaB activity through a gammaherpesvirus protein that assembles an EC5S ubiquitin-ligase. The EMBO journal **28:**1283-1295.
216. **Kim IJ, Flano E, Woodland DL, Lund FE, Randall TD, Blackman MA.** 2003. Maintenance of long term gamma-herpesvirus B cell latency is dependent on CD40-mediated development of memory B cells. Journal of immunology **171:**886-892.
217. **Gargano LM, Moser JM, Speck SH.** 2008. Role for MyD88 signaling in murine gammaherpesvirus 68 latency. Journal of virology **82:**3853-3863.
218. **Heslop HE.** 2005. Biology and treatment of Epstein-Barr virus-associated non-Hodgkin lymphomas. Hematology / the Education Program of the American Society of Hematology. American Society of Hematology. Education Program**:**260-266.
219. **Carbone A, Cesarman E, Spina M, Gloghini A, Schulz TF.** 2009. HIV-associated lymphomas and gamma-herpesviruses. Blood **113:**1213-1224.
220. **DePond W, Said JW, Tasaka T, de Vos S, Kahn D, Cesarman E, Knowles DM, Koeffler HP.** 1997. Kaposi's sarcoma-associated herpesvirus and human herpesvirus 8 (KSHV/HHV8)-associated lymphoma of the bowel. Report of two cases in HIV-positive men with secondary effusion lymphomas. The American journal of surgical pathology **21:**719-724.
221. **Carbone A, Gloghini A, Cabras A, Elia G.** 2009. The Germinal centre-derived lymphomas seen through their cellular microenvironment. British journal of haematology **145:**468-480.
222. **Boname JM, Coleman HM, May JS, Stevenson PG.** 2004. Protection against wild-type murine gammaherpesvirus-68 latency by a latency-deficient mutant. The Journal of general virology **85:**131-135.
223. **Bechtel JT, Liang Y, Hvidding J, Ganem D.** 2003. Host range of Kaposi's sarcoma-associated herpesvirus in cultured cells. Journal of virology **77:**6474-6481.

224. **Grogan E, Jenson H, Countryman J, Heston L, Gradoville L, Miller G.** 1987. Transfection of a rearranged viral DNA fragment, WZhet, stably converts latent Epstein-Barr viral infection to productive infection in lymphoid cells. Proceedings of the National Academy of Sciences of the United States of America **84:**1332-1336.
225. **Gruffat H, Sergeant A.** 1994. Characterization of the DNA-binding site repertoire for the Epstein-Barr virus transcription factor R. Nucleic acids research **22:**1172-1178.
226. **Liu C, Sista ND, Pagano JS.** 1996. Activation of the Epstein-Barr virus DNA polymerase promoter by the BRLF1 immediate-early protein is mediated through USF and E2F. Journal of virology **70:**2545-2555.
227. **Bowser BS, DeWire SM, Damania B.** 2002. Transcriptional regulation of the K1 gene product of Kaposi's sarcoma-associated herpesvirus. Journal of virology **76:**12574-12583.
228. **Haque M, Chen J, Ueda K, Mori Y, Nakano K, Hirata Y, Kanamori S, Uchiyama Y, Inagi R, Okuno T, Yamanishi K.** 2000. Identification and analysis of the K5 gene of Kaposi's sarcoma-associated herpesvirus. Journal of virology **74:**2867-2875.
229. **Jeong J, Papin J, Dittmer D.** 2001. Differential regulation of the overlapping Kaposi's sarcoma-associated herpesvirus vGCR (orf74) and LANA (orf73) promoters. Journal of virology **75:**1798-1807.
230. **Liu Y, Cao Y, Liang D, Gao Y, Xia T, Robertson ES, Lan K.** 2008. Kaposi's sarcoma-associated herpesvirus RTA activates the processivity factor ORF59 through interaction with RBP-Jkappa and a cis-acting RTA responsive element. Virology **380:**264-275.
231. **Sakaibara R, Uchiyama T, Kuwabara S, Kawaguchi N, Nemoto I, Nakata M, Hattori H.** 2001. Autonomic dysreflexia due to neurogenic bladder dysfunction; an unusual presentation of spinal cord sarcoidosis. Journal of neurology, neurosurgery, and psychiatry **71:**819-820.
232. **Song MJ, Brown HJ, Wu TT, Sun R.** 2001. Transcription activation of polyadenylated nuclear rna by rta in human herpesvirus 8/Kaposi's sarcoma-associated herpesvirus. Journal of virology **75:**3129-3140.
233. **Wong EL, Damania B.** 2006. Transcriptional regulation of the Kaposi's sarcoma-associated herpesvirus K15 gene. Journal of virology **80:**1385-1392.
234. **Willer DO, Speck SH.** 2005. Establishment and maintenance of long-term murine gammaherpesvirus 68 latency in B cells in the absence of CD40. Journal of virology **79:**2891-2899.
235. **Frederico B, May JS, Efstathiou S, Stevenson PG.** 2014. BAFF receptor deficiency limits gammaherpesvirus infection. Journal of virology **88:**3965-3975.
236. **Takeda K, Akira S.** 2002. [Role of toll-like receptor in innate immunity]. Tanpakushitsu kakusan koso. Protein, nucleic acid, enzyme **47:**2097-2102.
237. **Gargano LM, Forrest JC, Speck SH.** 2009. Signaling through Toll-like receptors induces murine gammaherpesvirus 68 reactivation in vivo. Journal of virology **83:**1474-1482.

238. **Haas F, Yamauchi K, Murat M, Bernasconi M, Yamanaka N, Speck RF, Nadal D.** 2014. Activation of NF-kappaB via endosomal Toll-like receptor 7 (TLR7) or TLR9 suppresses murine herpesvirus 68 reactivation. Journal of virology **88:**10002-10012.
239. **Forrest JC, Speck SH.** 2008. Establishment of B-cell lines latently infected with reactivation-competent murine gammaherpesvirus 68 provides evidence for viral alteration of a DNA damage-signaling cascade. Journal of virology **82:**7688-7699.
240. **Cheng BY, Zhi J, Santana A, Khan S, Salinas E, Forrest JC, Zheng Y, Jaggi S, Leatherwood J, Krug LT.** 2012. Tiled microarray identification of novel viral transcript structures and distinct transcriptional profiles during two modes of productive murine gammaherpesvirus 68 infection. Journal of virology **86:**4340-4357.
241. **Sanjabi S, Williams KJ, Saccani S, Zhou L, Hoffmann A, Ghosh G, Gerondakis S, Natoli G, Smale ST.** 2005. A c-Rel subdomain responsible for enhanced DNA-binding affinity and selective gene activation. Genes & development **19:**2138-2151.
242. **Ventura A, Meissner A, Dillon CP, McManus M, Sharp PA, Van Parijs L, Jaenisch R, Jacks T.** 2004. Cre-lox-regulated conditional RNA interference from transgenes. Proceedings of the National Academy of Sciences of the United States of America **101:**10380-10385.
243. **Collins CM, Speck SH.** 2012. Tracking murine gammaherpesvirus 68 infection of germinal center B cells in vivo. PloS one **7:**e33230.
244. **Tischer BK, Smith GA, Osterrieder N.** 2010. En passant mutagenesis: a two step markerless red recombination system. Methods in molecular biology **634:**421-430.
245. **Langmead B, Salzberg SL.** 2012. Fast gapped-read alignment with Bowtie 2. Nature methods **9:**357-359.
246. **Li H, Handsaker B, Wysoker A, Fennell T, Ruan J, Homer N, Marth G, Abecasis G, Durbin R, Genome Project Data Processing S.** 2009. The Sequence Alignment/Map format and SAMtools. Bioinformatics **25:**2078-2079.
247. **Upton JW, van Dyk LF, Speck SH.** 2005. Characterization of murine gammaherpesvirus 68 v-cyclin interactions with cellular cdks. Virology **341:**271-283.
248. **Jia Q, Sun R.** 2003. Inhibition of gammaherpesvirus replication by RNA interference. Journal of virology **77:**3301-3306.
249. **Frith MC, Saunders NF, Kobe B, Bailey TL.** 2008. Discovering sequence motifs with arbitrary insertions and deletions. PLoS computational biology **4:**e1000071.
250. **Grant CE, Bailey TL, Noble WS.** 2011. FIMO: scanning for occurrences of a given motif. Bioinformatics **27:**1017-1018.
251. **Pruitt KD, Tatusova T, Maglott DR.** 2005. NCBI Reference Sequence (RefSeq): a curated non-redundant sequence database of genomes, transcripts and proteins. Nucleic acids research **33:**D501-504.
252. **DeZalia M, Speck SH.** 2008. Identification of closely spaced but distinct transcription initiation sites for the murine gammaherpesvirus 68 latency-associated M2 gene. Journal of virology **82:**7411-7421.

253. **Adler H, Steer B, Freimuller K, Haas J.** 2007. Murine gammaherpesvirus 68 contains two functional lytic origins of replication. Journal of virology **81:**7300-7305.
254. **Howard PK, Shaw J, Otsuka AJ.** 1985. Nucleotide sequence of the birA gene encoding the biotin operon repressor and biotin holoenzyme synthetase functions of Escherichia coli. Gene **35:**321-331.
255. **de Boer E, Rodriguez P, Bonte E, Krijgsveld J, Katsantoni E, Heck A, Grosveld F, Strouboulis J.** 2003. Efficient biotinylation and single-step purification of tagged transcription factors in mammalian cells and transgenic mice. Proceedings of the National Academy of Sciences of the United States of America **100:**7480-7485.
256. **Driegen S, Ferreira R, van Zon A, Strouboulis J, Jaegle M, Grosveld F, Philipsen S, Meijer D.** 2005. A generic tool for biotinylation of tagged proteins in transgenic mice. Transgenic research **14:**477-482.
257. **Izumiya Y, Izumiya C, Hsia D, Ellison TJ, Luciw PA, Kung HJ.** 2009. NF-kappaB serves as a cellular sensor of Kaposi's sarcoma-associated herpesvirus latency and negatively regulates K-Rta by antagonizing the RBP-Jkappa coactivator. Journal of virology **83:**4435-4446.
258. **Grossmann C, Ganem D.** 2008. Effects of NFkappaB activation on KSHV latency and lytic reactivation are complex and context-dependent. Virology **375:**94-102.
259. **Sgarbanti M, Arguello M, tenOever BR, Battistini A, Lin R, Hiscott J.** 2004. A requirement for NF-kappaB induction in the production of replication-competent HHV-8 virions. Oncogene **23:**5770-5780.
260. **Moser JM, Upton JW, Gray KS, Speck SH.** 2005. Ex vivo stimulation of B cells latently infected with gammaherpesvirus 68 triggers reactivation from latency. Journal of virology **79:**5227-5231.
261. **AuCoin DP, Colletti KS, Xu Y, Cei SA, Pari GS.** 2002. Kaposi's sarcoma-associated herpesvirus (human herpesvirus 8) contains two functional lytic origins of DNA replication. Journal of virology **76:**7890-7896.
262. **Lin CL, Li H, Wang Y, Zhu FX, Kudchodkar S, Yuan Y.** 2003. Kaposi's sarcoma-associated herpesvirus lytic origin (ori-Lyt)-dependent DNA replication: identification of the ori-Lyt and association of K8 bZip protein with the origin. Journal of virology **77:**5578-5588.
263. **Hammerschmidt W, Sugden B.** 1988. Identification and characterization of oriLyt, a lytic origin of DNA replication of Epstein-Barr virus. Cell **55:**427-433.
264. **Fixman ED, Hayward GS, Hayward SD.** 1995. Replication of Epstein-Barr virus oriLyt: lack of a dedicated virally encoded origin-binding protein and dependence on Zta in cotransfection assays. Journal of virology **69:**2998-3006.
265. **Wu FY, Ahn JH, Alcendor DJ, Jang WJ, Xiao J, Hayward SD, Hayward GS.** 2001. Origin-independent assembly of Kaposi's sarcoma-associated herpesvirus DNA replication compartments in transient cotransfection assays and association with the ORF-K8 protein and cellular PML. Journal of virology **75:**1487-1506.

266. **Wang Y, Li H, Chan MY, Zhu FX, Lukac DM, Yuan Y.** 2004. Kaposi's sarcoma-associated herpesvirus ori-Lyt-dependent DNA replication: cis-acting requirements for replication and ori-Lyt-associated RNA transcription. Journal of virology **78:**8615-8629.
267. **Ellison TJ, Izumiya Y, Izumiya C, Luciw PA, Kung HJ.** 2009. A comprehensive analysis of recruitment and transactivation potential of K-Rta and K-bZIP during reactivation of Kaposi's sarcoma-associated herpesvirus. Virology **387:**76-88.
268. **Gregory SM, West JA, Dillon PJ, Hilscher C, Dittmer DP, Damania B.** 2009. Toll-like receptor signaling controls reactivation of KSHV from latency. Proceedings of the National Academy of Sciences of the United States of America **106:**11725-11730.
269. **Johnson LS, Willert EK, Virgin HW.** 2010. Redefining the genetics of murine gammaherpesvirus 68 via transcriptome-based annotation. Cell host & microbe **7:**516-526.